Optical Observations of Southern Hemisphere Blazars with the *WATCHER* Telescope

Peter Tisdall

School of Physics
Science Centre - North
University College Dublin

Submitted in fulfilment of the requirements
for the degree of Research Masters of Science

Head of Department:
Prof. P. Dunne

Supervisor:
Prof. L. Hanlon

2014

For Doireann

Contents

Abstract

Active galactic nuclei (AGN) are known to vary in brightness in all regions of the electromagnetic spectrum and over a wide range of timescales. Many statistical tests have been utilised to validate the detection of this variability. The C-statistic and F-test are commonly used tests for optical observations.

This thesis utilises the aforementioned tests to examine the results of an intense blazar monitoring campaign performed by the UCD Watcher robotic telescope. The blazars PKS 2005-489 and PKS 2155-304 were the focus of this monitoring campaign during the austral winter of 2013. During this time, PKS 2005-489 was confirmed to have small scale variations, on 10 of 56 nights. while PKS 2155-304 displayed no significant variability over 68 nights, during the campaign.

Simulations were used to assess the practicality of using the C-statistic and F-test to validate a detection of variability. These simulations found that the C-statistic is unreliable for fewer than 10 observations. The F-test proved to be significantly more resilient to smaller sample sizes.

In addition, the pilot outreach programme, 'Access All Skies', and the results of the feedback from the students and teachers in it, is presented. This programme was run by UCD, in conjunction with Blackrock Castle Observatory and Bradford University, during October 2012 and involved 5 primary schools and 5 secondary schools in Dublin, Wicklow and Cork. The goal of the programme is to inspire future scientists and engineers through the innovative use robotic telescope technology in education.

I hereby certify that the submitted work is my own work, was completed while registered as a candidate for the degree stated on the Title Page, and I have not obtained a degree elsewhere on the basis of the research presented in this submitted work.

Acknowledgements

I would like to acknowledge, first of all, my Mum, my Dad, and my family. Without you, none of this would have been possible. Thank you for all of the patience and support over the years. I love you all, big and small.

I would also like to thank my supervisor, Lorraine Hanlon, for all of the guidance and help you have given over the course of my undergraduate and postgraduate studies. Thank you for all you have taught me and the opportunities you have given me.

Thank you Antonio, Dave, Ger and Seamus for teaching me how to science. Its not funny how little I would have gotten done without your help. And the rest of the Space Science group, Colin, Dave T., Dave B., Oli, Suzanne, Sinéad, and Sinéad. Thanks for all of the wine and crazy conversations, you kept me sane.

Jon and Brian, thank you for being the best house-mates a man could ask for, and to all of my friends outside of UCD, sorry for being crap for the last few years. I swear it was worth it.

Special thanks to Rory Heffernan and Eoin Burke for all of the advice and laughs we have had. It means a lot to know you guys are there for me.
Finally, thank you Paul Hanratty, for teaching me banter, what it is and how to have it.

A lot of people have helped me in a lot of ways over the last 2 years, probably too many to mention, so if I have left you out, get over it.

List of Figures

List of Tables

Chapter 1

Introduction

The term Active Galactic Nuclei (AGN) refers to the incredibly energetic nuclei, or centre regions, of galaxies, whose luminosities are not attributable to the member stars of that galaxy. This is due to the observed spectrum appearing very different from regular stars and because they are bright in all wavelengths. There are several classification of AGN based on their observed properties, including Seyfert Galaxies, Quasars, Radio Loud Galaxies and Blazars. This chapter presents the historical context of AGN observations, following primarily the treatment given in *Urry* (1998), and outlines the observed properties of the different types of AGN.

1.1 Active Galactic Nuclei

1.1.1 Seyfert Galaxies

The first observations of AGN were made at the beginning of the twentieth century, when some astronomers were trying to classify the nature of 'spiral nebulae' (*Fath* 1909). In his investigation of the claim that the spectra of spiral nebulae were continuous, Fath noted that for the case of NGC 1068 'the spectrum is composite, showing both bright and absorption lines'. This observation differed from that of other spiral nebulae in the study, which showed continuous spectra with stellar absorption lines consistent with an unresolved collection of stars. Fath determined that the bright and dark spectral lines likely originated from the nucleus of the nebula, as the line widths were narrow, and that

this nucleus was not stellar in nature.

Fath made two plates of the spectrum of NGC 1068 in August and September of 1908 at the Lick Observatory, but his observations were not confirmed until 1917 (*Slipher* 1917) based on observations made in 1913 at the Lowell Observatory. In further observations of the galaxy made in 1917, Slipher noted that the emission lines were not images of the slit of the spectrograph, which is what he had become accustomed to finding in the gaseous emissions of nebulae. In contrast to the absorption lines, the emission lines were broadened, indicating that the emission was spread over a wide range of wavelengths. This nuclear emission was identified in a number of spiral galaxies, by several astronomers, over the following years (*Hubble* 1926).

Carl Seyfert began a study of the nuclear emission in spiral galaxies in 1943 (*Seyfert* 1943), in which he obtained the spectra of 6 galaxies (NGC 1068, 1275, 3516, 4051, 4151, 7469) with highly excited emission lines localised in the nuclei of the galaxies. In his study, Seyfert attributed the line broadening to a Doppler shift of up to $\sim 8,500\,\mathrm{km\,s^{-1}}$ for the hydrogen lines of NGC 3516 and 7469. Galaxies that have Doppler-broadened emission lines from their nucleus have since become known as 'Seyfert galaxies'. Seyfert galaxies were originally classified by whether they displayed broad emission lines (Type 1) or narrow emission lines (Type 2). As the quality of equipment and observations increased, it was seen that some Seyfert galaxies exhibited features of both classes, resulting in a fractional classification being introduced to identify these intermediate galaxies.

1.1.2 Radio Galaxies

The development of radio based astronomy in the 1940s provided the next step in the classification of AGN. The study of discrete sources was started when a small varying source was detected in Cygnus during a $60\,\mathrm{MHz}$ study of the Milky Way (*Hey et al.* 1947). They were able to place an upper limit of 2° on the angular diameter of the varying source with their 6° beam. This was later refined to an upper limit of 8' by *Bolton and Stanley* (1948). The variability in the intensity occurring on a time scale of seconds was found to be caused by processes in the Earth's ionosphere.

Optical observations of discrete sources of this kind were first made by *Bolton et al.*

(1948), aided by more accurate positions provided by the Sea Cliff Interferometer observations. They associated Taurus A with the Crab Nebula supernova remnant, Virgo A with Messier 87 and Centaurus A with NGC 5128. *Ryle et al.* (1950) performed a survey of the Northern Hemisphere 'radio-stars' using the Cambridge interferometer that showed a uniform distribution of these objects in the sky, and with this survey it was possible to find accurate positions for several bright object such as Tau A, Vir A, Cyg A and Cas A (*Smith* 1951). Accurate positions for these sources provided the means to perform optical identification of sources like Cas A and Cyg A with the Hale telescope (200") at Palomar Observatory (*Baade and Minkowski* 1954). The optical observations of Cyg A allowed a recessional velocity of $16,830\,\mathrm{km\,s^{-1}}$ to be calculated, placing Cyg A at a distance of $31\,\mathrm{Mpc}$ (for the accepted value of the Hubble constant, $H_0 = 540\mathrm{km\,s^{-1}\,Mpc^{-1}}$, at that time), placing it outside of the Milky Way. This large distance implied a very large luminosity for the object Cyg A in both optical ($6 \times 10^{42}\,\mathrm{erg\,s^{-1}}$) and radio ($8 \times 10^{42}\,\mathrm{erg}\,s^{-1}$) frequencies (Figure 1.1).

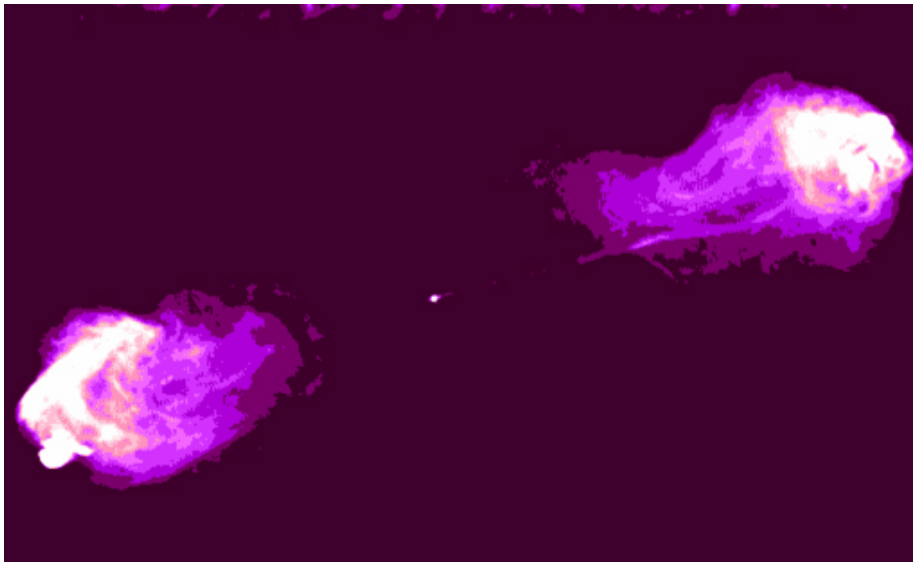

Figure 1.1: Radio Galaxy Cygnus A. The jets protruding from the central region of the galaxy ending in hot lobes as the material in the jet collides with the intergalactic medium. *Image courtesy of NASA/CXC/SAO*.

The discrete radio sources were classified into those that lay in the plane of the Milky Way (Class 1) and those that were distributed isotropically in the sky (Class 2), which suggested that these sources were extragalactic in nature. However, many of the Class 2 radio sources displayed very small angular sizes, and this popularised the view that many

of them were in fact 'radio stars' within our galaxy. In 1957, *Morris et al.* calculated an apparent brightness temperature lower limit of $\geq 2 \times 10^7$K, for three of these Class 2 sources. At the time, the only other known radio source of similar brightness was Cygnus A (Figure 1.1). This suggested that these three sources, were extragalactic of the Cyg A type.

During this time, the source of the galactic radio background was still under debate. *Alfvén and Herlofson* (1950) made the suggestion that the emission from the 'radio stars' was created by synchrotron radiation. This led *Kiepenheuer* (1950) to explain that the Galactic radio background was a result of synchrotron emission by cosmic rays. The synchrotron process became the accepted explanation for extragalactic discrete sources by the end of the 1950s. This theory implied extreme energies for the 'double lobed' radio galaxies ($\sim 10^{60}$ ergs, *Burbidge et al.* (1966)), named for the large jets emitted from the nucleus that form lobes as the ejected material slows.

The third Cambridge survey at 159 MHz, and the revised survey at 178 MHz, provided accurate positions for many of the discrete sources, which allowed the optical identification process to continue, and many of the sources catalogued in this survey are still known by the names given at this time (e.g. 3C 273, 3C 279). Some AGN were also discovered via optical telescopes based on the apparent 'compactness' and the strong UV continuum observed in the sources (*Zwicky* 1966).

As the studies advanced, radio galaxies were classified into broad-line radio galaxies (BLRG), which have spectra very similar to Seyfert 1 galaxies, and narrow-line radio galaxies (NLRG), which have spectra that are similar to Seyfert 2 galaxies. While there are several differences between the radio galaxies and the Seyfert galaxies, the most obvious is that all the radio galaxies are giant elliptical galaxies, whereas Seyfert 1's are almost exclusively hosted by spiral galaxies. Radio galaxies were also classified into two classes by the morphology of their radio emission. Fanaroff and Riley (1974) noted that there was an abrupt division in the radio luminosity distribution in radio galaxies. Fanaroff-Riley 1 (FR1) type galaxies display much greater brightness towards the nucleus, whereas Fanaroff-Riley 2 (FR2) type galaxies have radio lobes and brighter advancing edges caused by hotspots (*Fanaroff and Riley* 1974).

1.1.3 Quasars

Towards the end of the 1950's, astronomers began searching for optical identifications and the redshifts of the radio galaxies that had been identified. In 1960, an image of 3C 48 was obtained at the Mt. Wilson and Palomar Observatory, and was initially identified as a stellar object with a visual magnitude of 16 that exhibited a strange nebulosity. 3C 48 was also found to have very broad emission lines and photometry showed it to be variable and have an excess of UV emission when compared with normal stars. This and several other objects that exhibited similar features became known as Quasi Stellar Radio Sources (QSRS), or Quasars, and it was said to be a 'remote possibility that it [3C 48] may be a distant galaxy of stars' but 'general agreement' that it was 'a relatively nearby star with most peculiar properties' (*Matthews et al.* 1961).

A group of subsequent papers (*Hazard et al.* (1963); *Schmidt* (1963); *Oke* (1963); *Greenstein and Matthews* (1963)) were the first to propose the explanation that these quasars were extragalactic objects. The findings of these papers were based on the analysis of the spectrum of the quasars 3C 273 and 3C 48. The optical spectrum of 3C 273 exhibited unusual broad emission lines that were similar to the Balmer series in their spacing towards the blue. Using this, Schmidt was able to identify the $H_\beta, H_\gamma, H_\delta$ and H_ϵ lines in the spectrum ($z = 0.16$), and was then able to pinpoint the location of the Mg II λ2798 lines in the UV part of the spectrum. Oke showed in his paper the location of the λ7600 emission line from the optical spectrum of 3C 273, and, with the proposed redshift, agreed with the results of Schmidt on the location of the H_α line of the spectrum.

More detailed studies of 3C 48 and 3C 273 were performed in order to investigate the origin of the calculated redshifts (*Greenstein and Schmidt* 1964). They investigated the rapid motion of objects in or near the Milky Way, gravitational redshifts, and cosmological redshifts as possible origins. The radial velocities of the objects and the apparent lack of proper motion indicated a lower limit of 10 Mpc distant, and this coupled with the fact that the 4 quasars with known redshifts were receding and their luminosities were more like galaxies than stars excluded the explanation of rapid motion within our galaxy. It was argued that for the redshift observed to be caused by gravitational effects the widths of the emission lines would require the line emitting gas to be confined to a small fractional

radius around the massive object producing the redshift. In the case of a $1M_{\odot}$ object, the observed H_{β} flux implied an electron density of $N_e \approx 10^{19}\,\mathrm{cm}^{-3}$, which is prohibited by the presence of forbidden emission lines in the observed spectrum. This emission line constraint, combined with a requirement that the massive object not disturb stellar orbits in the Galaxy, required a mass that is $\geq 10^9\ M_{\odot}$ (*Greenstein and Schmidt* 1964).

The cosmological explanation for the redshift was adopted for many further studies, and was used to approximate the radii of the emitting regions of the quasars. A model was proposed of a central source of optical continuum, surrounded by an emission-line region, and a still larger radio emitting region surrounding that. This model used the observed optical variability (*Matthews and Sandage* 1963) to define light travel time constraints. Schmidt and Greenstein also noted that it was possible for 3C 48 and 3C 273 to be surrounded by galaxies, but the luminosity of the nucleus is so great that they are obscured from view.

Quasars were known to exhibit a large UV excess when compared with normal stars on a colour-colour diagram. This led to the technique of exposing the same plate to U and B filters, with small offsets, which allowed for identification of sources with excess UV continua (*Matthews and Sandage* 1963). Sandage noted that many of the sources found in this manner did not match up with known radio sources, and were dubbed 'interlopers' or 'quasi stellar galaxies' (QSG), known as quasi stellar objects (QSO). He also found that for magnitudes fainter than 15^{th}, the UV excess sources populated the region occupied by quasars on the colour-colour diagram, whereas optically brighter sources were found to be main sequence stars. The spectra of these fainter sources revealed they had large redshifts of $z \approx 1.2$ (*Sandage* 1965), and Sandage also estimated, at the time, that these QSOs outnumbered radio loud galaxies by a factor of ~ 500. QSOs are now known as radio quiet quasars (RQQ).

The large redshifts and high luminosities of these sources, made them ideal subjects for the study of extragalactic astronomy. In particular, the study of the Inter Stellar Medium (ISM) uses the narrow absorption lines observed in the spectra of many QSOs. In the cases where $z_{abs} < z_{em}$ the absorption lines are thought to be caused by intervening matter between the object and the observer (*Bahcall and Salpeter* 1965) or matter that is being expelled by the quasar. In some cases, broad absorption lines (BAL) have been ob-

served in radio quiet QSOs. These BAL are still among the least well understood features of the spectra of QSOs.

1.1.4 Blazars

The object BL Lacertae (BL Lac) was originally identified as an irregularly variable star, (*Hoffmeister* 1929), that varied from 13th to 16th magnitude, in the visual band, over a period of several days. As the identification of radio sources continued, BL Lac was determined to coincide with the radio source VRO 42.22.01 (*Schmitt* 1968). Schmitt found there to be a slight nebulosity around the object, and stated that its radio polarisation and the unusual microwave spectrum made it an 'outstandingly interesting' object.

Further study of BL Lac showed that it was also rapidly variable at radio frequencies, and possessed a circular radio polarisation (*Biraud and Veron* 1968). Similarities between BL Lac and some other radio sources previously identified were used to hypothesise a new class of QSOs (*Strittmatter et al.* 1972), characterised by:

1. rapid variability in radio, infrared and optical wavelengths
2. non-thermal continuum with the majority of the luminosity radiated in the infra-red
3. absence of emission lines in the central source
4. strong and rapidly varying polarization at visual and radio wavelengths.

Sources that displayed these attributes became known as BL Lacertae type sources, after the prototype. By 1976, $\sim$30 objects of this new class had been identified (*Stein et al.* 1976), but the redshift for some of these sources was still under debate due to the mostly featureless spectra of the core source, but it was becoming accepted that BL Lac sources were associated with elliptical galaxies (*Colla et al.* (1975); *Disney et al.* (1974)).

As studies of BL Lac sources continued, similarities between them and many QSOs and Seyfert galaxies were found. *Stein et al.* (1976) put forward the idea that the classes of these sources were not clear cut or distinct. Stein also noted that many low redshift QSOs displayed evidence of surrounding nebulosity, which was attributed to elliptical galaxies (*Kristian* 1973), and that this nebulosity disappeared at higher redshifts.

A closely-related family of sources are the flat spectrum radio quasars (FSRQ), which are highly variable sources in both radio and optical wavelengths that exhibit many of the same features as BL Lac sources. They differ in that they possess strong, broad emission lines, very similar to those emitted by classical quasars. These sources are found at a generally higher redshift, $0.1 \leq z \leq 2$, to the BL Lac sources, $z \leq 0.2$, (*Longair* 2011). The term 'Blazar' is used to encompass both the FSRQ and BL Lacertae sources.

1.2 The Unified Model

The Unified Model proposes that all AGN are fundamentally the same type of object and that the observable properties of AGN depend only on their orientation, particularly the angle at which they are observed (*Urry and Padovani* 1995). Figure 1.2 shows the main components that are believed to make up the nucleus of an active galaxy; the super-massive black hole (SMBH), the accretion disk, the gas and dust torus, the broad-line emission region (BLR), the narrow-line emission region (NLR) and the relativistic jet from which lobes originate. The presence of the jet and lobes appears to be dependent on the class of AGN, which, as hypothesized by the unified model, is based on the orientation of the galaxy to the observer.

1.2.1 Seyfert Galaxies

It is believed that the angle of observation plays a significant role in the classification of Seyfert 1 and Seyfert 2 galaxies. In a study of the Seyfert 2 galaxy NGC 1068 *Antonucci and Miller* (1985) found, in their spectropolarimetric observations, that the polarised line emission was as broad as the broad permitted lines observed in Seyfert 1 galaxies. From this they inferred that there was some obscuring torus around the nucleus, such that at a small viewing angle, with respect to the axis perpendicular to the torus, the nucleus is seen to be emitting the characteristic Seyfert 1 broad-line regions and the strong blue and UV continuum. At larger angles, the nucleus of the galaxy is obscured, allowing only the narrow-line regions which are located further from the nucleus to be observed in direct light. The central regions that are obscured can be observed in light that is reflected by

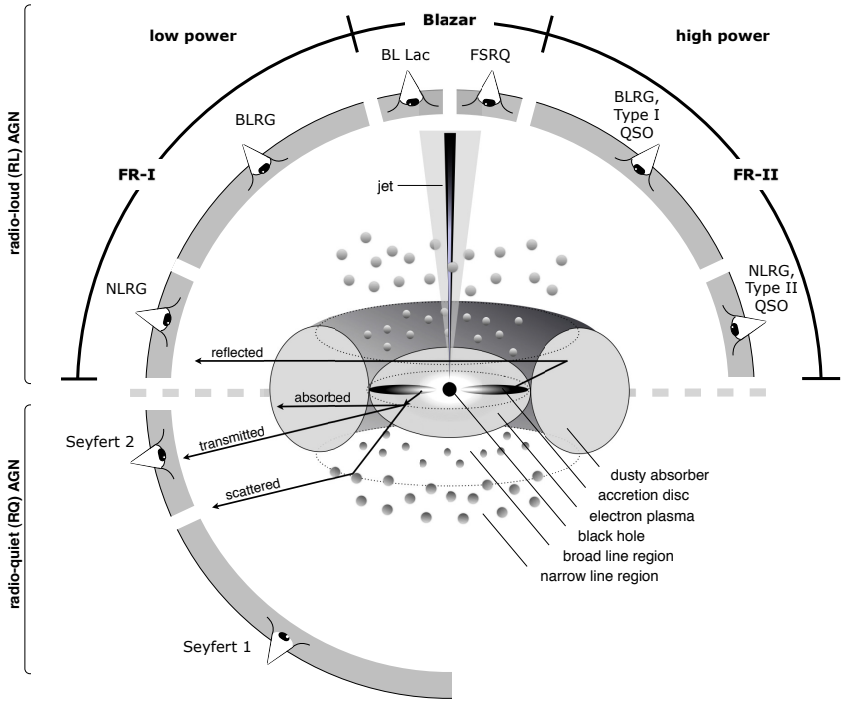

Figure 1.2: Unification scheme for AGN (*Beckmann and Shrader* 2012).

clouds of dust and gas outside the region of the torus in the narrow-line regions. The continuum and broad line emission from the nuclear regions of the galaxy is polarised by the process of reflection, either by Thompson or Rayleigh scattering.

As shown in Figure 1.2, Seyfert galaxies are observed when the galaxy is viewed at an angle of $\sim$45° (Seyfert 1), where both narrow and broad-line regions are visible, and at smaller angles (Seyfert 2), where the broad-line region is hidden by the torus.

1.2.2 Radio Galaxies and Quasars

The idea of the unification of radio galaxies and quasars that appear as bright radio sources was first discussed by *Barthel* (1989, 1994). He focused on the properties of the double radio sources, known as FR2 radio sources (Figure 1.2), and the effect of projection effects on these sources. Barthel argued that, in order for the superluminal motion that is observed in many compact radio sources to be apparent, the axis of the relativistic jet must lie at a small angle to the line of sight.

It is currently unclear how FR1-type galaxies fit into this scheme (*Torres and Anchordoqui* 2004). The different radio morphologies observed between FR1 and FR2 are possibly caused by an unknown physical mechanism.

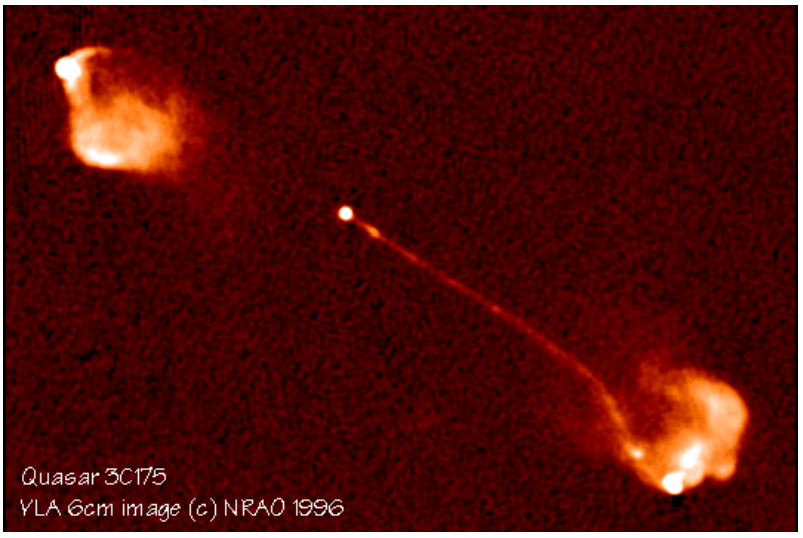

Figure 1.3: Radio Quasar 3C 175. The highly collimated, relativistic jets expand into bright lobes, with 'knots' of higher intensity, as the material in the jet comes into contact with the intergalactic medium. The effect of redshift is seen in the decreased intensity of the jet orientated away from the line of sight. *Image courtesy of NRAO/AUI*

A commonly-observed trait of radio quasars is the presence of only one jet, with two strong lobes visible. Figure 1.3 shows the radio quasar 3C 175, which possess two distinct radio lobes, but with only one jet visible. This effect is attributed to the combination of relativistic Doppler and aberration effects, i.e. the intensity of the jet is being enhanced by the blueshift while the intensity of the counter-jet is being reduced due to redshift, making it too faint to observe. Further evidence for the unification of radio quasars and the radio galaxies is that the projected linear sizes of the radio galaxies appear larger than those of the quasars at the same redshifts. This apparent difference in size is easily explained with the quasars being observed at a smaller angle to the line of sight. Barthel also noted that the optical emission observed from some of the radio galaxies was linearly polarised, which is expected for radiation emitted by an obscured nucleus that is then scattered, as in Seyfert 2 galaxies.

Similar to the Seyfert 1 galaxies, radio quasars are observed when the nucleus lies at an angle of $\sim 45°$, and at more acute angles the object appears as a radio galaxy.

1.2.3 Blazars

The highly-collimated jets that are emitted from the nucleus, perpendicular to the plane of the torus, fuel the radio lobes observed in many of these sources. An object is classified as a blazar when this jet lies very close to, or on the line of sight. When the jet is observed in this orientation, the emission is highly enhanced by Doppler and aberration effects, obscuring much of the underlying double radio lobe. In some cases, the underlying double lobe can be observed with high dynamic range observations. For example, the BL Lac object 3C 371 has been observed to have the appearance of an FR2 double-lobed radio source that is being observed end-on (*Longair* 2011).

Similarities between BL Lac sources and FR1 galaxies have been observed when the BL Lac sources are observed with very high dynamic range. With these observations, weak extended radio sources have been found about the radio source, and their low luminosity radio structures are very similar to those of FR1 type radio galaxies.

1.3 Blazar Theory

As mentioned above, the term 'Blazar' refers to both BL Lac type sources and FSRQs. They can simply be defined as AGN that have their relativistic jets along, or close to, the line of sight (Figure 1.2). This makes blazars very important to the study of AGN as a whole, as they provide a direct view of the central engine, and the emission processes involved (*Urry* 1996).

Blazars emit broadband continuum radiation from radio to γ–rays and their Spectral Energy Distributions (SED) are characterised by two broad emission peaks (Figure 1.4). The first peak occurs at lower energies between radio and X–rays and the emission is accepted as being non-thermal synchrotron radiation produced by relativistic electrons in the jet. The higher energy bump in the γ–ray energy regime is thought to be a result of inverse Compton processes.

FSRQs have strong, clear, distinguishable emission lines in their optical spectra and are typically found at higher redshifts, while BL Lacs exhibit weak or absent emission lines and appear more luminous. BL Lacs also show a higher degree of brightness vari-

ability with this flux peaking at higher energies than observed in FSRQs.

Blazars are further divided into subclasses, based on the frequency at which the synchrotron peak occurs (*Abdo et al.* 2010):

LSP or *Low Synchrotron Peaked* blazars. These are sources where the synchrotron power peaks in the far IR or IR band ($\nu_{peak} \lesssim 10^{14}$ Hz), meaning that their X–ray emission is flat due to the rising part of the inverse Compton component.

ISP or *Intermediate Synchrotron Peaked* blazars. These are sources where the peak occurs at intermediate energies ($10^{14} \lesssim \nu_{peak} \lesssim 10^{15}$ Hz). In this case the X–ray band includes both the tail of the synchrotron emission and the rise of the inverse Compton component.

HSP or *High Synchrotron Peaked* blazars. These sources peak in the UV band or higher ($\nu_{peak} \gtrsim 10^{15}$ Hz) as the emitting particles are accelerated to much higher energies. Under these conditions the synchrotron emission dominates the observed flux in the X–ray band.

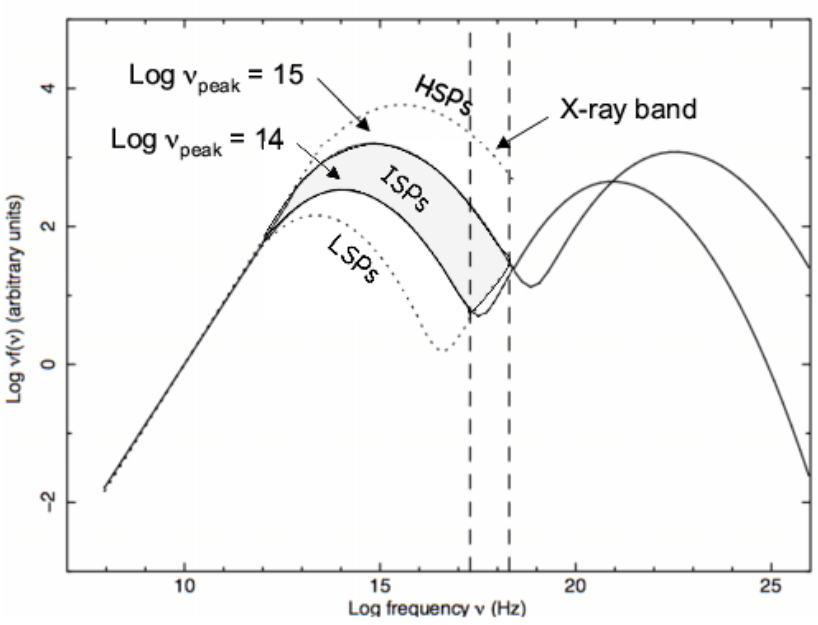

Figure 1.4: Definition of different blazar types based on the location of the synchrotron peak in the SED (*Abdo et al.* 2010).

Another of the observational differences between FSRQ and BL Lac type sources is the ratio of the magnitude of the synchrotron peak to the inverse Compton peak. The spectra of FSRQ are more likely to be dominated by the γ–ray emission, with the inverse Compton peak being higher in amplitude than the synchrotron. It is also seen that the majority of FSRQs are of the LSP type at microwave, X–ray and γ–ray frequencies, with no HSP type FSRQs being identified at any frequency to date. The distribution of the synchrotron peak of BL Lac type objects is quite different. In the microwave band, HSP type sources are rare, whereas HSPs are much more abundant at X–ray and γ–ray frequencies (*Abdo et al.* 2010).

1.3.1 Emission Processes

The emission from blazars is dominated by non-thermal jet radiation. All non-thermal processes involve strong electromagnetic fields that accelerate or decelerate charged particles, either by being deflected by a magnetic field or by colliding with other particles. A brief description of the processes involved in the production of the high energy emission in blazars is given here. The description presented follows primarily that of *Longair* (2011).

Synchrotron Radiation

When charged particles are accelerated to relativistic energies by strong magnetic fields, they follow a curved path, producing synchrotron radiation. Figure 1.5 shows the curved path that a high-energy electron follows in a uniform magnetic field.

The frequency at which the electron gyrates, its gyrofrequency, is constant through the field lines in the direction of the magnetic field. It is expressed as:

$$\nu_g = \frac{eB}{2\pi\gamma m_e} \tag{1.1}$$

where $\gamma = (1 - v^2/c^2)^{-1/2}$ is the Lorentz factor for relativistic particles and B is the strength of the magnetic field.

This means that the electron is accelerated towards the guiding centre of its orbit with a radiation loss rate given by:

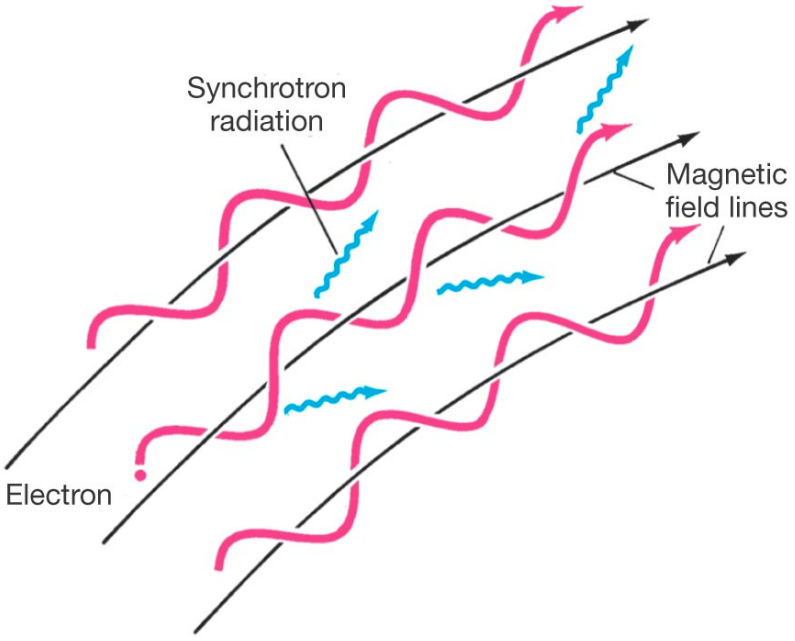

Figure 1.5: Helical motion of a charged particle in a uniform magnetic field (*Pearson Education, Inc.* 2008)

$$-\left(\frac{dE}{dt}\right) = \frac{e^4 B^2}{6\pi\epsilon_0 c m_e^2}\frac{v^2}{c^2}\gamma^2 sin^2\alpha \tag{1.2}$$

where v is the velocity of the electron, ϵ_0 is the permittivity of free space and α is the pitch angle of the electron. The pitch angle distribution is likely to be randomised by either Alfvén and hydromagnetic waves or irregularities in the magnetic field distribution, meaning that there is an isotropic distribution for a population of high-energy electrons. Thus, the average energy loss rate can be described by Equation 1.3, where σ_T is the Thompson cross-section and $u_{mag} = B^2/2\mu_0$ is the energy density of the magnetic field:

$$-\left(\frac{dE}{dt}\right)_{sync} = \frac{4}{3}\sigma_T c u_{mag}\left(\frac{v^2}{c^2}\right)\gamma^2 \tag{1.3}$$

One of the general features of the radiation from the relativistic electrons is that it is beamed in the direction of the motion of the electrons. This is determined through relativistic transformations considering that the radiation is emitted isotropically in the rest frame. The opening angle θ, in the laboratory frame can be expressed as:

$$sin\theta \approx \theta \approx \pm\gamma^{-1} \tag{1.4}$$

In the observer's frame, the dipole beam pattern is very elongated in the direction of motion of the electron (Figure 1.6). As it sweeps past the line of sight of the observer, a pulse of radiation is observed every time the electron's velocity vector lies within an angle $\pm\,\gamma^{-1}$ with respect to the observer's line of sight.

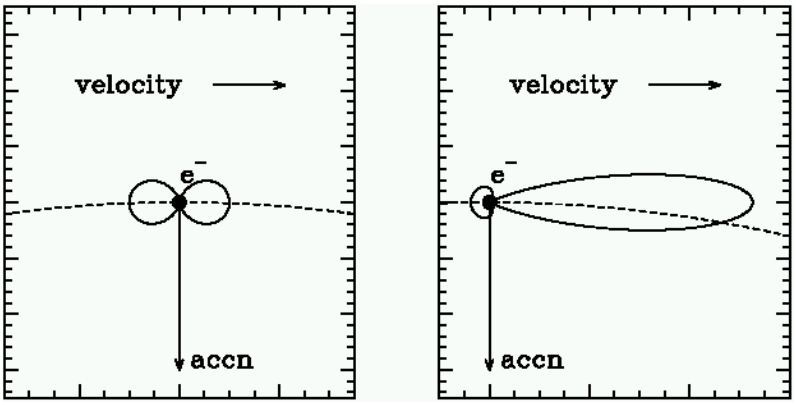

Figure 1.6: Beaming effect for a relativistic electron (*Flynn* 2005). The left panel shows the diagram of the isotropic radiation in the instantaneous rest frame, and the right panel shows the beaming effect seen in the observer's frame.

The observed frequency, ν, compared to the relativistic gyrofrequency, ν_r, can be written as:

$$\nu \approx \gamma^2 \nu_g = \gamma^3 \nu_r = \frac{\gamma^3 \upsilon}{2\pi r_g} \tag{1.5}$$

where r_g is the radius of the electron's orbit, or the instantaneous radius of curvature. Equation 1.5 allows the frequency at which the radiation was emitted to be determined.

Synchrotron radiation is generally accepted to be the source of the low energy emission (1st hump) in the SED of blazars.

Inverse Compton Scattering

Compton scattering involves the collision of high-energy photons with a stationary electron (Figure 1.7). The result of this interaction is an increase in the wavelength of the photon due to it imparting some of its energy to the electron, which ejects the electron from its atom, ionizing it.

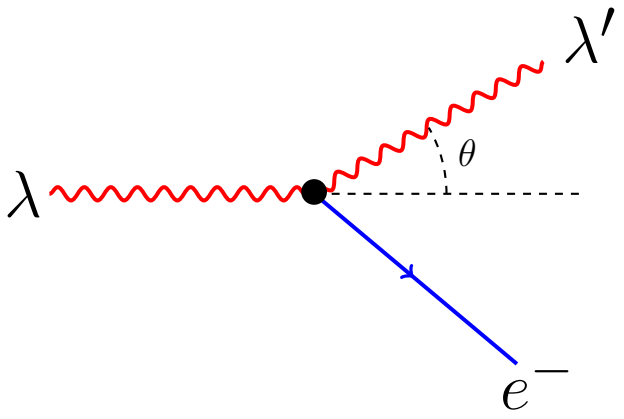

Figure 1.7: Feynman diagram of Compton scattering

In the inverse Compton (IC) scattering process, ultra-relativistic electrons scatter low-energy photons to higher energies so that the photons gain energy at the expense of the electrons kinetic energy (Figure 1.8). The rate of energy gain by the photons can be written as:

$$\left(\frac{dE}{dt}\right)_{IC} = \frac{4}{3}\sigma_T c u_{rad} \left(\frac{v^2}{c^2}\right) \gamma^2 \tag{1.6}$$

This expression is true provided that the energy of the photon in the rest-mass frame of the electron is $\ll m_e c^2$, or $\gamma\hbar\omega \ll m_e c^2$. Equation 1.6 is quite similar to the energy loss rate equation for synchrotron radiation (Equation 1.3). This is due to the dependency of the energy loss rate on the electric field which accelerates the electron in its rest frame, and the origin of this field does not matter.

The maximum energy which a photon can acquire through IC scattering corresponds to a head-on collision. In this case the photon is reflected back along its original path and the maximum energy is given by:

$$E_{max} = (\hbar\omega)_{max} \approx 4\gamma^2 \hbar\omega_0 \tag{1.7}$$

where $\hbar\omega_0 = E_p$, the initial energy of the photon.

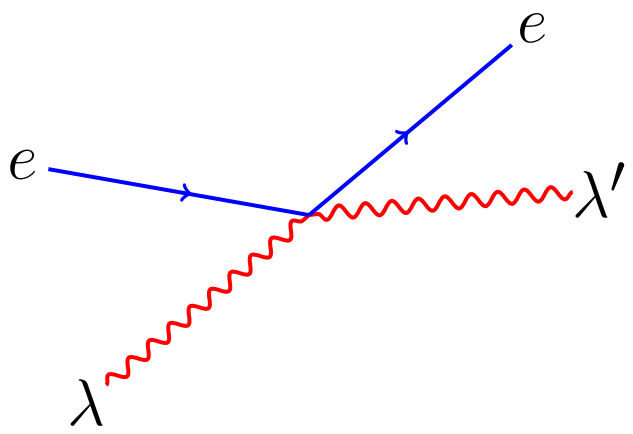

Figure 1.8: Feynman diagram of Inverse Compton scattering

Synchrotron-Self-Compton Radiation

Synchrotron-self-Compton (SSC) radiation results from the IC scattering of synchrotron radiation by the same relativistic electrons that produced the synchrotron radiation. When the energy density of low-energy photons is sufficiently high that the majority of the electrons energy is lost through SSC, rather than synchrotron radiation, ultra-high γ–rays can be produced.

The source high energy emission (2nd hump) in the SED of blazars is typically attributed to IC or SSC processes.

1.3.2 Leptonic Models

Leptonic models are the most common models used to explain the high-energy peak in blazar emission (*Chatterjee et al.* 2008; *Bonning et al.* 2012). These models attribute this peak to the either SSC radiation from photons within the jet, or from the up-scattering of photons external to the jet (external Compton, EC).

In the EC model, the photons that undergo the IC scattering enter the jet from an external source, such as the accretion disk or dusty torus. The SSC model describes a situation in which a population of relativistic electrons move along the jet and generate synchrotron radiation through the magnetic field present in the jet. These photons are then up-scattered by the same population of electrons that produced them.

These models are not mutually exclusive, and many models incorporate both. Multi-component SSC models also exist and allow for the presence of multiple electron populations.

1.3.3 Hadronic Model

In hadronic models, the high-energy peak in the SED is attributed to the production of γ–rays by VHE protons in the jet through pion decay (Eq. 1.8). This model requires extreme magnetic fields in order to accelerate the protons. The protons can then produce secondary γ–rays though further interactions with matter in the jet (*Pohl and Schlickeiser* 2000), or by interacting with synchrotron photons (*Böttcher* 2005).

$$p + \gamma \rightarrow \begin{cases} p + \pi^0 \\ n + \pi^+ \end{cases} \tag{1.8}$$

A notable feature of this emission model is the production of neutrinos through the pion decay. The detection of neutrinos from a blazar would strongly indicate a hadronic model for the source. Hadronic models are also well suited for the explanation of 'orphan' flares, or flares that unrelated to the synchrotron component. Due to the nature of the SSC model, any flare at γ–ray energies should be accompanied by a correlated flare in the synchrotron component. In hadronic models, relativistic protons may interact with an external photon field generated by the electron synchrotron radiation to produce independent VHE emission.

1.3.4 Variability

Variability across multiple wavelengths is one of the defining properties of blazars, and can be used to probe the location and physical processes related to the emission by careful examination of the timescale of these variations (*Agudo et al.* 2011; *Marscher* 1996; *Chatterjee et al.* 2008).

For example, in the leptonic models, the same population of seed photons is responsible for the emission in low (optical) and high energies (γ–ray), meaning that variations seen at these energies should be well correlated. In hadronic models, this correlation may

be weak or non-existent (*Chatterjee et al.* 2012). Correlation studies between variability at different energies are an important tool for the modelling of the emission process for a blazar, explained in Sections 1.3.2 and 1.3.3.

The timescales of variability can be broken down into intra-day variability (IDV), short-term variability (STV, days–weeks), and long-term variability (LTV, months–years) (*Gaur et al.* 2012; *Villforth et al.* 2010).

Most models used to describe IDV involve shocks propagating down the blazar jet, and these jet fluctuations almost certainly dominate the variations seen when blazars are in a high state (*Gupta et al.* 2012). Analysis of this IDV can be used to provide an estimate for the mass of the central engine of the blazar, generally accepted to be a super-massive blackhole (SMB). Assuming that the emission region is close to the central engine, a short timescale of variability implies a small engine. This is calculated with the inequality:

$$R \leq \frac{\delta c \Delta t}{1+z} \tag{1.9}$$

where R is the radius of the emitting region, Δt is the observed variability timescale, z is the redshift of the source and δ is the Doppler factor. The Doppler factor is used to correct for the Doppler shift in the observed frequency versus the emitted frequency.

1.4 Synopsis of Thesis

This dissertation presents the results of an observing campaign, during the austral winter of 2012, undertaken by the Watcher robotic telescope to observe two blazars, PKS 2005-489 and PKS 2155-304. The 'Access All Skies' outreach and education programme using robotic telescopes is also presented. This project was run by University College Dublin (UCD) in conjunction with Blackrock Castle Observatory (BCO), the Bradford Robotic Telescope (BRT) and Dublin City of Science 2012, in autumn 2012.

Chapter 2 discusses multi-wavelength observations and the role of robotic telescopes. Chapter 3 discusses the method of analysis that was used in the production of the light curves presented in Chapter 5. Chapter 4 provides a detailed overview of the target sources. Chapter 6 discusses the results of the Access All Skies project and presents an implementation programme for future outreach.

Chapter 2

Blazar Multi-Wavelength Observing Campaigns

Many sources, including blazars, show very different behaviour and characteristics at different wavelengths and over different timescales. For this reason there are many different telescopes, both space- and ground-based, observing the night sky across the entire spectrum. Coordinated multi-wavelength (MWL) observations allow this behaviour to be characterised and physical insight to the processes to be derived.

Telescopes such as Watcher are primarily designed to make target of opportunity (ToO) observations of sources like γ–ray bursts. Due to the transient nature of these sources, the remainder of the observing time for such telescopes may be used for observing campaigns and source monitoring. This chapter presents the role of monitoring campaigns in modern astronomy.

Multi-wavelength campaigns are conducted primarily in response to an increase in activity, at one or more wavelengths, from a source. Planned intensive campaigns may also be performed in order to provide a better understanding of the source at times when it may not be in an active state. Both of these types of campaigns require a large amount of coordination between telescopes and institutions.

Due to the variable nature of AGN, it is vital for the observations to be synchronised. Each telescope involved provides a very important aspect of the information that is built up about the source. It is only with these simultaneous observations across the spectrum

that it is possible to fully describe the physical process responsible for the emission.

2.1 Spectral Energy Distribution

A spectral energy distribution (SED) is a plot of source brightness or flux density versus frequency or wavelength. Flux density (in units of $\mathrm{Wm^{-2}Hz^{-1}}$) is the standard measure of the power received from a source, which is the energy incident per second per unit area per unit frequency band at the telescope (*Longair* 2011). The SED for a blazar is characterised by a double-humped appearance, reflecting different physical processes operating at different frequencies (Figure 1.4 and 2.1).

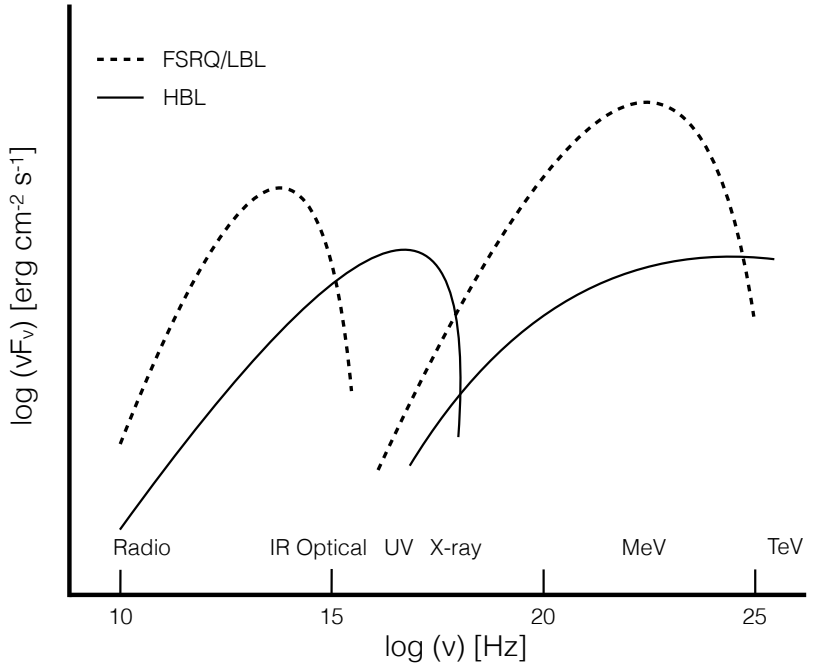

Figure 2.1: Typical SED for blazars. FSRQ and LBL type blazars (dashed line) typically have a synchrotron peak in the IR to far-IR, whereas the HBL type blazars (solid line) have a synchrotron peak at much higher frequencies.

The first hump in Figure 2.1 is commonly attributed to synchrotron radiation from high-energy electrons within the jet, which peaks between 10^{13} and 10^{17} Hz for BL Lac type objects and between $10^{12.5}$ and $10^{14.5}$ Hz for FSRQ's (*Abdo et al.* 2010).

By combining observations made in the optical and X–ray bands the location of this synchrotron peak can be determined, and from this, the energy of electrons within the jet. The second hump in the SED extends up to γ–rays, and peaks in the GeV to TeV range. One of the primary theories for the source of this emission is inverse-Compton scattering of 'seed' photons off electrons within the jet, either through synchrotron self-Compton (SSC) or external Compton radiation (see Section 1.3).

2.1.1 Target of Opportunity Campaigns

The primary reason for having a large number of telescopes monitoring the sky is to detect and report on any changes in the emission from a wide range of sources.

Figure 2.2 describes the basic data flow whereby flares and transient sources are detected by telescopes and are communicated to robotic telescopes and users around the globe. Systems such as the GRB Coordinate Network (GCN) use such an approach to rapidly and automatically provide large numbers of telescopes with the information to point towards the same region of the sky and to observe at different wavelengths.

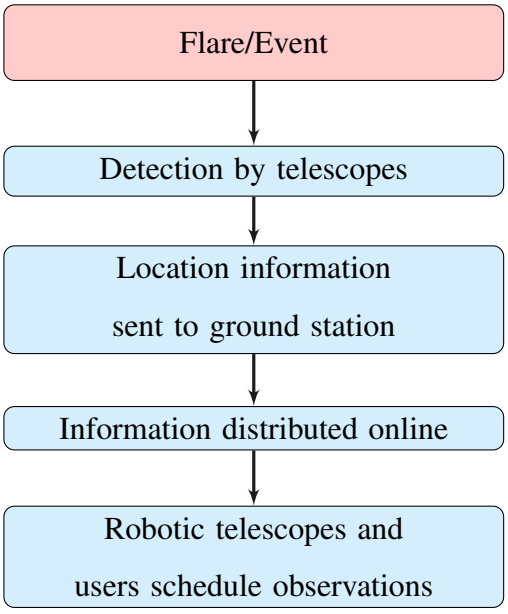

Figure 2.2: Basic description of a transient detection network.

The Astronomers Telegram (ATEL) is another web based short-notice publication system that is used for reporting and commenting on new astronomical observations (*Rut-*

ledge 1998). This system is not as automated as that of the GCN, and still requires a person to write and send the notice to the website. It does however, allow for a greater amount of information to be included in the notice, it is not dependent on one or two energy bands for detections and it isn't focussed on a particular astronomical source like γ–ray bursts.

These communication networks allow simultaneous MWL observations to be made in response to sudden events such as flares in the output of an AGN, supernovae or GRBs. Once the observations have been made, it is then possible for people to collaborate and combine their results to form a full picture of the event at different energies.

2.1.2 Planned Intensive Campaigns

In order to build up a full picture of a source, it is necessary to observe its behaviour for longer periods of time and at times when it is in a quiescent state. Planned Intensive Campaigns (PIC) also permit the best wavelength and temporal coverage for the source. These campaigns involve coordinated observations from ground and space based telescopes over pre-determined lengths of time, and require months of planning to organise.

The coordination required is one of the greatest challenges involved in MWL campaigns. Large numbers of observing proposals are required to request time on the different telescopes. Each of these telescopes has its own observing constraints which need to be taken care of, like different hours of darkness for ground telescopes, different integration times and avoidance of the sun for satellites. The varied data types will involve different data reduction techniques, and the gathering of this data from many sources can introduce large delays.

The nature of the different telescopes used, combined with the difficulties in coordination, means that constant simultaneous observation is not always possible. For example, in the 2009 campaign undertaken by the HESS collaboration to observe PKS 2005-489, the HESS Cherenkov telescopes observed the source, non-continuously, from May 22 to July 2, while the RXTE X–ray telescope only observed PKS 2005-489 on 6 nights for 2-4 ks per pointing, between May 22 and June 3 (*H.E.S.S. Collaboration et al.* 2011).

2.1.3 Multi-Wavelength Campaigns of Other Sources

There is a wide range of sources that are good candidates for MWL campaigns. Sources like γ–ray bursts, pulsars and γ–ray binaries are often the focus of MWL campaigns for a variety of reasons.

One of the primary goals of MWL of transient sources like γ–ray bursts, is the determination of the redshift of the progenitor. The redshift allows for the proper estimation of the physical mechanisms involved, such as the circumburst environment, true energy release and the opening angle of the jet. By observing these sources at multiple wavelengths it is possible to study the population of stars in galaxies that would otherwise not be visible.

Pulsars emit over a wide range of wavelengths, from radio to γ–rays, and often display different behaviour at these wavelengths. The locations of the various emitting regions within the pulsar, and the correlation of the pulsed emission observed at different wavelengths is a common goal of MWL campaigns (*Kisaka and Kojima* 2011).

MWL studies of γ–ray binaries are used to better model the position and rotation of the binary system. For example, in a recent MWL study of the γ–ray binary system PSR B1259-63 (*Chernyakova et al.* 2014), the position of the binary system was constrained to be within a region of $\sim$100 AU.

2.2 Role of Robotic Telescopes

Robotic telescopes (RT) offer full automated control of an observatory and its instruments. The key ability of a robotic system is that it can observe without any human intervention. RTs generate their own observing schedule according to pre-determined criteria and observing conditions.

Research goals that involve long time baselines or rapid response times can be restrained by the inflexibility of larger, more traditional ground based observatories that have limited availability and require human intervention in order to observe a source.

The main advantage of RTs lies in their flexibility, that allows them to efficiently monitor sources for very long periods of time, while still allowing for the rapid response

to a transient source (*Ferrero et al.* 2010). This makes them excellent instruments for the monitoring of blazars.

One of the most important roles for RTs is the supporting of planned satellite observing campaigns. These campaigns are often very long in duration, yet only involve the satellite observing for a short period of time (*Hudec* 2010). RTs are very useful to provide observational coverage for the entire duration of the campaign, in particular in the period directly before and after the satellite observation window.

Monitoring for triggering satellite ToO observations is another role in which RTs excel. RTs can monitor a range of sources, and if there is a detection of brightening in a source, satellites can then be triggered to make further observations.

2.2.1 Watcher

The Watcher robotic telescope is located at the Boyden Observatory in Bloemfontain, South Africa. Watcher is a 40 cm Classical Cassegrain reflecting telescope that is equipped with an Andor iXon electron-multiplying CCD (*French et al.* 2004).

Primary Mirror	40.64 cm
Focal Length	570cm
CCD	Andor iXon+ 888
Field of View	10”$\times$10”
Filters	V, R, v′, r′, i′, clear, Hα, OIII
Mount	Paramount ME

Table 2.1: Watcher Telescope Specifications

Watcher was built by UCD's Space Science Group primarily to observe γ–ray burst afterglows and to provide supporting optical observations for a range of telescopes that operate in the γ–ray (MeV - TeV) and X–ray regions of the spectrum. These telescopes include Fermi, INTEGRAL, Swift, XMM-Newton, NuSTAR and the HESS Cherenkov array.

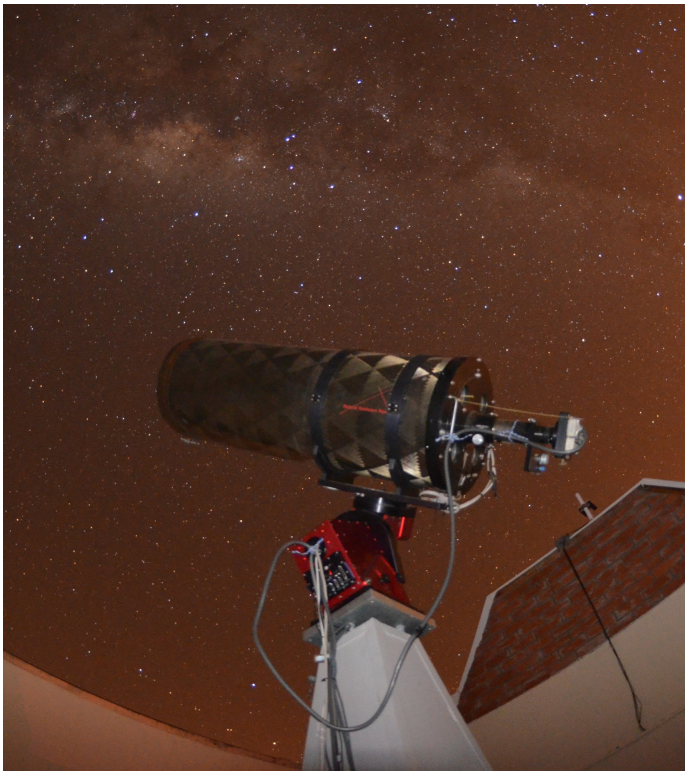

Figure 2.3: The Watcher Robotic Telescope

Given its similar geographical longitude to the HESS array in Namibia, Watcher provides supporting optical observations for several GeV sources as optical variability has been linked to changes in GeV γ–ray emission (*Bonning et al.* 2012; *Chatterjee et al.* 2012). Watcher supports contemporaneous optical/VHE gamma-ray observations to be undertaken to further explore the nature of correlated optical-VHE variability. Furthermore, long term monitoring of specific sources can be used to trigger HESS observations if evidence of flaring is identified in real-time data.

2.3 Conclusions

As detailed in this chapter, performing MWL campaigns is critical for the full understanding of the physics involved in many astronomical sources. Without observations across the entire electromagnetic spectrum it would not be possible to distinguish between several of the emission mechanisms of high energy sources and that the emission could not be accurately modelled or explained.

The careful coordination of these campaigns is essential for their success and the

rapid response to triggers is fundamental in many situations such as blazars and GRBs. In this case, robotic telescopes are a vital tool for the final success of these campaigns. By absorbing most of the observing time needed for detailed monitoring, which is rarely available in large ground-based telescopes, RTs offer the flexibility needed for these campaigns to operate.

Chapter 3

Calibration and Processing of Astronomical Images

In order to produce accurate and scientifically valid results from the images taken by Watcher it is first necessary to process raw images into clean, usable ones from which it is possible to obtain photometric measurements, this is defined as image calibration. The method used for the image calibration is based primarily on that presented in *The Handbook of CCD Astronomy*, by Steve B. Howell (2000).

3.1 Data Reduction

Standard CCD image reduction makes use of a basic set of images that form the core of the calibration and reduction processes. Image reduction refers to the production of corrected and meaningful results the from raw images through calibration. The basic set of images that was used for this body of work consisted of two calibration frames – flat and dark fields.

The image calibration is performed using the Image Reduction and Analysis Facility[1] (IRAF) software package (*Tody* 1993).

[1]IRAF is distributed by the National Optical Astronomy Observatories, which are operated by the Association of Universities for Research in Astronomy, Inc., under cooperative agreement with the National Science Foundation.

3.1.1 Bias Frames

The majority of CCD's are adjusted to produce a non-zero output when the signal from the detector is zero. This is known as the bias level. In order to obtain the bias level, images are taken in total darkness and with an integration time of zero. The bias level should be identical across all pixels since no photo- or thermal electrons are collected and the level arises from the on-chip amplifiers. The CCD read noise can be calculated by simply taking the root mean square (rms) of the bias level. The read out noise of for the Andor iXon CCD used by Watcher is 11.2 e^- per pixel.

It is possible for the bias level to fluctuate in patterned or unpatterned ways. Patterned effects can be caused by light emitting circuitry within the telescope system, and are easily accounted for due to their obvious pattern and presence in every image. Unpatterned fluctuations can be caused by nearby electronics. Although they are typically very small, care should be taken to minimise these effects.

Watcher does not take nightly bias frames as it does not have a shutter available.

3.1.2 Dark Frames

Dark field images, or darks, are images taken in total darkness with an integration time greater than zero, which is ideally the same exposure time as the object images. Dark frames provide a method of recording the thermal noise (dark current) in a CCD, and can also be used to detect 'hot' pixels on the CCD.

The Andor CCD is cooled to $\sim$ -80° C, which means that there is almost no contribution from thermal electrons for integration times longer than zero seconds. Therefore dark frames are used in the calibration of images taken by Watcher, in place of bias frames (Figure 3.1).

In order to obtain darks with Watcher a hood is placed over the telescope to prevent any light from reaching the CCD. Several images are then taken at various different integration times. These images are then averaged with the IRAF *darkcombine* task, using the median value for each pixel. In the case where there are an even number of pixels, the median is taken as the average of the two central values.

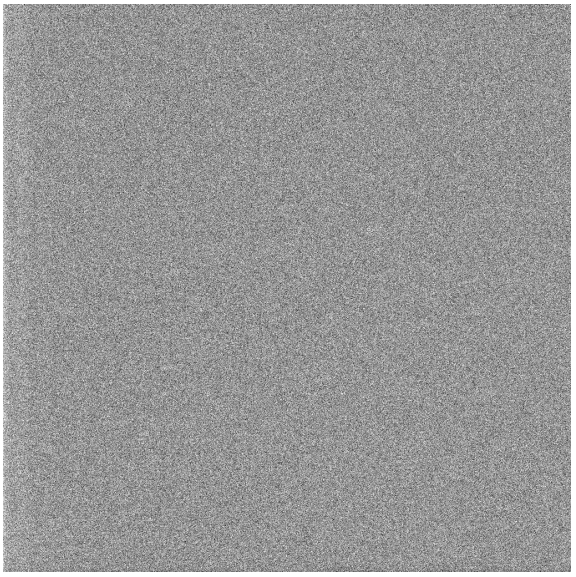

Figure 3.1: Sample dark frame for Watcher (60s integration time). In this image a black pixel represents a value of 398 and a white pixel represents a value of 401. The average bias level derived from the Watcher dark frame is ∼400.

3.1.3 Flat Field Images

Flat-field images, or flats, record the response of the entire optical system, including the telescope, filters, cover glass and the CCD itself (*Berry and Burnell* 2005). Flats are typically taken by either exposing the CCD to an evenly illuminated dome (dome flats) or at twilight or dark sky (sky flats), and in each filter to be used during the observation. This is done to try and achieve a high signal to noise ratio, and a uniformly illuminated calibration image (Figure 3.2). For each night's observing, several flat field images (of the same exposure time and filter) are combined to create a master flat for each filter.

The flats are combined using the *flatcombine* task in IRAF by taking the median of each pixel value similar to the production of the master dark. The final step in producing the master flat is then to subtract the bias level or, in Watcher's case, the master dark from this combined flat.

Watcher uses sky flats for its calibration images as the current set-up is not configured to obtain dome flats. There are risks associated with using sky flats. For example, the images may not be uniformly illuminated due to changing sky brightness, cloud presence or early stars being in the field. This risk is minimized by pointing the telescope in the

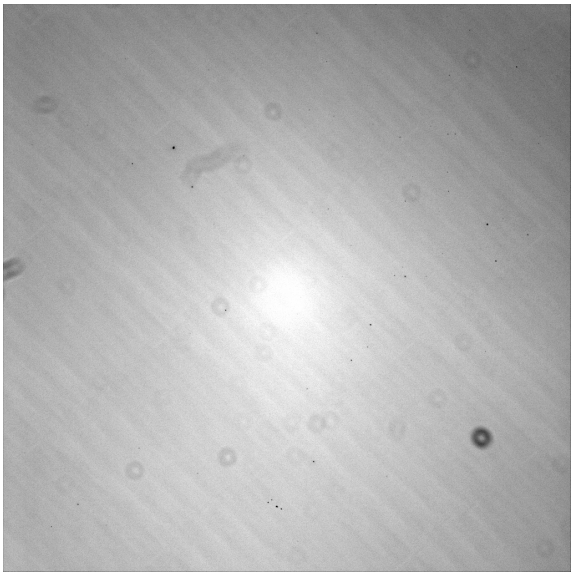

Figure 3.2: Example flat field image for Watcher (V Band). The circular patterns are caused by dust particles in the system. Vignetting and striation effects can be seen clearly.

direction opposite to the setting and rising sun, and by using several different exposure times for each filter.

To create the final calibrated frame, the master dark is first subtracted from the raw object image, and the resulting frame is divided by the master dark in the correct filter. This simple process produces a clean and scientifically usable image. This procedure can be written as:

$$\text{Final Reduced Object Image} = \frac{\text{Raw Object Image} - \text{Master Dark}}{\text{Master Flat}} \tag{3.1}$$

3.2 Aperture Photometry

Photometry is the method of determining the amount of flux emitted by an object as a function of wavelength. In order to obtain reliable photometric results there are three key tasks to perform: *a*) centroiding; *b*) estimation of the background level; and *c*) calculation of the source flux contained within the region of interest.

The region of interest is defined as the collection of pixels that contain the feature or

source that is to be measured. It is typically determined by specifying a central coordinate, and selecting a circular area, or aperture, around this point. Determining the radius of this aperture is a very important part of aperture photometry, and is discussed in greater detail in Section 3.2.3.

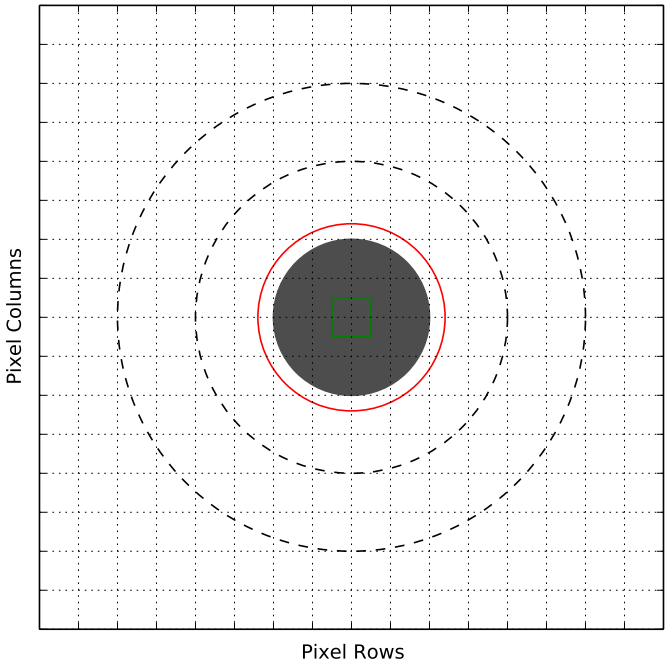

Figure 3.3: Diagram of source on a pixel grid. The centroid is calculated using a small region at the centre of the source (green square). The flux of the source is calculated from the central aperture (solid line). The background level is calculated using the region within the annulus (dashed line).

3.2.1 Centroiding

When given the position of a source it is important to determine the ”centre of mass” in order to maximise the signal to noise ratio when measuring the flux within an aperture. This process is known as centroiding.

This can be done by taking a small region of the source around an initial estimation of the centre and reading intensity values for each pixel into an array (Figure 3.3). The centre of mass of this array can then be calculated. This process is then repeated using the new centre of mass location calculated. An accurate position for the centroid is calculated when the derived position is no longer changing between iterations.

3.2.2 Background Estimation

The background level in an image contains photons from unresolved astronomical sources, instrumental effects such as read noise and thermal dark current and the dispersion of nearby sources in the image caused by atmospheric effects. This level is present in all of the pixels, including those that capture the source of interest, and as such needs to be corrected for before the final flux of a source can be determined.

The background is estimated by placing an annulus around the source of interest and the calculating the average intensity within this annulus, per pixel (Figure 3.3). In order to ensure that the background level is well estimated the annulus typically contains about three times the number of pixels of the source aperture.

3.2.3 Calculation of Flux

With the centroid calculated it is then possible to determine the flux from the source itself using a circular aperture (Figure 3.3), centred on this point. By summing the values from each pixel within this aperture it is possible to calculate an instrumental magnitude for the source.

$$I = S - n_{pix}\bar{B} \tag{3.2}$$

$$\text{Magnitude} = -2.5\log_{10}(I) + C \tag{3.3}$$

Where I is the source intensity (ADU), S is the sum of the pixel values within the aperture (ADU), n_{pix} is the number of pixels in the aperture, $\bar{B}$ is the background level (ADU/pixel) and C is an arbitrary constant used to bring the magnitude to a standard scale (*Johnson and Morgan* 1953; *Strómgren* 1956).

Due to the nature of the pixel array and the circular aperture used, it is not possible to avoid partial pixels from being included in the calculations. For these pixels, the ratio of the area of the pixel outside the aperture to the area inside is used as a weighting scheme for the counts in the partial pixel.

The radius of the aperture is chosen to maximise the signal to noise ratio (S/N) for the measurement of the point source flux, as the S/N ratio is not constant as a function of radius (Figure 3.4). Figure 3.5 shows that for larger aperture sizes, dim sources are

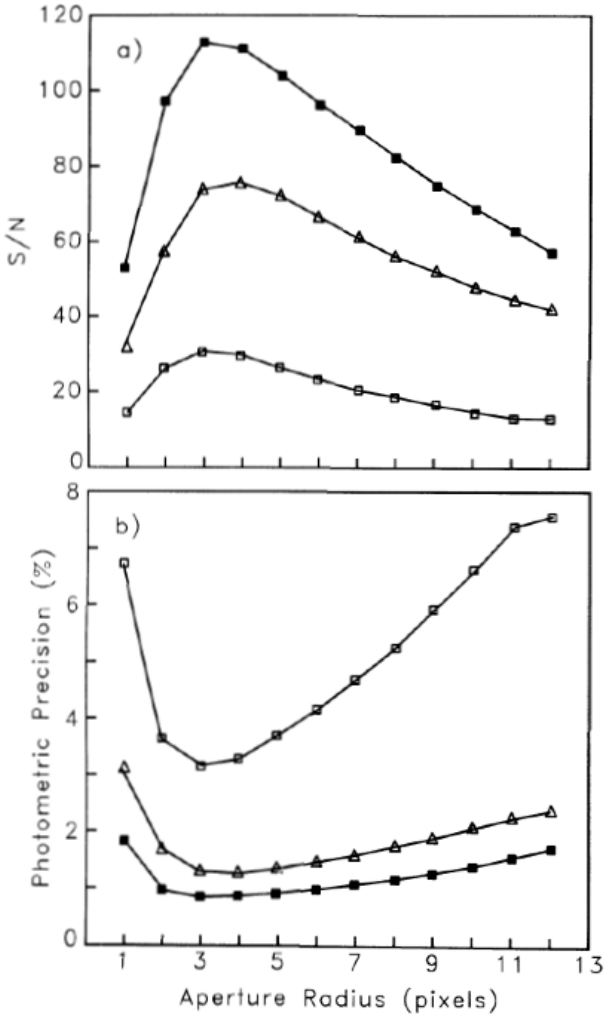

Figure 3.4: The S/N of a source is not constant with aperture radius. The top graph shows this for 3 point sources that differ by 0.3 magnitudes (middle curve, △) and 2.0 magnitudes (bottom curve, □) from the top curve (■). The bottom graph shows the same three stars as a function of photometric precision, *Howell* (1989).

strongly affected by the increased contribution of the background.

Equation 3.4 shows the equation used to calculate the S/N for a source within the aperture.

$$\frac{S}{N} = \frac{N_\star}{\sqrt{N_\star + n_{pix}(1 + \frac{n_{pix}}{n_B})(N_S + N_D + N_R^2 + G^2\sigma_f^2)}} \tag{3.4}$$

$N_\star$ is the total number of photons (ADU) collected from the source itself, or the signal. The term $1 + (n_{pix}/n_B)$ is a measure of the uncertainty introduced by any error in the

background calculation, where n_B is the number of pixels in the background annulus. N_S is the number of photons per pixel from the background (ADU), N_D is the number of dark current electrons per pixel, N_R is the number of electrons per pixel introduced by the read noise, G is the gain of the CCD and $\sigma_f = 0.288675$ and is the error introduced by the A/D converter in the CCD.

The gain of a CCD is the conversion factor of detected photons (photoelectrons) and the number of digital units (ADU).

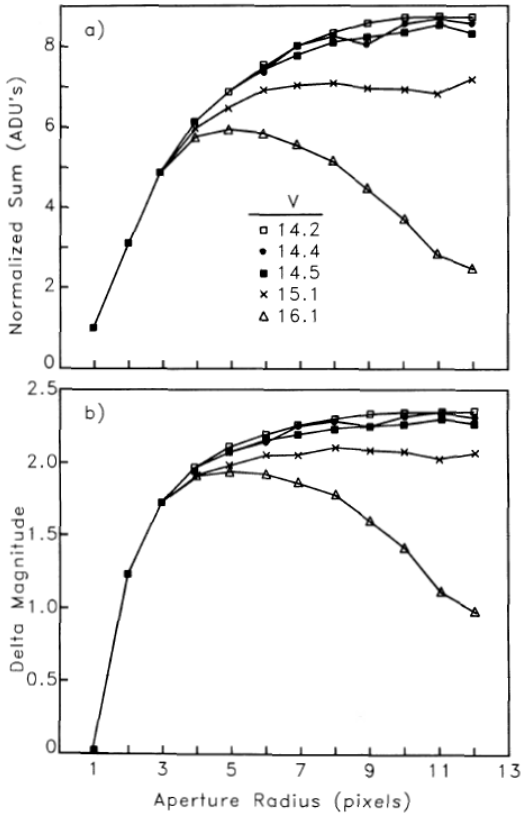

Figure 3.5: Growth curves for five stars on a single CCD frame. The bright stars follow a similar path, but the dimmer stars are strongly affected by the background as the aperture radius increases (*Howell* 1989).

A larger aperture radius collects more signal, but also includes a larger number of pixels, which increases the contribution from the background. In order to calculate the ideal aperture size for a source the pipeline uses a curve of growth method. A range of different radii is tested and the aperture which produces the highest S/N for the source is selected. This is done for each source in an image, as the S/N ratio will depend on the

source magnitude (Figure 3.5).

3.2.4 Differential Photometry

Photometry involves the comparison of the measured flux from one source to the flux of another. 'Absolute Photometry', the comparison is made against a source of known flux to produce an absolute measurement with a physical unit, whereas 'Differential Photometry' is the comparison against an unknown source (in the absolute sense) to produce a relative result. Differential Photometry allows for very high precision measurements to be made.

In CCD astronomy, all of the stars in one image have been observed at the same time, exposure, in the same filter and through the same atmospheric path. This means that the extinction and variations caused by atmospheric effects is the same for all sources in that image. It is for this reason that Differential photometry is so well suited for studies based on variability or colour indices (B - V).

Common practice in Differential Photometry is to compare the source of interest against two (or more) non-varying stars on a frame-by-frame basis, and to also check the two comparison stars by comparing them against each other. This check is done to ensure that the comparison stars are truly non-variable and there is no false detection of variability.

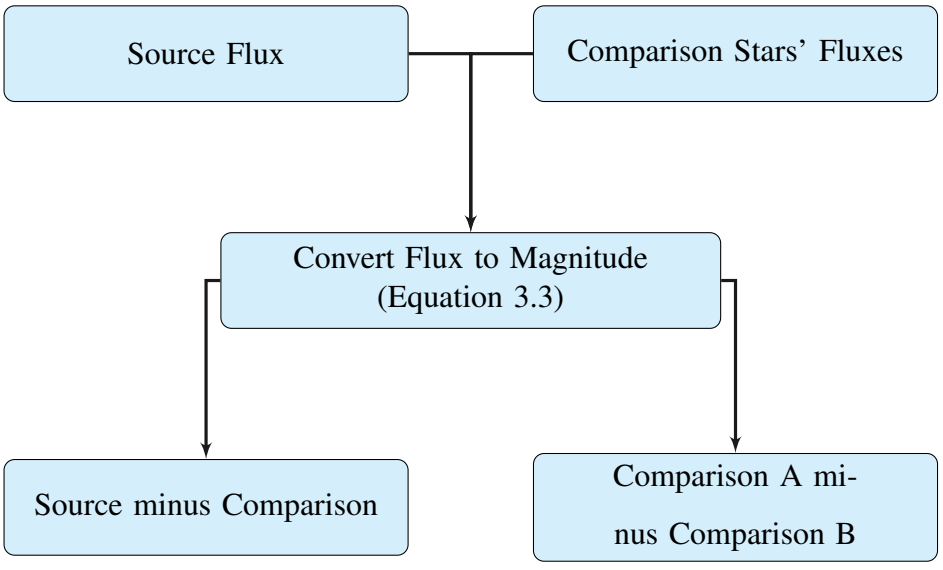

Figure 3.6: Basic description of the Differential Photometry process.

3.2.5 PynAPPle

The **Py**thon **A**perture **P**hotometry **P**ipe**l**in**e** (PynAPPle) is under development in the UCD Physics Space Science group to provide fast photometric analysis of images taken by Watcher, both in real time and for archival images. It is being developed completely in Python in order to reduce the reliance on extra software like IRAF, which often involves difficult installations and complicated dependencies.

PynAPPle currently has two methods of analysing images. The first method allows PynAPPle to connect to any running instance of the DS9[2] image visualisation software. This provides a fully interactive method with which to analyse images within DS9.

The second method uses a customisable configuration file that allows the user to specify specific inputs, actions, and outputs for PynAPPle to perform, which is then run in a terminal environment. Using PynAPPle in this fashion allows for greater flexibility and efficiency in the analysis of images. Custom functions can easily be integrated into the pipeline, such as the variability tests used for this body of work, when it is used in this manner.

The method that PynAPPle uses to analyse images taken by Watcher is as described in this chapter. The data presented in this thesis has been analysed using PynAPPle.

[2] http://ds9.si.edu

Chapter 4

The Watcher Blazar Observing Program

This chapter provides a description of the criteria used to select blazars for the Watcher monitoring programme. Detailed information about the individual targets that were selected as a focus for the monitoring campaign during the austral winter of 2013 is also presented.

A full description of the observations made can be found in Appendix A.

4.1 Target Selection

The sources selected for observation in the Watcher monitoring campaign were chosen from the 2nd Fermi Catalogue (*Ackermann et al.* 2011). The catalogue contains more than 800 blazars that were detected over a 24 month period in the 100MeV – 100GeV range. The wide range of sources detailed in this catalogue provided an excellent basis for the selection of sources to be monitored. The possibility of correlation studies between γ–ray and optical wavelengths was also part of the motivation for using this catalogue. Selection criteria must be applied in order to eliminate those targets which are unsuitable for monitoring by Watcher.

The first constraint on the sample was a declination limit of $\leq 20^{\circ}$. This was enforced to eliminate those targets which would not be visible by Watcher for either a significant portion of the night, or at all. In order to detect intra-night variability it is necessary for

the targets to be visible for a significant portion of the dark hours. This constraint reduced the sample to about 400 blazars.

Secondly, no source dimmer than 14th magnitude (USNO B1 Catalogue) was accepted for monitoring. This constraint was placed in order to ensure good photometric accuracy that is necessary for intra-night variability studies. The magnitude of intra-night variability is typically quite low ($\leq$0.5mag), which means that it is necessary to observe targets with a high signal to noise ratio to maximise the possibility of detecting small amplitude variability.

The list of 10 sources that met these criteria is given in Table 4.1.

Source	Class	SED Class	z	B Mag. *(USNO)*	Observing Season $\geq 30^\circ$
PKS 2005-489	BL Lac	HSP	0.071	11.29	May-Sept
PMN J2022-4513	BL Lac	–	–	13.91	May-Sept
PKS 2155-304	BL Lac	HSP	0.116	12.54	Jun-Oct
AP Librae	BL Lac	LSP	0.048	11.06	Mar-Jul
PMN J0617-1715	BL Lac	LSP	0.098	13.15	Oct-Feb
PMN J0152+0146	BL Lac	HSP	0.08	11.82	Aug-Dec
3C 273	FSRQ	LSP	0.158	13.94	Feb-May
4C +04.77	BL Lac	ISP	0.027	9.98	Jun-Oct
BZB J0912+1555	BL Lac	HSP	0.212	13.46	Dec-Mar
S3 1741+19	BL Lac	HSP	0.083	11.4	May-Jul

Table 4.1: List of observable sources based on the selection criteria. The observing season refers to the time of the year that the source is at least 30° above the horizon.

PKS 2005-489 and PKS 2155-304 were selected as the primary targets for the 2013 austral winter monitoring campaign with Watcher which is the subject of this thesis. They were selected due to their history of variability in multiple wavelengths.

4.2 PKS 2005-489

PKS 2005-489 is one of the brightest BL Lac objects visible in the southern hemisphere (Table 4.1). It was first identified during the Parkes 2.7GHz survey (*Wall et al.* 1975) and is located at α_{J2000} = 20:09:25.35 δ_{J2000} = -48:49:54.3 at a redshift of z = 0.071 (*Falomo*

et al. 1987). PKS 2005-489 is shown marked by a reticule in Figure 4.1. The numbered stars are the comparison stars that are used for photometry (Table 4.2).

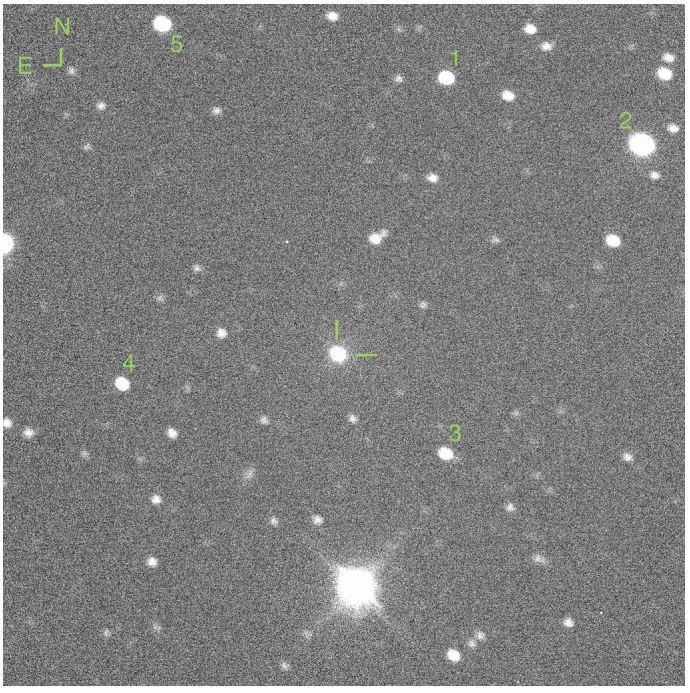

Figure 4.1: Finding chart for PKS 2005-489 (7' × 7'). R Band image taken by Watcher on 12/07/13.

Star	**Identifier**	**B** (mag)	**R** (mag)	**I** (mag)
1	2MASS J20091904-4846431	15.5	13.3	13.42
2	TYC 8400-900-1	12.4	11.4	10.79
3	2MASS J20091767-4850566	15.6	14.3	14.29
4	2MASS J20094003-4850218	15.8	13.7	13.85
5	2MASS J20093867-4846178	14.4	12.9	12.55

Table 4.2: Comparison stars for PKS 2005-489 (*Monet* 1998)

Historically, PKS 2005-489 has exhibited extensive variability at numerous wavelengths, this behaviour is one of the primary reasons for this source being selected for monitoring by Watcher.

Perlman et al. (1999) first reported on an X–ray flare detected and monitored by the Rossi X–ray Timing Explorer (RXTE), during which the peak in activity was observed to reach 30 times the quiescent flux level. Very high energy (VHE) γ–rays were first

detected from PKS 2005-489 by the HESS Cherenkov telescopes in 2004 (*Aharonian et al.* 2005a), making it the second such AGN in the southern hemisphere to be detected at these energies. The first AGN that was detected at VHE in the southern hemisphere, by the University of Durham Mark 6 γ–ray telescope, was PKS 2155-304 (*Chadwick et al.* 1999).

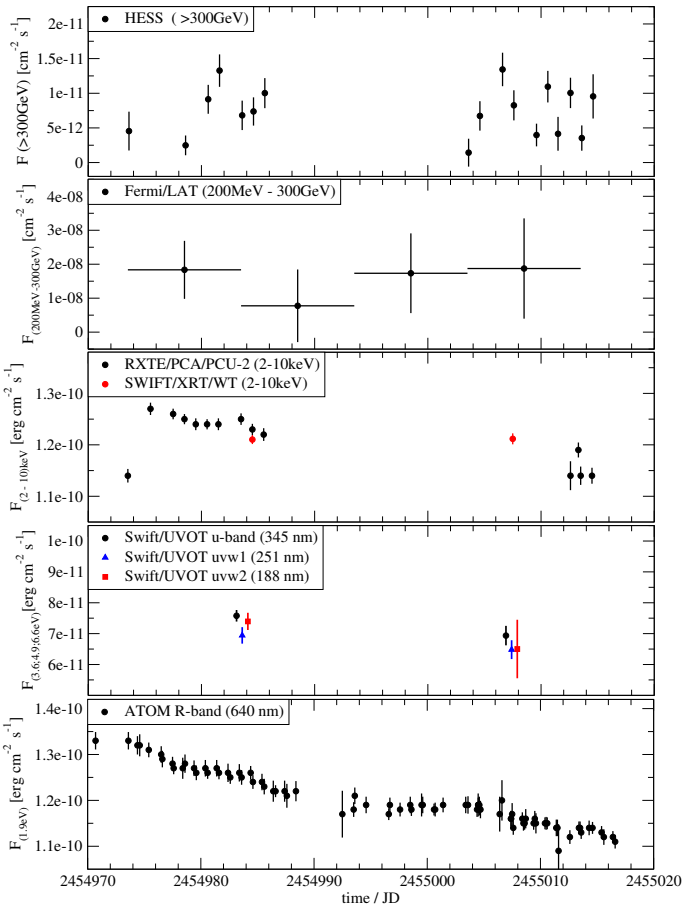

Figure 4.2: Lightcurves of PKS 2005-489 during the HESS MWL campaign from May 22 to July 2, 2009. The HESS, RXTE and Swift lightcurves are shown in nightly binning and the Fermi/LAT lightcurve is shown in a 10 day binning (*H.E.S.S. Collaboration et al.* 2011).

Since then PKS 2005-489 has been the focus of several multi-wavelength (MWL) monitoring campaigns by the HESS collaboration. PKS 2005-489 was monitored in multiple wavelengths between 2004 and 2009 with simultaneous observations by both space and ground based telescopes including Fermi/LAT, XMM-Newton, RXTE, Swift, HESS, the Automatic Telescope for Optical Monitoring (ATOM) and the Robotic Optical

Transient Search Experiment (ROTSE) (*H.E.S.S. Collaboration et al.* 2010, 2011). The lightcurves for this time period are shown in Figure 4.2.

The regular optical monitoring performed by both ATOM and ROTSE has confirmed that variability on the scale of years is present in PKS 2005-489 as well as some smaller variability on a monthly time scale. The peak in the flux observed in 2005 was followed by a slow decline for ∼1.5 years before rising again to similar peak levels in 2009 (*Kaufmann et al.* 2009).

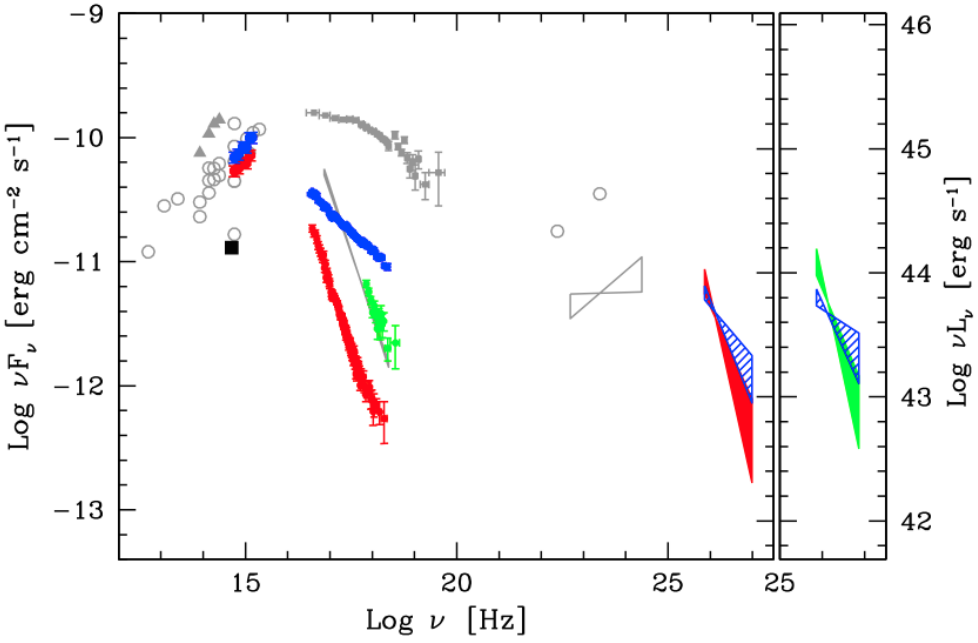

Figure 4.3: SED for PKS 2005-489 at different times and states (*H.E.S.S. Collaboration et al.* 2010). This SED shows archival BeppoSAX data (grey), data measured by XMM-Newton on Oct. 4, 2004 (red filled circles), Sept. 26, 2005 (blue filled circles) and also from RXTE in Aug.-Sept. 2005 (green filled circles). The bow-ties represent data from Fermi (grey open bow-tie) and HESS in 2004 (red filled bow-tie) and in 2005 (blue hatched bow-tie). The right hand sub-plot depicts the HESS spectrum in 2005, divided into two subsets: before the XMM pointing (green filled bow-tie) and during the XMM epoch (blue hatched bow-tie). The flux in the R band from the host galaxy is plotted as a filled black square.

The HESS Collaboration (2010) assembled the SED of PKS 2005-489 with data taken during 2004 and 2005 (Figure 4.3). The SED appears to show the typical double humped nature that is associated with HBL type blazars, with a peak in the UV–soft X–ray band. In the 2004 dataset, the X–ray spectrum is characterized by the lowest flux that has ever been recorded for this source (*H.E.S.S. Collaboration et al.* 2010). As a result of this it

is possible for the onset of the inverse-Compton emission to be observed in the SED as a slight concavity as the spectrum hardens at $\sim 10^{18}$ Hz. This is typically not visible in the SED of HBL blazars due to the dominance of the synchrotron emission from high-energy photons at these energies.

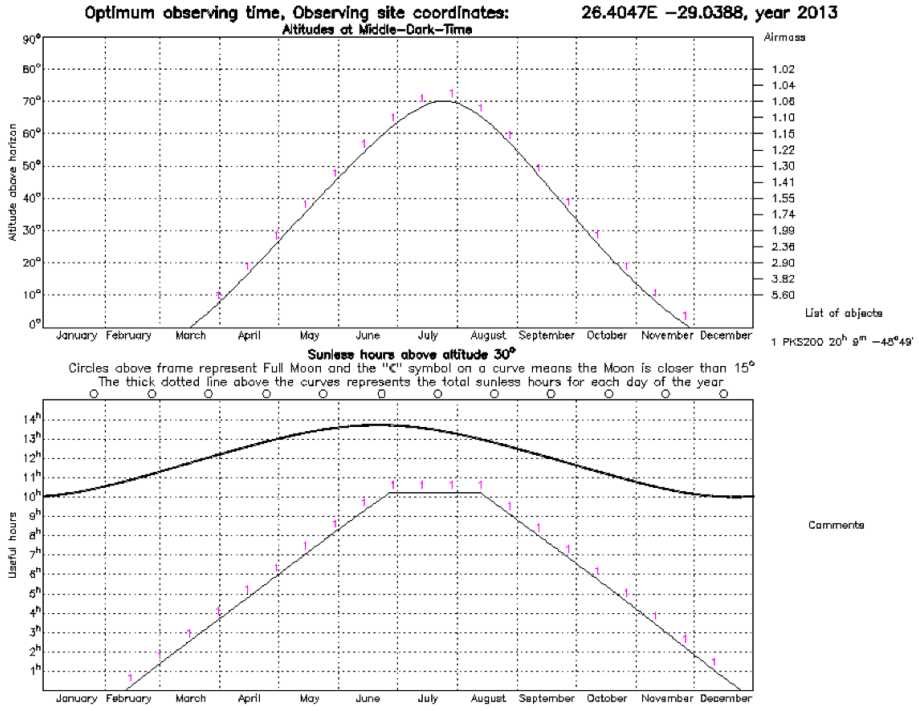

Figure 4.4: Visibility chart of PKS 2005-489 from Boyden Observatory

The visibility of PKS 2005-489 from the Boyden observatory for 2013 is shown in Figure 4.4. The altitude of the source above the horizon, at the middle dark time of the night, is shown for 2013 in degrees and as a function of the airmass in the upper plot. The thin black line in the lower plot shows the number of sunless hours the source spent above 30° over the course of the year, corresponding to an airmass of ≤ 2. The thick black line represents the total number of sunless hours for each day of the year.

4.3 PKS 2155-304

PKS 2155-304 is a HBL source discovered by the HEAO 1 X–ray satellite (*Griffiths et al.* 1979). It is one of the optically brightest AGN that is visible in our skies and was the first AGN with confirmed VHE emission in the southern hemisphere (*Chadwick et al.* 1999).

It is located at α_{J2000} = 21:58:52.065 δ_{J2000} = -30:13:32.12 at a redshift of z = 0.116 (*Falomo et al.* 1987). PKS 2155-304 is shown marked by a reticule in Figure 4.5, the numbered stars are the comparison stars that are used for photometric calculations (Table 4.3).

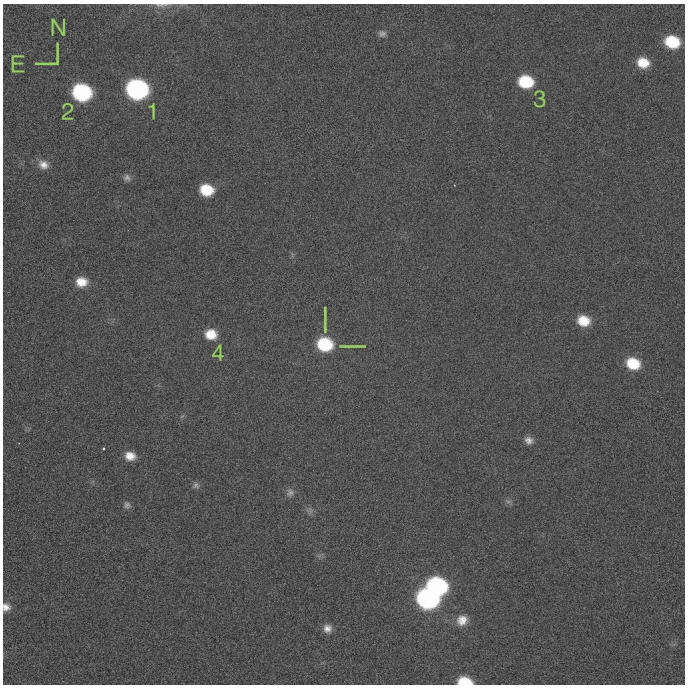

Figure 4.5: Finding chart for PKS 2155-304 (7' × 7'). R Band image taken by Watcher on 11/07/13.

Star	**Identifier**	**V** (mag)	**R** (mag)	**I** (mag)
1	TYC 7488-3401-1	12.05	11.67	11.3
2	2MASS J21590534-3010510	13.00	12.47	12.02
3	2MASS J21584233-3010274	14.28	13.92	13.56
4	STAR 21585788-3013272	15.35	15.01	14.69

Table 4.3: Comparison stars for PKS 2155-304 (*Hamuy and Maza* 1989)

Due to its history of strong variability at optical, radio, X–ray and γ–ray energies (*Patiño-Álvarez et al.* 2013; *Lenain et al.* 2008), PKS 2155-304 was one of the primary sources selected for monitoring with Watcher. PKS 2155-304 has been included in many MWL monitoring campaigns involving a wide variety of different instruments including the Hartebeesthoek Radio Astronomy Observatory (HartRAO), Nançay decimetric Radio

Telescope (NRT), Australia Telescope Compact Array (ATCA), Swift, ATOM, Chandra, RXTE, Fermi and HESS (*H.E.S.S. Collaboration et al.* 2012).

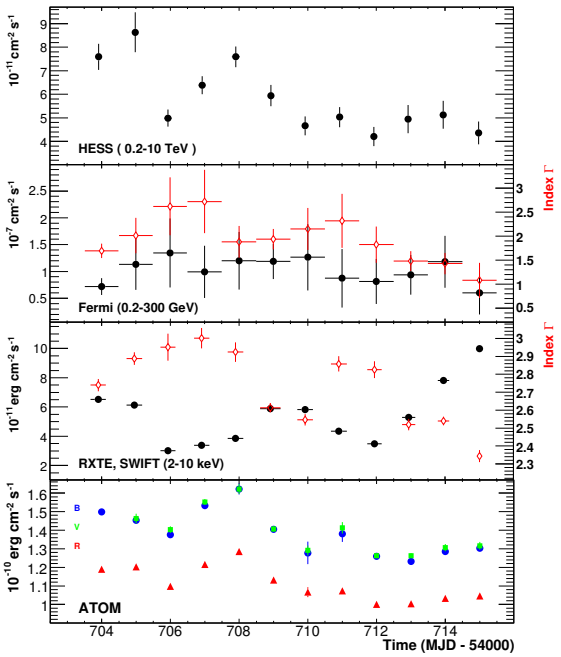

Figure 4.6: Lightcurves for PKS 2155-304 from Aug. 25 - Sept. 6, 2008 (*Aharonian et al.* 2009). The Fermi and RXTE/Swift panels also show the spectral index measurements (red empty circles) for each night

PKS 2155-304 was monitored by BeppoSAX between 1996 and 1999, during which X–ray variability on the scale of ∼1h was observed (*Zhang et al.* 2002). Then in November of 2007, an outburst from PKS 2155-304 was detected in both X–rays and γ–rays by BeppoSAX, RXTE and the Energetic Gamma Ray Experiment Telescope (EGRET). During the following years, it remained in a low state of activity, with no γ–ray detection above 420 GeV (*Nishijima* 2002).

The HESS collaboration confirmed PKS 2155-304 as a TeV γ–ray source based on observations made during 2002 and 2003 (*Aharonian et al.* 2005b), with a detection with a significance of 45σ at energies in excess of 160 GeV. The first MWL campaign of PKS 2155-304 was begun in 2003 including optical observations from ROTSE. This campaign found intra-night variability to be present in the VHE and X–ray band, with the shortest time scales being detected at ∼25 min by RXTE. The optical band showed some intra-night variability over the course of the campaign, despite having only a moderate change

in overall flux output (*Aharonian et al.* 2005c).

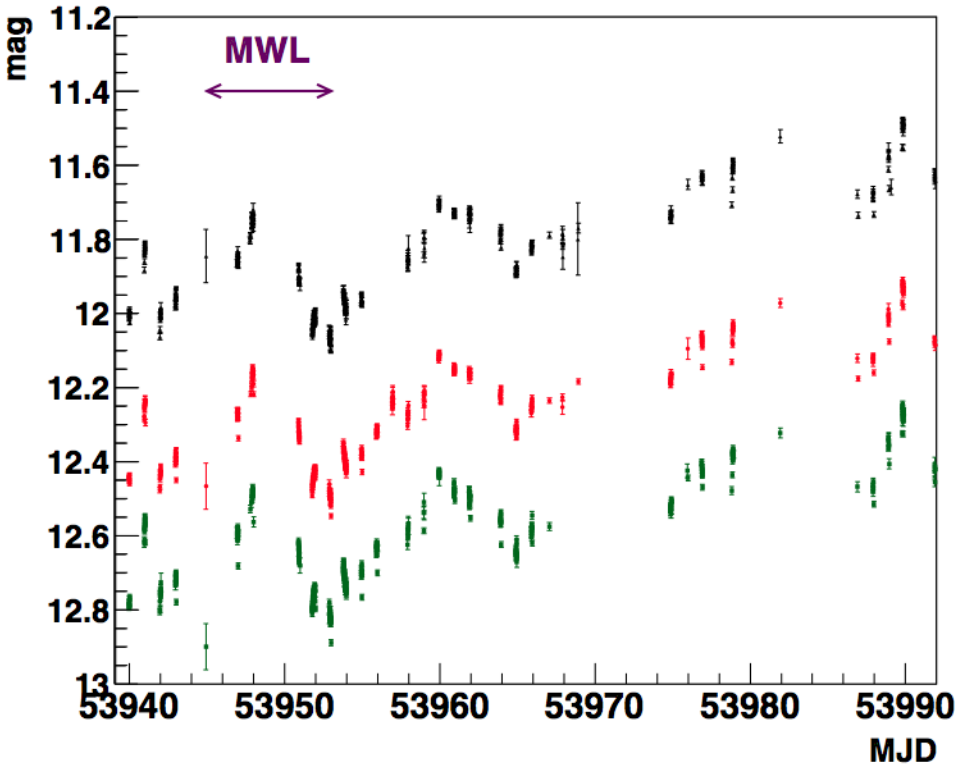

Figure 4.7: Watcher optical light curves for the 2006 flare of PKS 2155-304, I band (upper points; black), R band (middle points; red) and V band (lower point; green). The arrow indicates the interval of the MWL campaign (*H.E.S.S. Collaboration et al.* 2012).

In July of 2006, PKS 2155-304 underwent a spectacular flaring event, with an overnight increase in γ–ray flux that was measured at over 20 times the typical level along with variability time scales down to 200s (*Aharonian et al.* 2007). This flare prompted a full two week MWL monitoring campaign with optical observations being provided, in part, by Watcher. Figure 4.7 shows the Watcher light curves in the R, V and I bands for this flaring period. The intra-night variations that were observed during the campaign were on the order of $\simeq$0.1mag, and were present for several months after the flare. The amplitude of the observed optical variability is similar to that seen during a low state of activity (*H.E.S.S. Collaboration et al.* 2012).

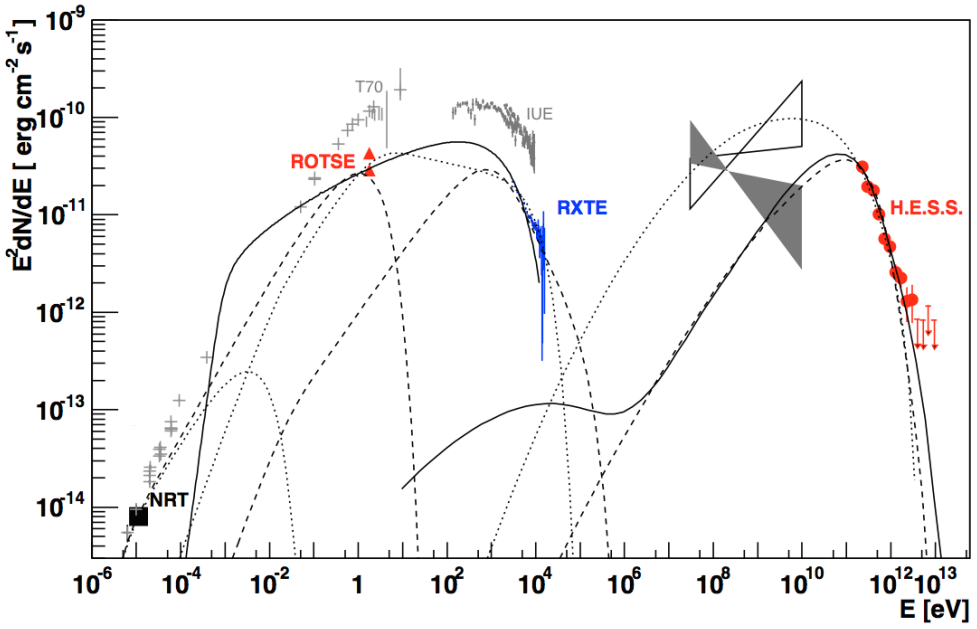

Figure 4.8: SED for PKS 2155-304 modified from *Aharonian et al.* (2005c). The grey points correspond to data that was taken separately from the 2003 MWL campaign. Archival EGRET data from the third EGRET catalogue is shown by the shaded bow-tie (*Hartman et al.* 1999), and the unshaded bow-tie represents the EGRET data from a very high γ–ray state, as described in *Vestrand et al.* (1995). The dotted and dashed lines are the same leptonic model with different assumptions for the source of the emission. The solid line describes the hadronic model for the SED.

Figure 4.8 shows the spectral energy distribution for PKS 2155-304, based on the 2003 MWL observations made by the HESS collaboration (*Aharonian et al.* 2005c). Despite more recent campaigns being completed, this SED shows the greatest detail across the largest range of energies for this source. The coloured data points (NRT, ROTSE, RXTE, HESS) show the results of this particular MWL campaign. The NRT radio point (filled square) is the average value for the observations carried out between October and November of 2003, while the grey data from BeppoSAX represents the high state that was observed in 1997 (*Chiappetti et al.* 1999). The two data points from ROTSE (red triangles) are the highest and lowest measurements made for this time period.

The broadband spectral morphology of PKS 2155-304 is typical of the BL Lac type, showing the double-humped structure corresponding to a low-energy and high energy component (Figure 4.8). Current models suggest that the low-energy component is dominated by synchrotron radiation from non-thermal electrons emitted in collimated jets, whereas the source of the higher energy emission can be described by multiple models.

The dotted line in Figure 4.8 describes the leptonic model of synchrotron self-Compton (SSC) scattering, which assumes a common origin for the optical and X–ray synchrotron emission. The dashed line shows the same leptonic model with the assumption that the optical emission originates in the core of the jet (see Section 1.3.2). The hadronic model is shown in the solid line in Figure 4.8 (see Section 1.3.3). This model assumes that the observed γ–ray emission is initiated by accelerated protons interacting with ambient matter.

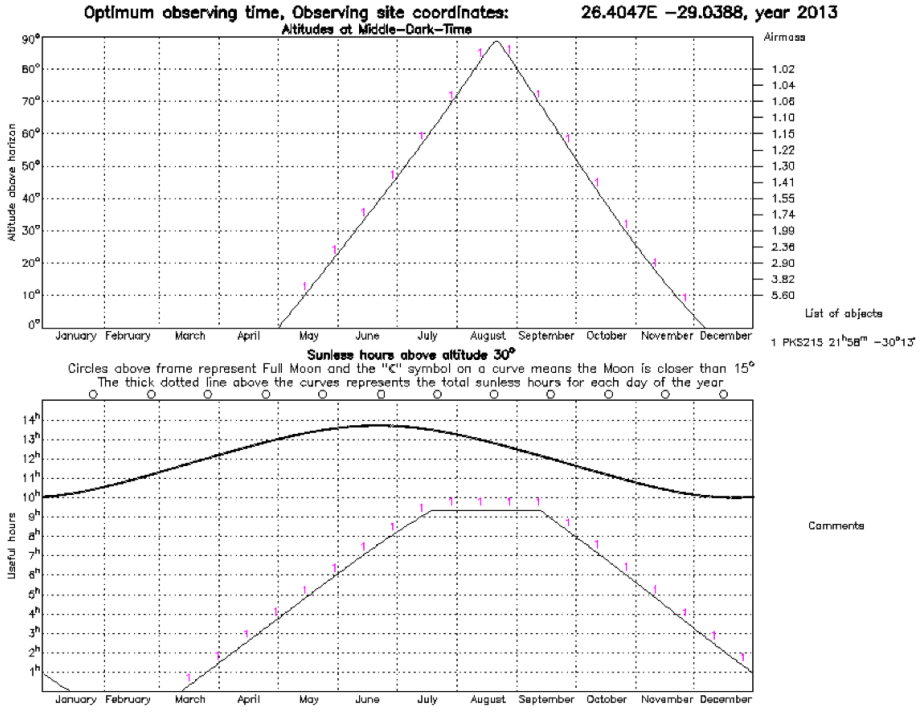

Figure 4.9: Visibility chart of PKS 2155-304 from Boyden Observatory

Figure 4.9 shows the visibility of PKS 2155-304 from Boyden for 2013. The top plot shows the altitude, in degrees above the horizon (left axis), of the source at the middle dark time over the course of the year and shows the airmass for this point on the right axis. The thin black line in the lower plot shows the number of sunless hours the source spends above 30°, which corresponds to an airmass of $\sim$2. The thick black line represents the total number of sunless hours for the year.

4.4 Conclusions

Ten sources were selected from the 2nd Fermi Catalogue as a part of a new blazar monitoring programme with the Watcher telescope. The sources were selected based on their optical brightness and declination, such that they were visible to Watcher, and provided a high enough SNR sufficient for high accuracy photometry. During the austral winter of 2013, the two sources PKS 2005-489 and PKS 2155-304 were observed on a near nightly basis with the V, R and I filters. These sources were chosen as the focus for the austral winter as they have displayed variability across the entire electromagnetic spectrum, and are common targets of MWL campaigns involving ground and space-based telescopes.

Chapter 5

Results

This chapter details the results of the Watcher blazar monitoring campaign during the austral winter of 2013. The two blazars, PKS 2005-489 and PKS 2155-304, were the focus of the monitoring campaign during this period. PKS 2005-489 was observed on 56 nights, while PKS 2155-304 was observed on 68 nights over the course of the campaign.

A sample set of the differential lightcurves for PKS 2005-489 and PKS 2155-304 is presented Appendix B[1]. The gaps that appear in some of the lightcurves are caused by automatic dome closures to prevent Watcher from being damaged by rain or wind. Full details of the nightly observations for each source are presented in Appendix A.

For each night of observations the lightcurves were tested for variability using both the C-test and F-test (Section 5.1). Variability is said to be present where both tests detected a signal greater than 3σ. Nights with fewer than 10 images were excluded from the analysis, due to the increased likelihood of a false detection with a small number of observations.

5.1 Variability Tests

The unpredictable and non-periodic nature of AGN variability and the difficulty of obtaining confirmation by other observers means that claims of variability are often met with scepticism (*de Diego* 2010). In order to increase the confidence in the detection of variability, several statistical tests are applied to the data.

[1]The full database of nightly lightcurves can be found at www.watchertelescope.ie/files/petetisdall/AppendixB.pdf

The first statistical test of variability used in this body of work is the C-statistic, which is a simple comparison of the standard deviations of the source and a reference star (*Jang and Miller* 1997):

$$C = \frac{\sigma_T}{\sigma} \tag{5.1}$$

where σ_T is the standard deviation of the target differential lightcurve and σ is the standard deviation of the reference star differential light curve. The adopted criterion for variability requires that for a variable source $C \geq 3$. This corresponds to a 99.73% confidence level of variability detection.

The second statistical test used is a comparison of the variances for the target and for a non-variable reference source and is known as the *F*-test (*Howell et al.* 1988):

$$F = \frac{s_T^2}{s_\star^2} \tag{5.2}$$

where s_T^2 and $s_\star^2$ refers to the sample variance of the target source and reference star instrumental light curve respectively. This is then compared against a critical value, $F_{\nu_T,\nu_\star}^{(\alpha)}$, where α is the significance level set for the test. Here, ν is the degrees of freedom involved, and is typically $\nu = N - 1$ where N is the number of images in the data set (*de Diego* 2010).

Simulated lightcurves were created with no variability, and statistical variation based on the average standard deviation of the observed reference stars, and with a range of different 'images' (5 - 30). This was done to verify the validity of the statistical tests and to investigate the likelihood of a false detection due to, for example, a small number of images. These lightcurves were then simulated 50,000 times and the distribution of the C-test values for different numbers of 'images' are plotted (Figure 5.1).

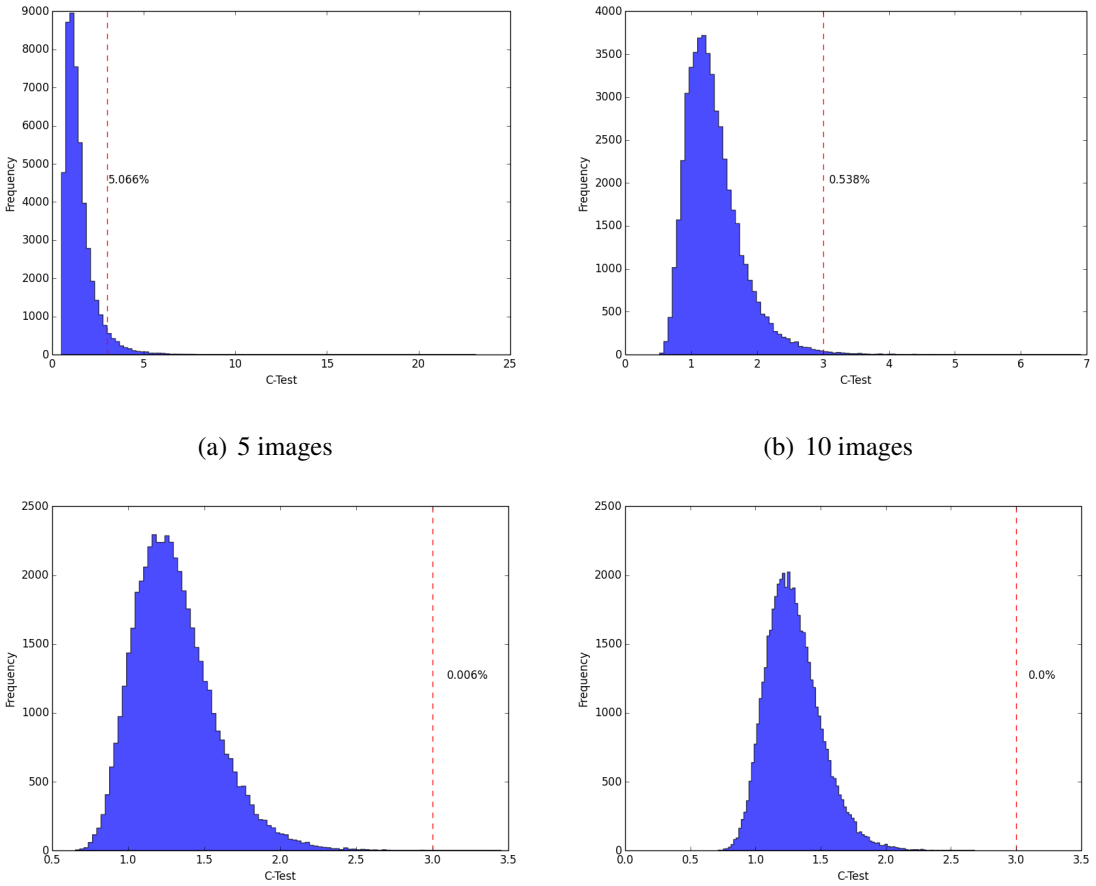

(a) 5 images

(b) 10 images

(c) 20 images

(d) 30 images

Figure 5.1: C-test values for simulated light curves with a varying range of data points. The dashed red line indicates the point of a 3σ detection. The false detection rate is shown as the percentage of the histogram that lies beyond this point.

Figure 5.1 demonstrates the sensitivity of the C-test to sample size. For the simulated lightcurves with only 5 data points, there is a 5% chance of a false detection of variability with this test. This demonstrates the importance of having a well-sampled source in order to accurately verify any observed variability.

Similar simulations were run to investigate the effect of sample size variations on the F-test. The light curves that were simulated for these tests were created using the same standard deviation for both the source of interest and the reference star, such that there is no differences in the variance of the sources. The distribution of the F-test values for various sample sizes is shown in Figure 5.2.

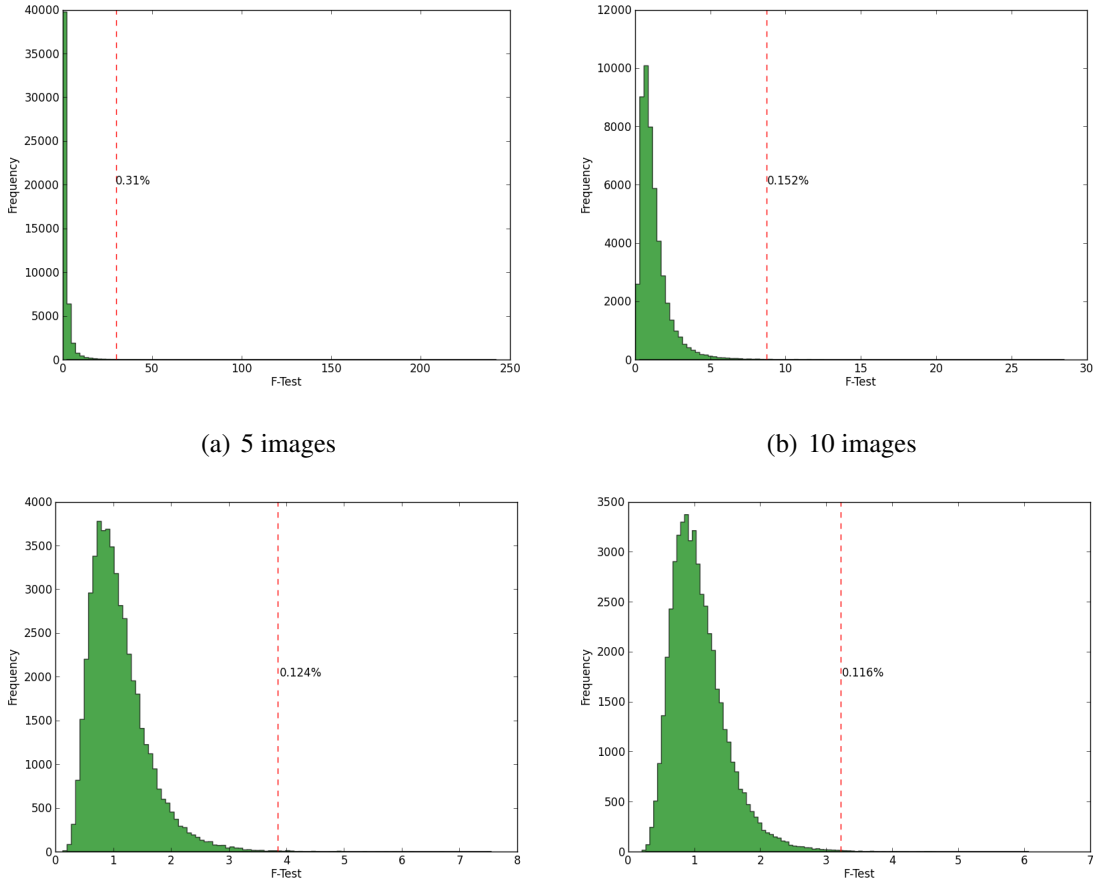

(a) 5 images

(b) 10 images

(c) 20 images

(d) 30 images

Figure 5.2: F-test values for simulated light curves with varying numbers of 'images'. The dashed red line indicates the point of a 3σ detection ($F_{crit}^{(0.001)}$). The false detection rate for this number of images is shown as the percentage of the histogram that lies beyond this point.

The F-test is considerably less sensitive to small sample sizes than the C-test. For a simulated lightcurve with 5 images there is only a 0.31% chance of a false positive detection of variability when there is no distinct variability present.

From the results of these simulations, any nights with detected variability, and with fewer than 10 observations were ignored.

5.2 PKS 2005-489

PKS 2005-489 was quite active and exhibited variability on multiple occasions during the observing period of July – October 2013. Unfortunately there was no gamma-ray

data available from Fermi during this time period for comparison. A summary of the observations in which variability was detected is given in Table 5.1. The lightcurves for those nights with detected variability are presented in Figures 5.3 – 5.26, along with the distribution of C-test and F-test values for the simulated lightcurves for each night in question. The error bars for the points are smaller than the markers. The complete set of observations made is presented in Appendix A

Date	Filter	Observations	C-test	F-test	F Critical Value
2013-07-12	I	100	3.28	2.003	1.87
2013-07-31	I	53	3.20	2.67	2.38
2013-08-02	I	88	3.65	2.98	1.95
2013-08-22	R	160	3.24	2.39	1.64
2013-09-30	I	38	3.85	3.81	2.81
2013-09-30	V	37	4.06	5.6	2.85
2013-10-01	I	37	3.36	4.94	2.85
2013-10-01	R	38	3.76	4.51	2.81
2013-10-07	R	35	4.19	7.78	2.94
2013-10-09	R	17	3.05	6.73	4.93
2013-10-13	I	23	3.08	4.27	3.98
2013-10-17	I	20	3.2	7.87	3.86

Table 5.1: Nights of observed variability in PKS 2005-489.

The C-test was performed using the comparison stars provided in the USNO 2.0 catalogue (*Monet* 1998). In order to verify the validity of the C-test result the test was also performed using only the comparison stars.

The first two reference stars (2MASS J20091904-4846431 and TYC 8400-900-1) displayed no variability and were used to test the remaining comparison stars in the field. The result of this test indicated that two of the comparison stars (2MASS J20091767-4850566 and 2MASS J20094003-4850218) were exhibiting some variability, meaning that they could not be used for differential photometry. The final comparison star in the field (2MASS J20093867-4846178) was typically very close to the edge of the field of

view and was not consistently in the image frame. For this reason, it could not be used for the purpose of differential photometry.

Number	Comparison Star *Identifier*	R *Magnitude*	I *Magnitude*	Comments
1	2MASS J20091904-4846431	13.3	13.42	Non variable
2	TYC 8400-900-1	11.4	10.79	Non variable
3	2MASS J20091767-4850566	14.3	14.29	Variability detected
4	2MASS J20094003-4850218	13.7	13.85	Variability detected
5	2MASS J20093867-4846178	12.9	12.55	Unreliable in frame

Table 5.2: Summary of comparison stars for PKS 2005-489 (*Monet* 1998)

For each night with detected variability, lightcurves were simulated 50,000 times using the same number of images as were obtained that night. For each simulation the C-test was calculated. The actual C-test value for the night was compared against the distribution of these values in order assess the probability of the C-test value arising due to a statistical fluctuation.

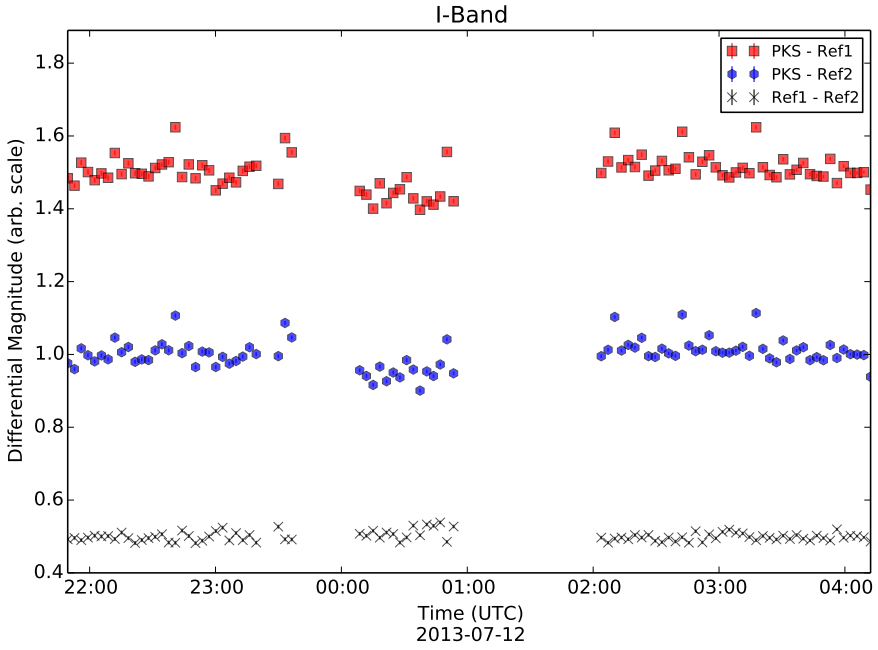

Figure 5.3: PKS 2005-489 I-Band Differential Lightcurve for 12/07/13

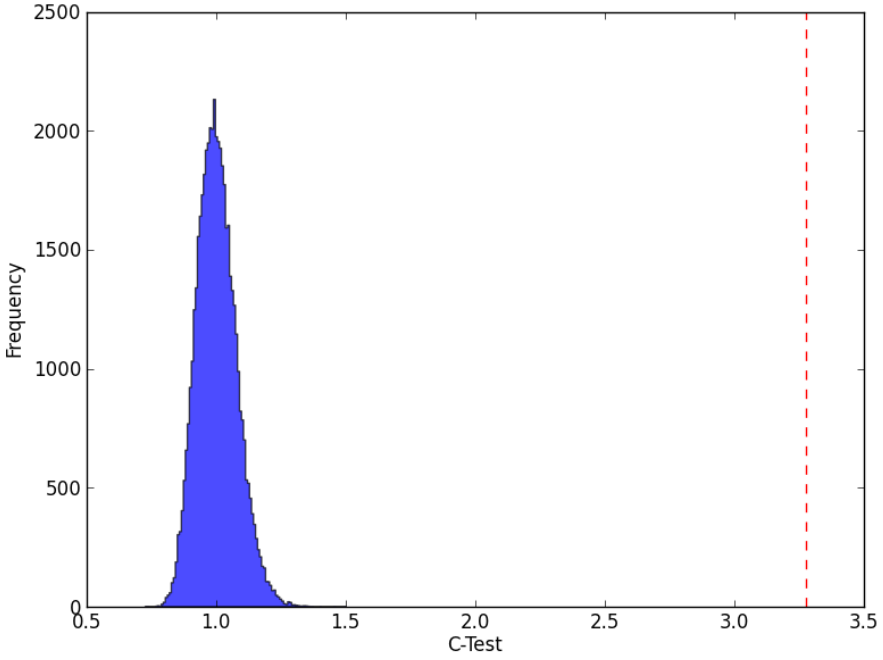

Figure 5.4: Distribution of C-test values for simulated lightcurves based on the observations of 12/07/13. The red dashed line indicates the calculated C-test value for this night.

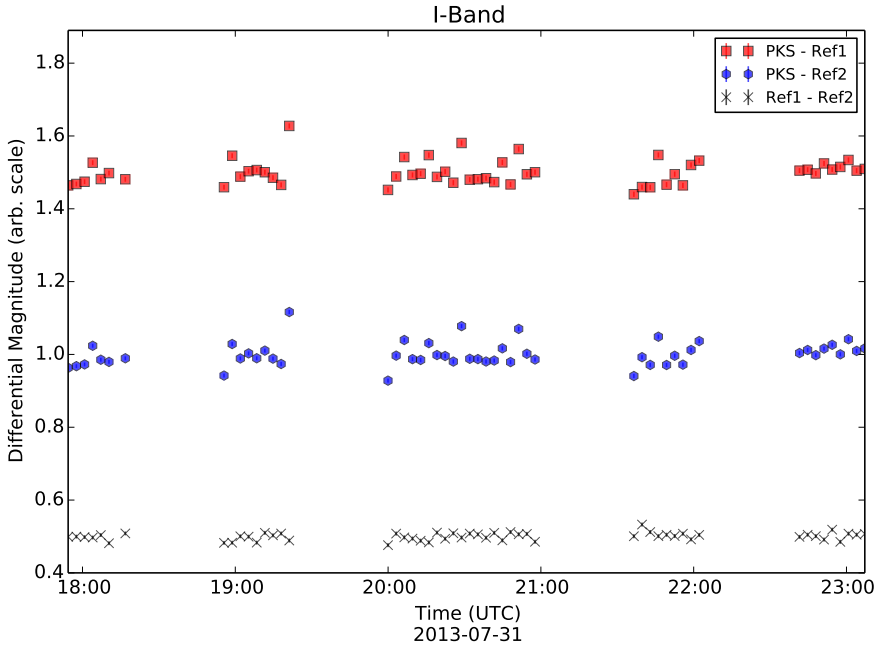

Figure 5.5: PKS 2005-489 I-Band Differential Lightcurve for 31/07/13

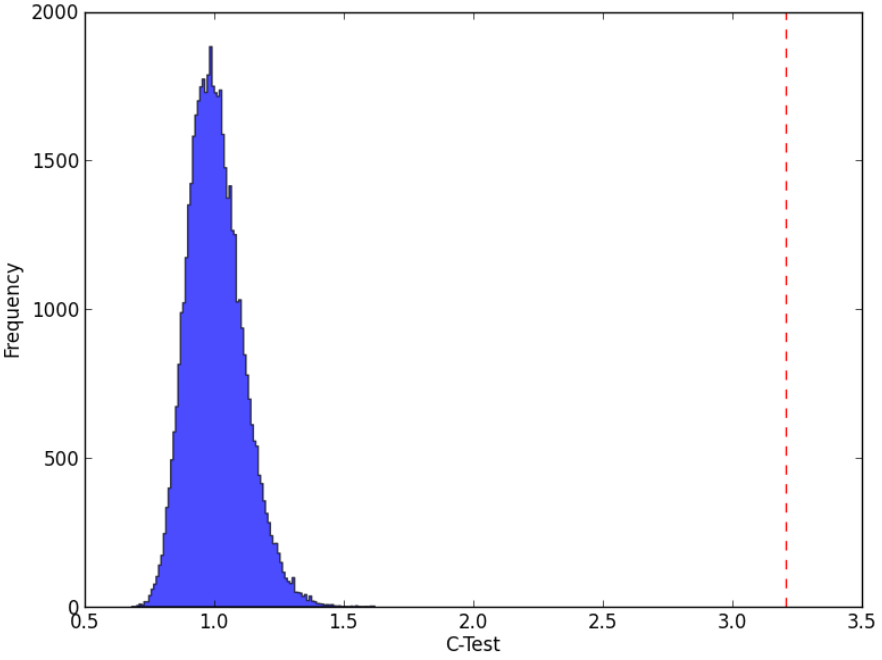

Figure 5.6: Distribution of C-test values for simulated lightcurves based on the observations of 31/07/13. The red dashed line indicates the calculated C-test value for this night.

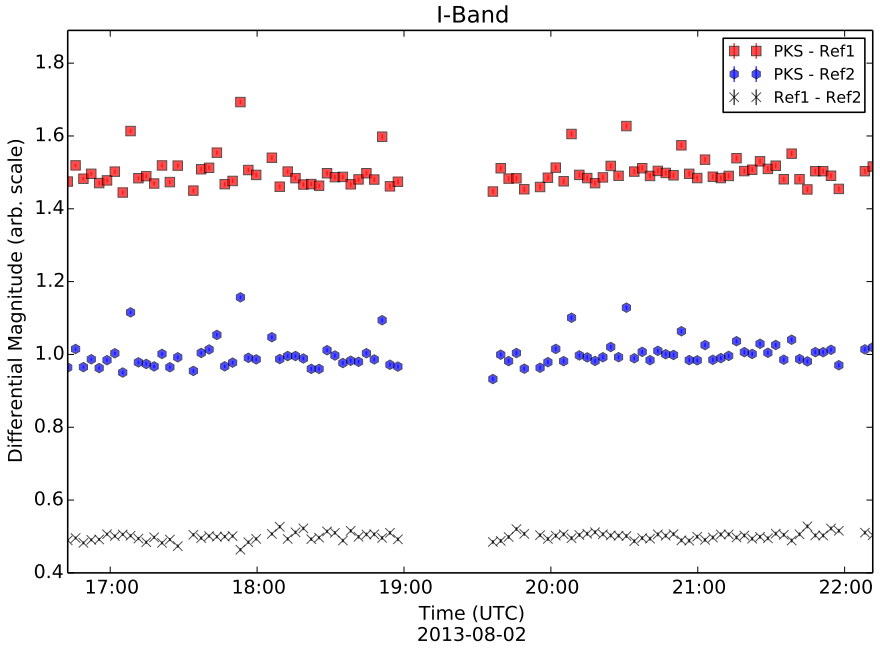

Figure 5.7: PKS 2005-489 I-Band Differential Lightcurve for 02/08/13

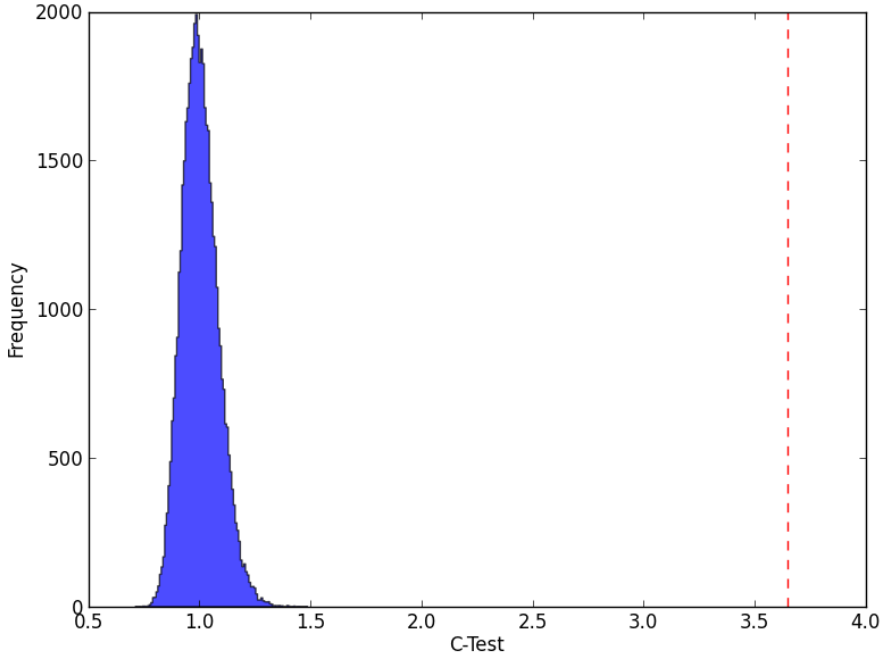

Figure 5.8: Distribution of C-test values for simulated lightcurves based on the observations of 02/08/13

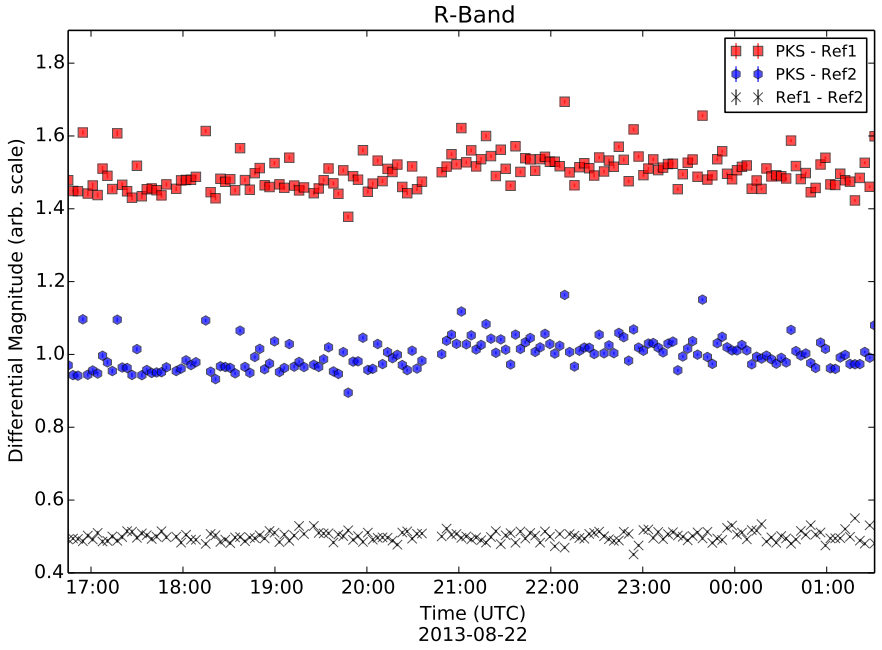

Figure 5.9: PKS 2005-489 R-Band Differential Lightcurve for 22/08/13

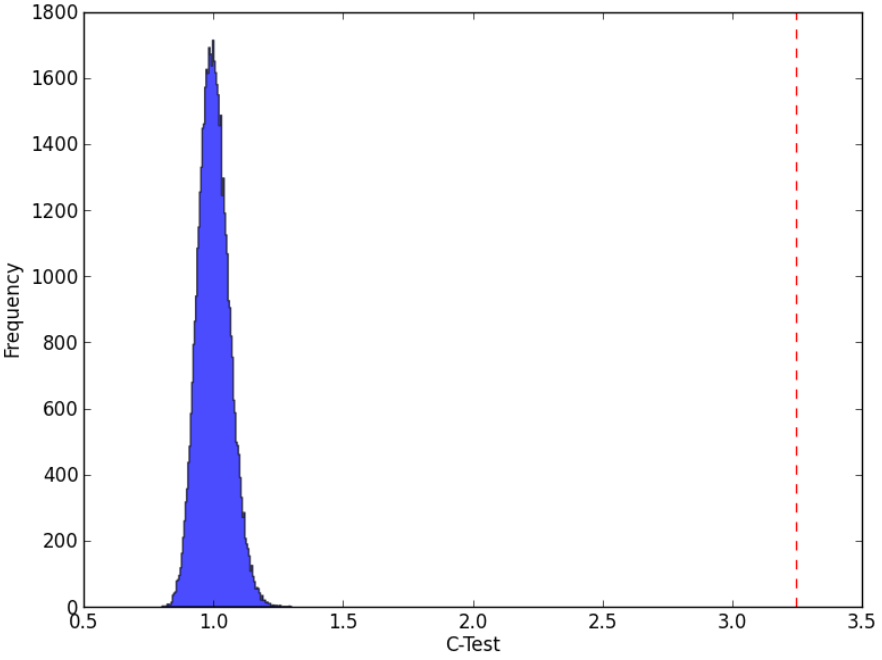

Figure 5.10: Distribution of C-test values for simulated lightcurves based on the observations of 22/08/13.

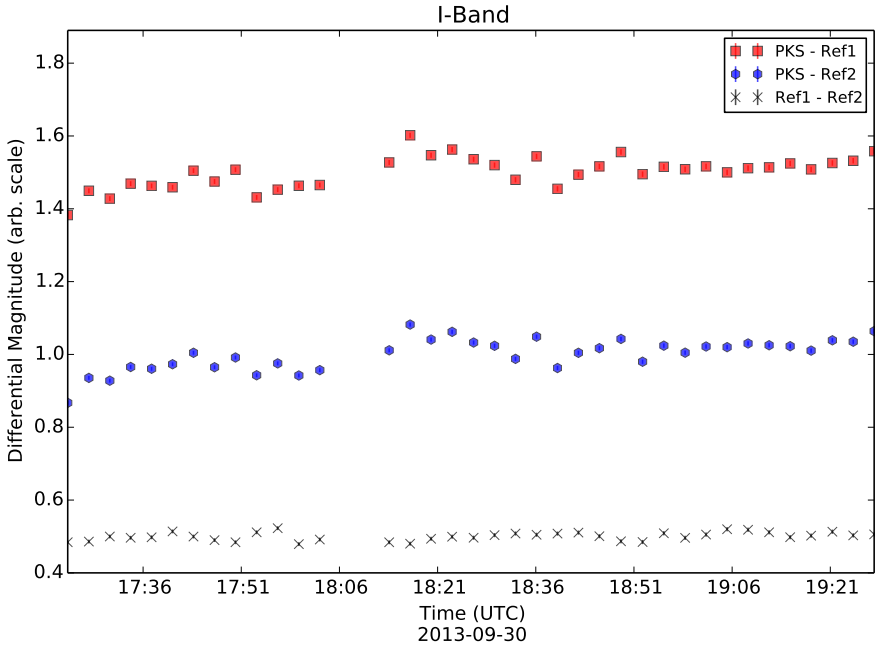

Figure 5.11: PKS 2005-489 I-Band Differential Lightcurve for 30/09/13

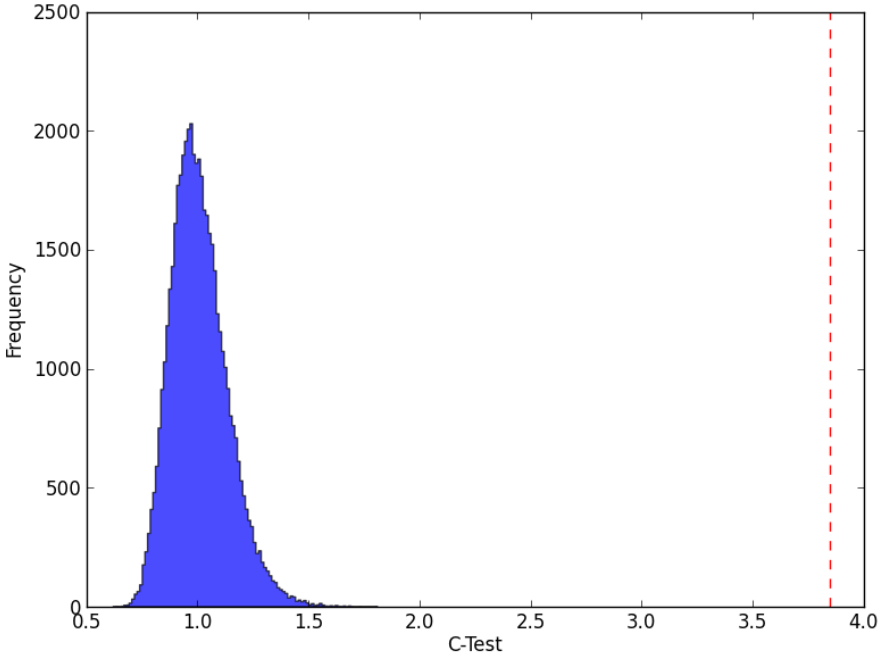

Figure 5.12: Distribution of C-test values for simulated lightcurves based on the I-band observations of 30/09/13.

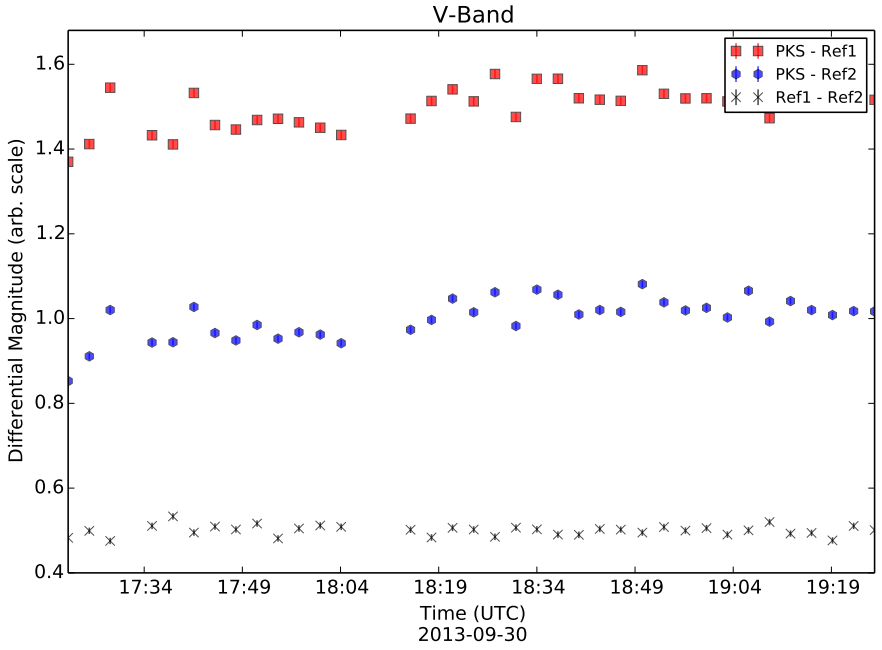

Figure 5.13: PKS 2005-489 V-Band Differential Lightcurve for 30/09/13

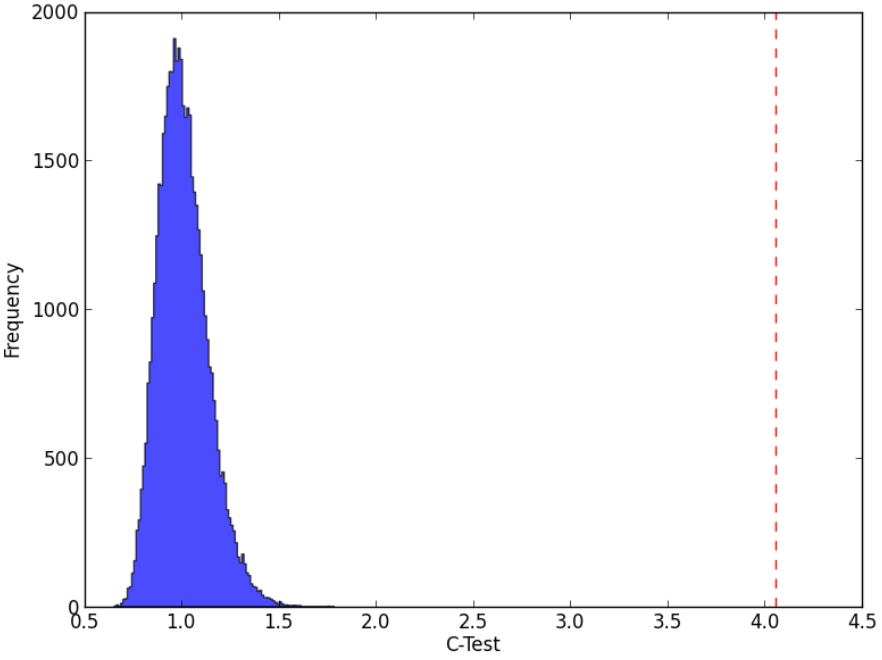

Figure 5.14: Distribution of C-test values for simulated lightcurves based on the V-band observations of 30/09/13.

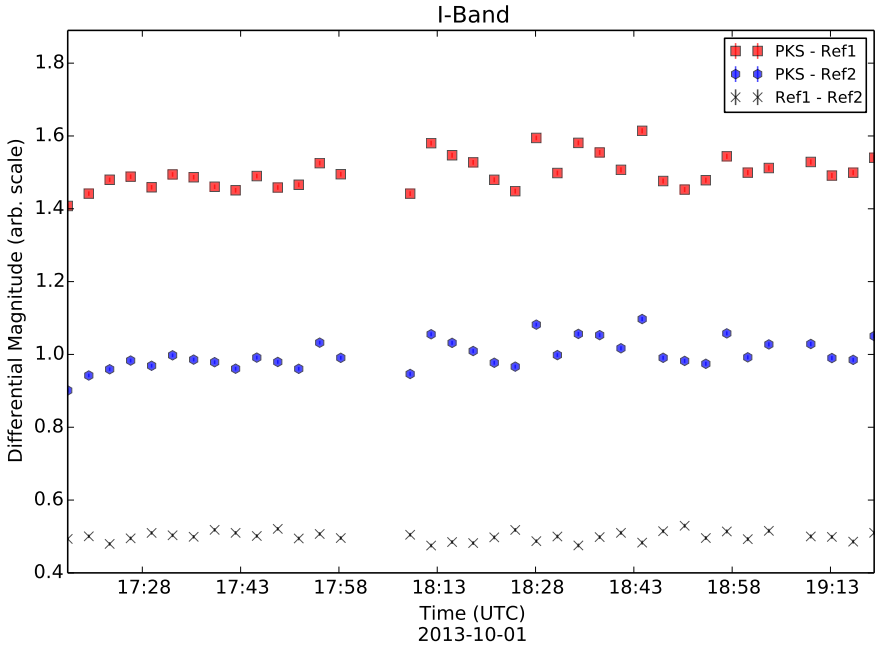

Figure 5.15: PKS 2005-489 I-Band Differential Lightcurve for 01/10/13

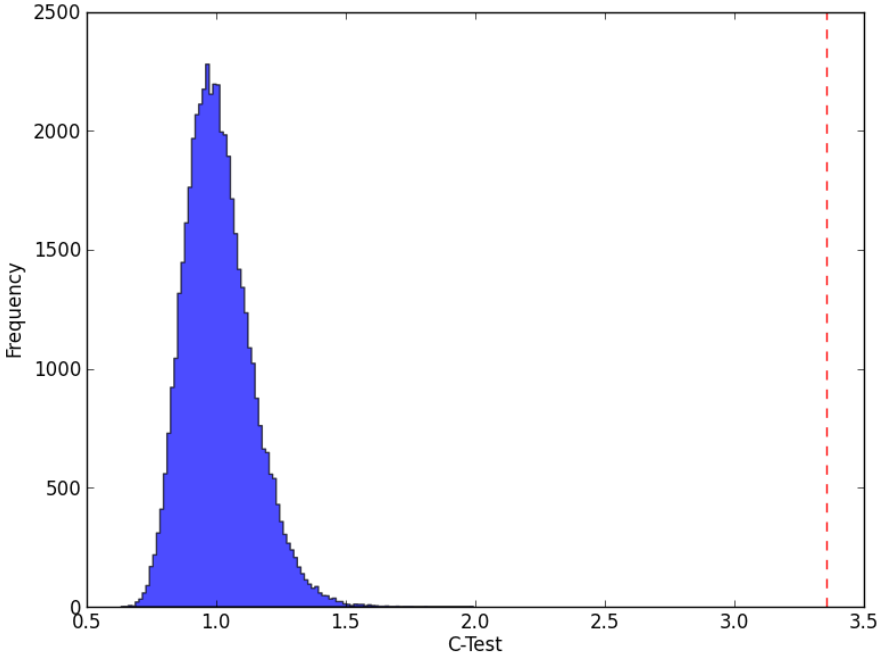

Figure 5.16: Distribution of C-test values for simulated lightcurves based on the I-band observations of 01/10/13.

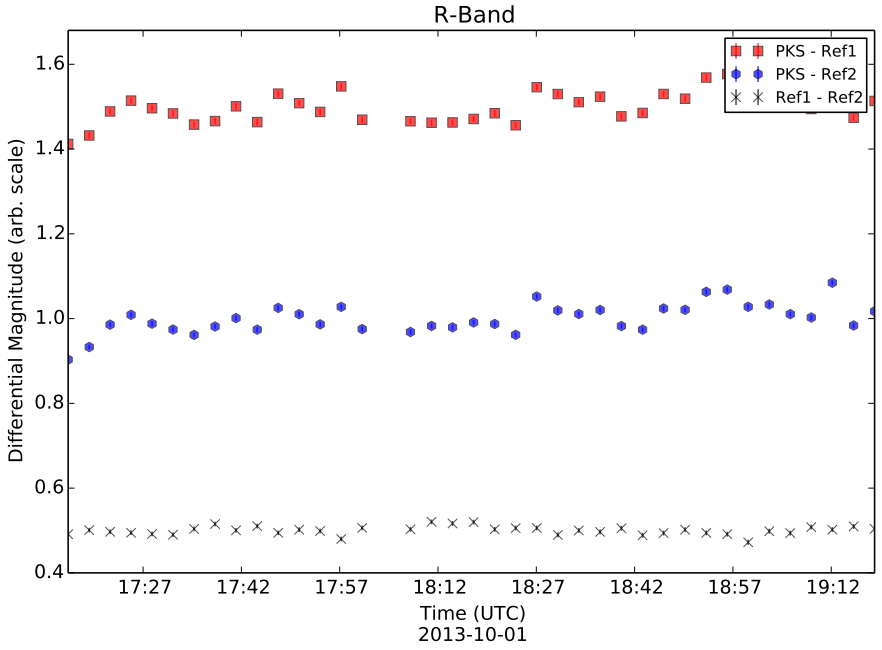

Figure 5.17: PKS 2005-489 R-Band Differential Lightcurve for 01/10/13

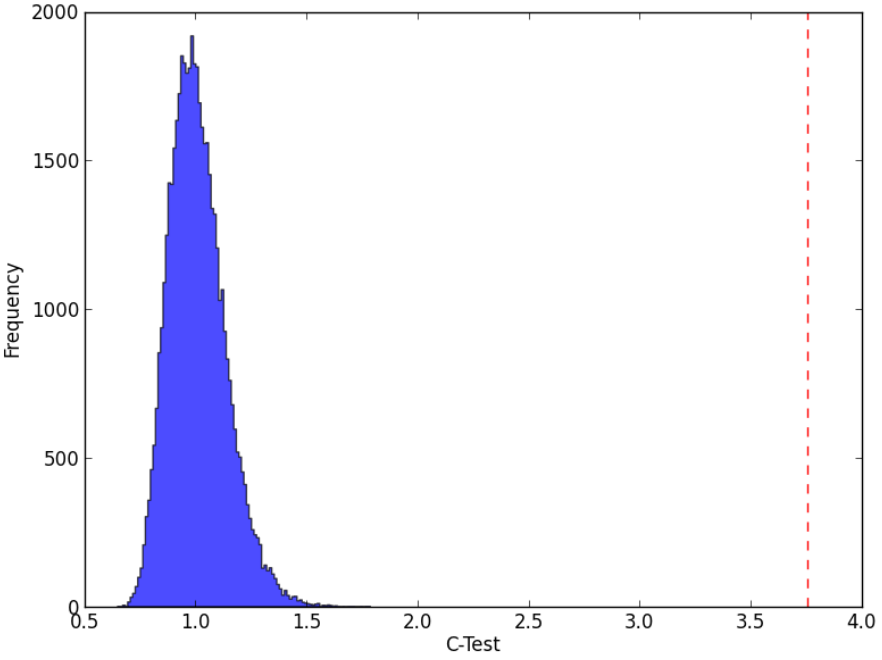

Figure 5.18: Distribution of C-test values for simulated lightcurves based on the R-band observations of 01/10/13. The red dashed line indicates the calculated C-test value for this night.

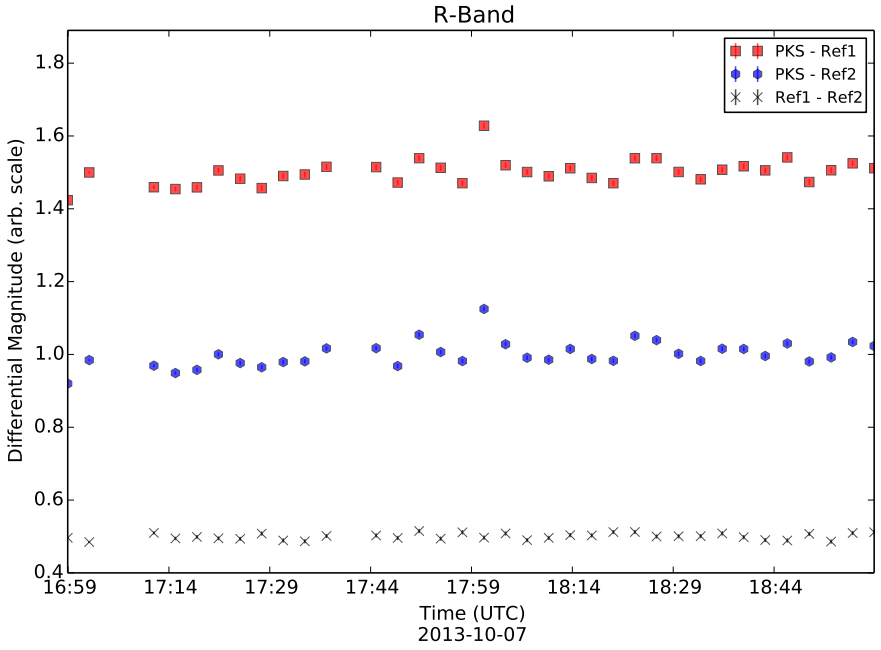

Figure 5.19: PKS 2005-489 R-Band Differential Lightcurve for 07/10/13

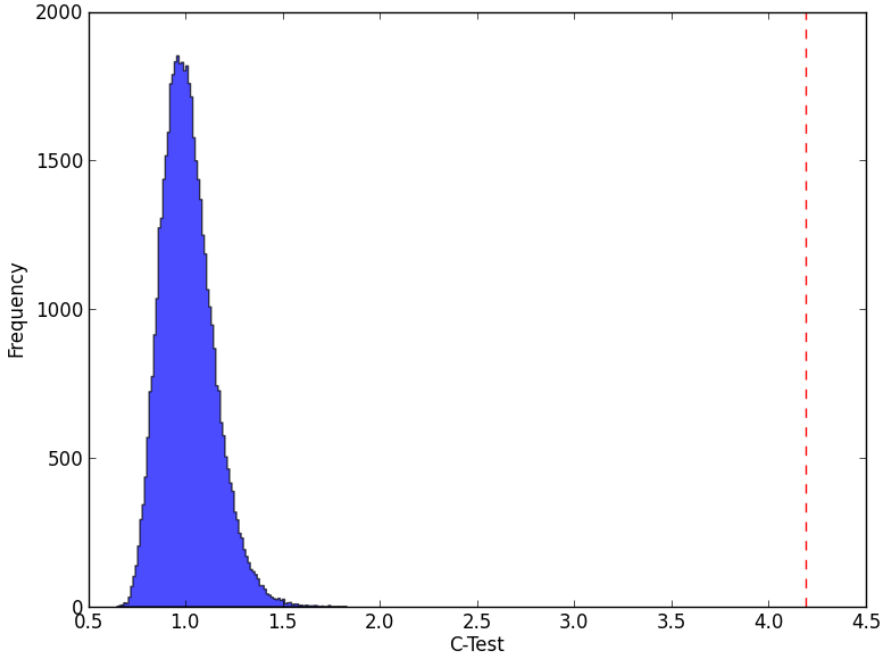

Figure 5.20: Distribution of C-test values for simulated lightcurves based on the observations of 07/10/13. The red dashed line indicates the calculated C-test value for this night.

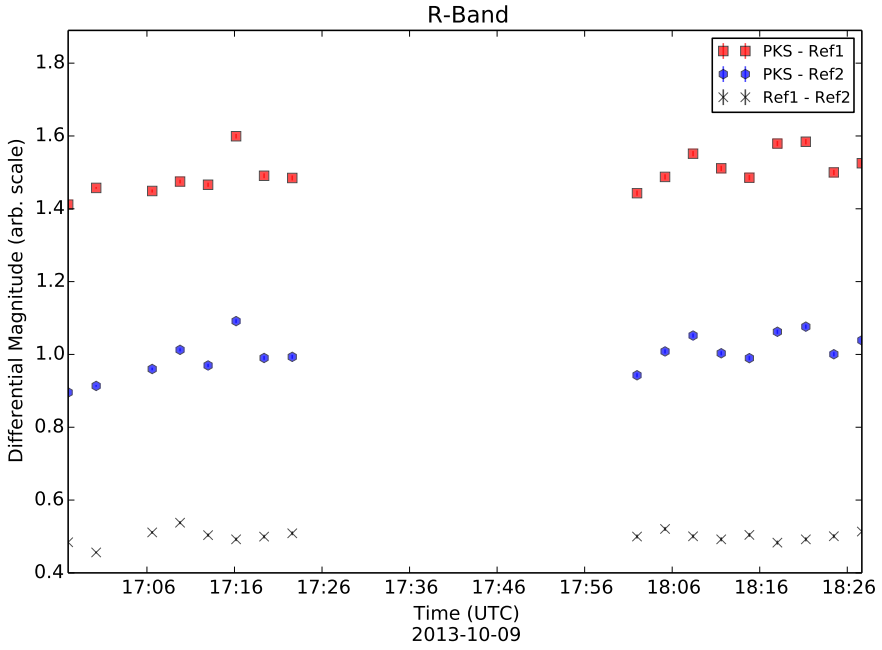

Figure 5.21: PKS 2005-489 R-Band Differential Lightcurve for 09/10/13

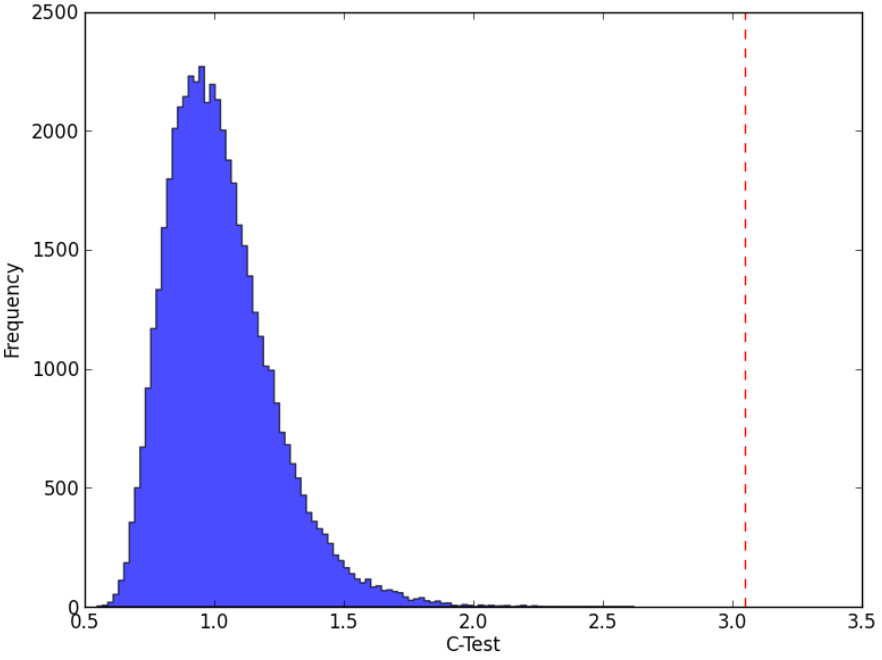

Figure 5.22: Distribution of C-test values for simulated lightcurves based on the observations of 09/10/13. The red dashed line indicates the calculated C-test value for this night.

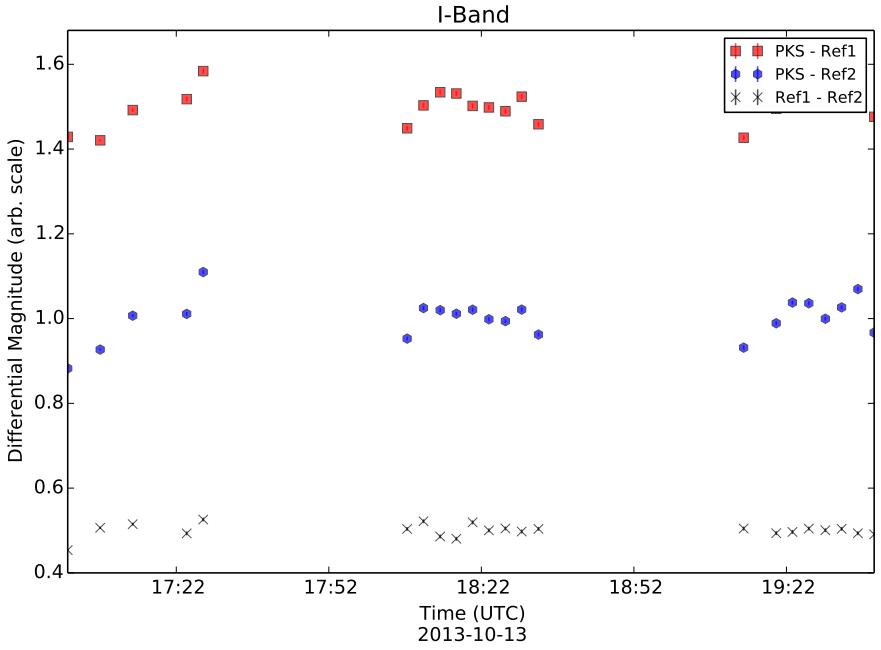

Figure 5.23: PKS 2005-489 I-Band Differential Lightcurve for 13/10/13

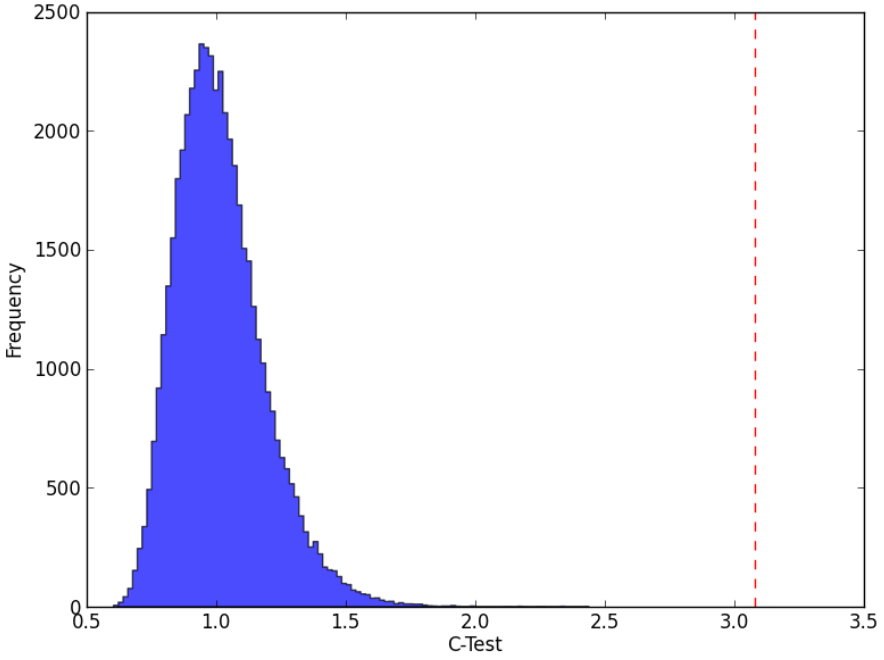

Figure 5.24: Distribution of C-test values for simulated lightcurves based on the observations of 13/10/13. The red dashed line indicates the calculated C-test value for this night.

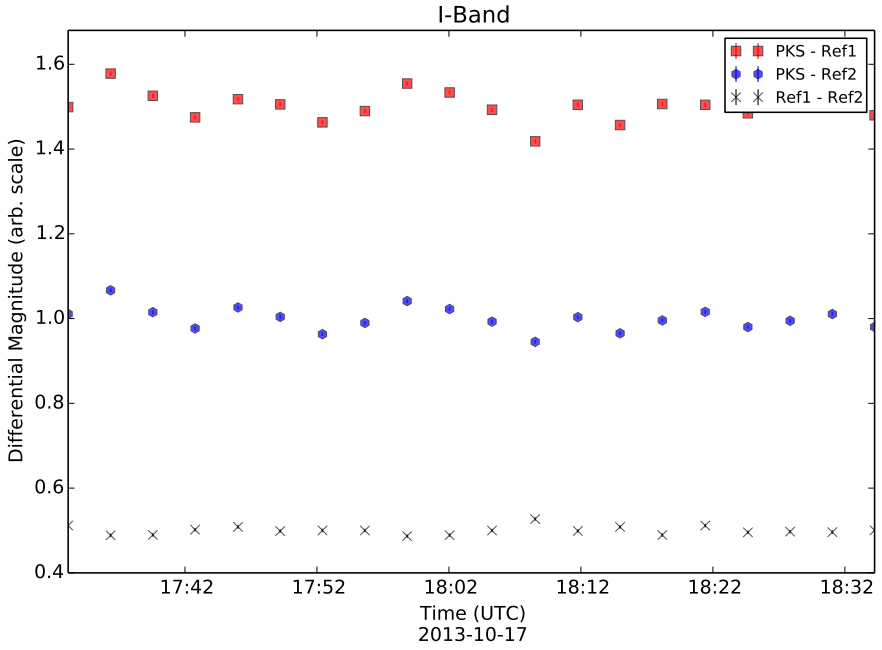

Figure 5.25: PKS 2005-489 I-Band Differential Lightcurve for 17/10/13

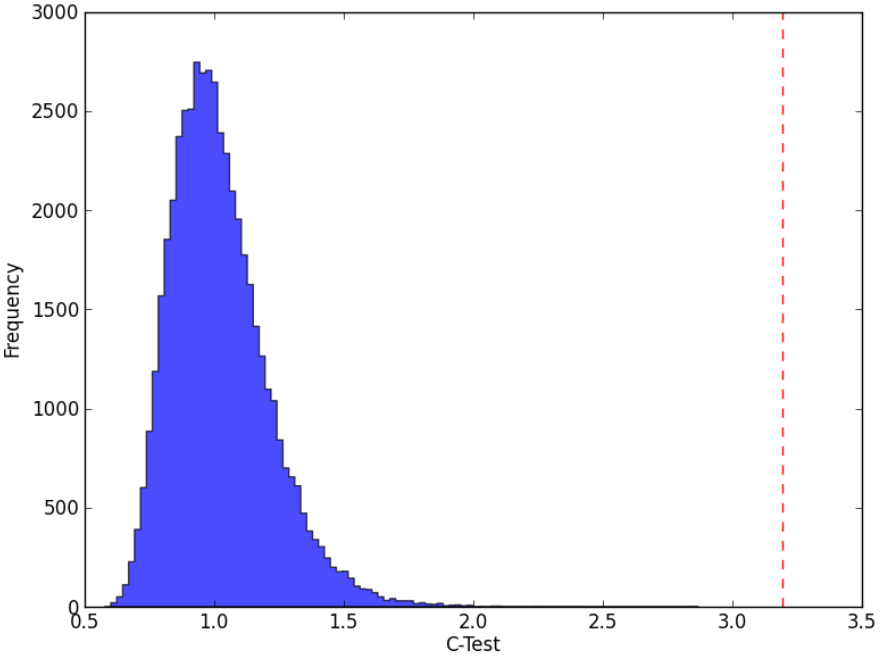

Figure 5.26: Distribution of C-test values for simulated lightcurves based on the observations from the 17/10/13. The red dashed line indicates the calculated C-test value for this night.

5.3 PKS 2155-304

The second source intensely observed during this monitoring programme was the BL Lac PKS 2155-304. No significant optical variability was detected in this source, despite showing some variation in its γ–ray flux (Figure 5.27). The C-test and F-test were both performed for this source, and found no sign of variability $> 3\sigma$.

Lightcurves obtained during particularly good nights are presented in Figures 5.28 – 5.33. A sample of the nightly lightcurves is presented in in Appendix B[2].

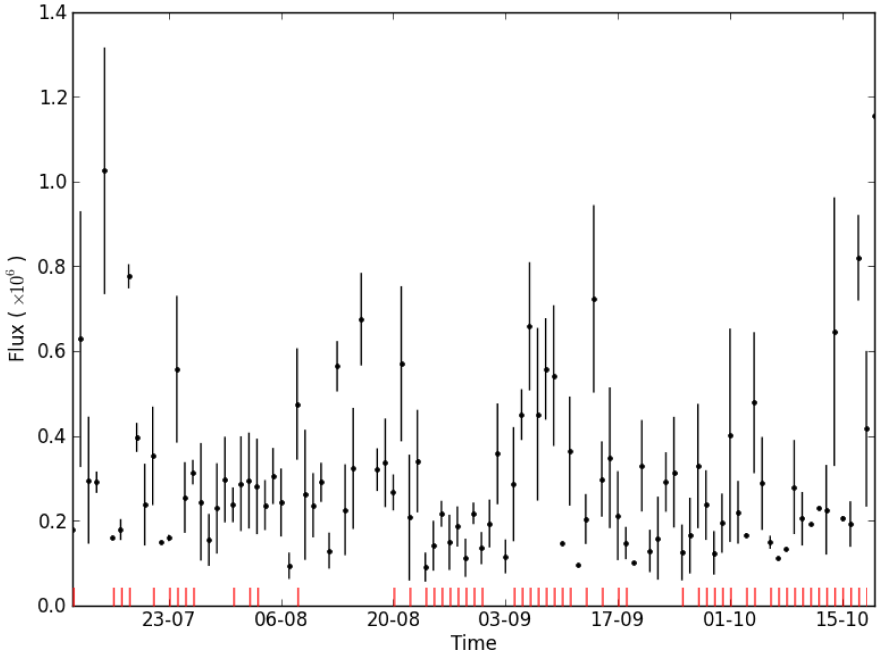

Figure 5.27: Fermi LAT monitored light curve in the 100MeV – 300GeV energy rangefor PKS 2155-304 during the austral winter of 2013 [*data retrieved from http://heasarc.gsfc.nasa.gov/xamin/xamin.jsp*]. The red lines indicate the dates with Watcher observations for this source.

[2]The full database of nightly lightcurves can be found at www.watchertelescope.ie/files/petetisdall/AppendixB.pdf

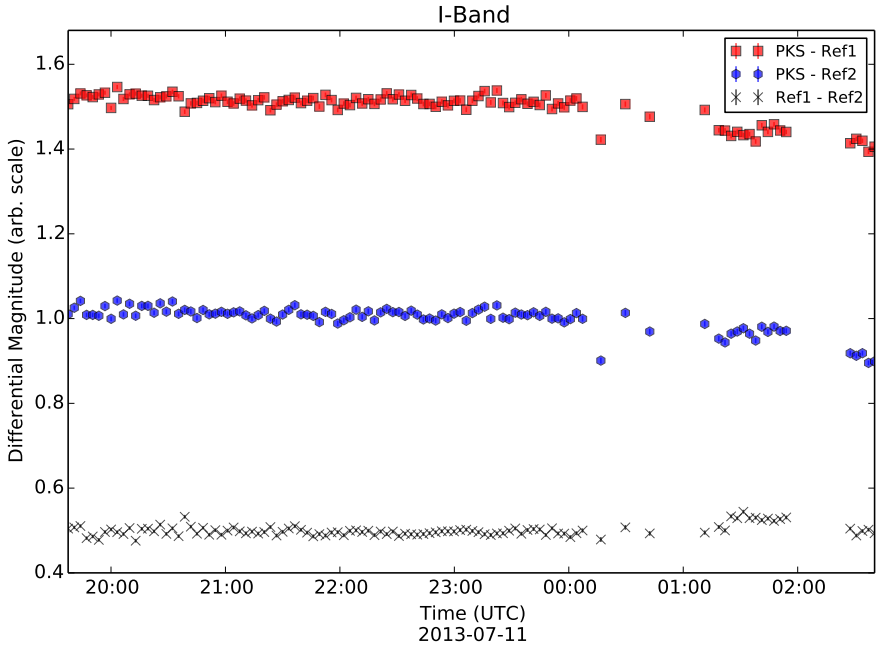

Figure 5.28: PKS 2155-304 I-Band Differential Lightcurve for 11/07/13

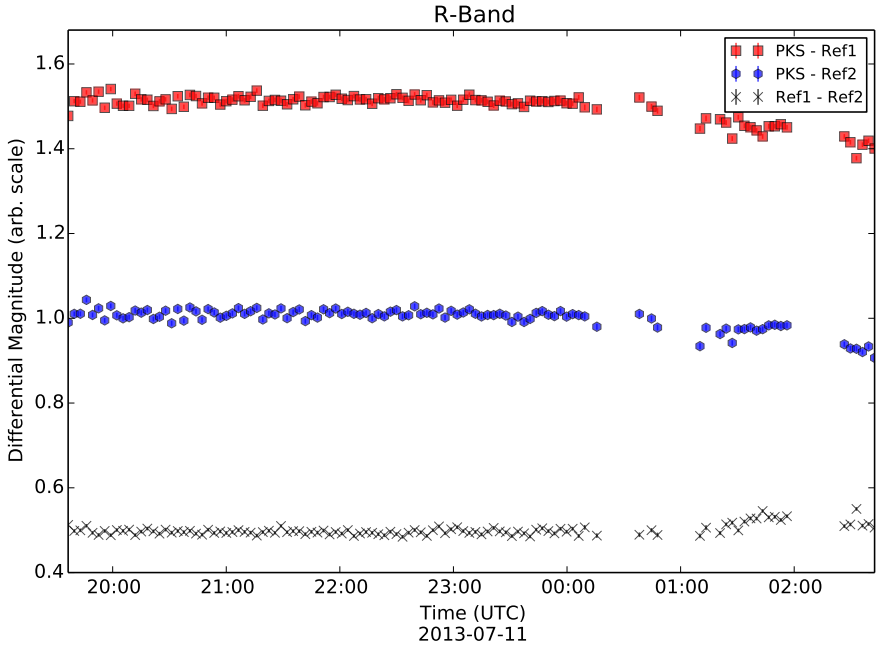

Figure 5.29: PKS 2155-304 R-Band Differential Lightcurve for 11/07/13

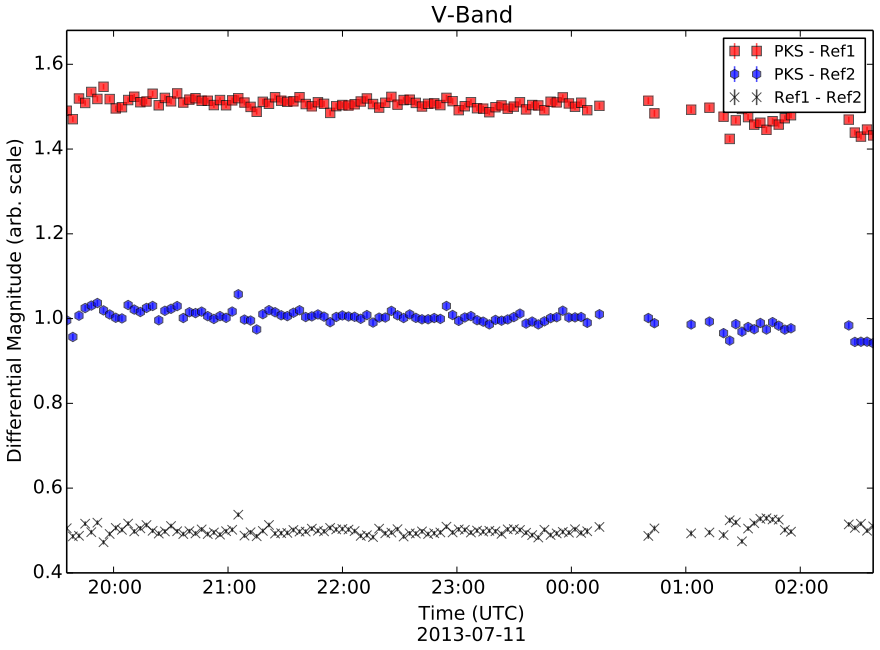

Figure 5.30: PKS 2155-304 V-Band Differential Lightcurve for 11/07/13

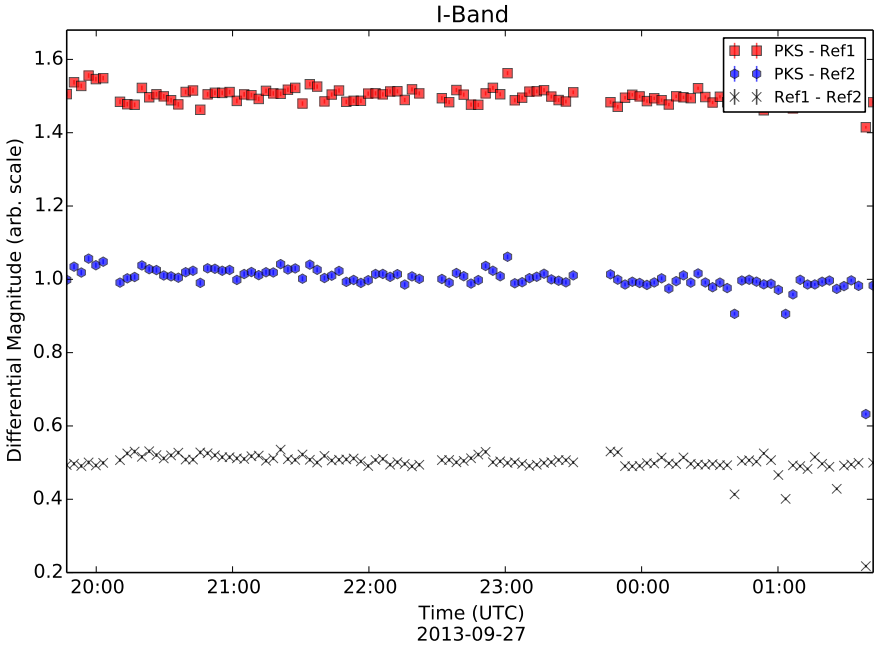

Figure 5.31: PKS 2155-304 I-Band Differential Lightcurve for 27/09/13

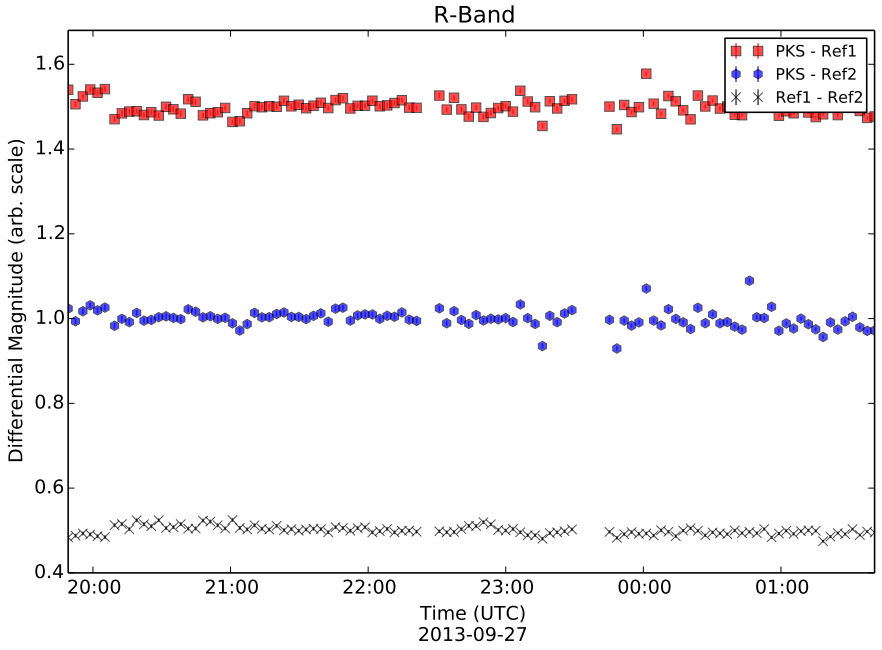

Figure 5.32: PKS 2155-304 R-Band Differential Lightcurve for 27/09/13

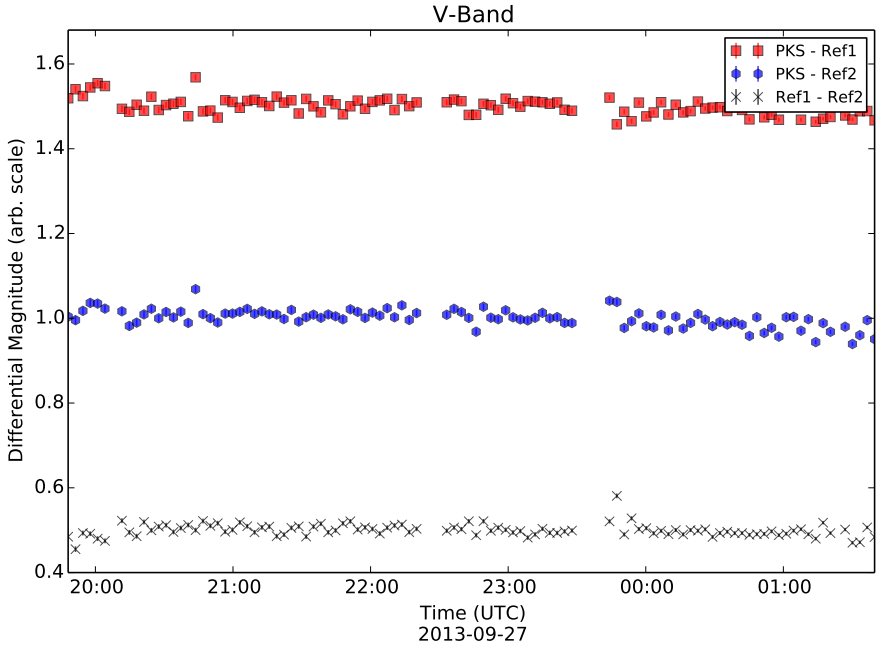

Figure 5.33: PKS 2155-304 V-Band Differential Lightcurve for 27/09/13

5.4 Discussion and Conclusions

In this chapter a comparison of two statistical tests is provided. The C-test is a method for testing variability based on the ratio between the standard deviations of a source of interest and a comparison star and is commonly used in studies of AGN (*Stalin et al.* 2004; *Gupta et al.* 2008; *Andruchow et al.* 2005). The F-test compares, instead, the variance of the source and a comparison star to verify the existence of any variability in the source. Both tests were used to confirm the existence of variability in order to minimise the chance of a false detection due to statistical effects.

The C-test was found to be strongly influenced by the number of data points in the sample (Figure 5.1), such that having a small sample size dramatically increased the likelihood of a false detection of variability. The F-test however, was found to be much more resilient to size of the sample, showing only a small increase in the false detection rate (Figure 5.2).

The two blazars PKS 2005-489 and PKS 2155-304 were the focus of an intense monitoring campaign during the austral winter of 2013. During this monitoring period, both targets displayed a relatively low level of activity with some small variations seen in PKS 2005-489, and no significant detection in PKS 2155-304. Historically, both of these sources have displayed a range of different behaviours at multiple wavelengths, including extreme flares as well as small scale variability during periods of lower activity (*Rector and Perlman* 2003; *Paltani et al.* 1997).

Variability was detected in PKS 2005-489 on 10 of the 56 nights, between July and October 2013 (Table 5.1), based on the results of the C-test and F-test. Simulations were used to verify the validity of each of these detections, the results of which indicate that the variability is significant and is not a false positive.

The variability observed in PKS 2005-489 during this monitoring campaign consisted primarily of small scale perturbations, or 'flickering', in the apparent brightness of the source. The 'flickering' nature of the variability could indicate that the variations are caused by turbulence within the jet emanating from the central engine. PKS 2005-489 has been observed to undergo periods of low activity followed by short periods of higher activity (*H.E.S.S. Collaboration et al.* 2010; *Kaufmann et al.* 2009). The variability ob-

served in this analysis is consistent with previous observations detailed in the literature.

There was no significant variability identified in PKS 2155-304 during the monitoring period. However, during this time, there was some variability seen in the γ–ray flux with the LAT telescope on board the Fermi satellite (Figure 5.27). It is not possible to make a direct comparison between the optical data obtained with Watcher and the γ–ray data from the LAT as the γ–ray data is binned on a nightly basis, and no absolute measurements have been made with the optical data.

The absence of variability at optical wavelengths could indicate that the observed high energy emission, from PKS 2155-304, may have been hadronic in origin, i.e. caused by the production of VHE photons within the jet. A more rigorous comparison of the source's emission in γ–ray and optical wavelengths would be required to model the emission process and potentially constrain the emission mechanism.

Previous studies of this source have shown that it undergoes periods of high activity, with short-timescale variability observed on the order of $\sim$1mag, and periods in a low, or quiescent, state with peak-to-peak variations on the order of $\sim$0.1mag (*Aharonian et al.* 2005c). During this monitoring campaign, PKS 2155-304 was in a very quiet state, with little to no activity at optical wavelengths. This is consistent with previous findings for this source.

The Watcher robotic telescope will continue to monitor the blazars detailed in Table 4.1 as part of its ongoing monitoring campaign. Recent upgrades to the telescope will allow for more detailed analysis to be made in the future.

Chapter 6

Access All Skies

'Access All Skies' was a pilot project that was run by University College Dublin (UCD) and Blackrock Castle Observatory (BCO) during October and November of 2012. The key objective of the project was to inspire future scientists and engineers through the innovative use of robotic telescope technology in education.

Ten schools (five secondary and five primary) in Dublin, Wicklow and Cork took part in the project to introduce the Bradford Robotic Telescope (BRT) and practical astronomy to Irish schools. The schools were visited on two occasions by members of the BRT, UCD and BCO teams. The details of these visits and the results of the feedback from this project are presented in this chapter.

During this project I was actively involved in the organisation and coordination of the school visits, including the creation and moderation of the students website accounts. As part of the initial session in the schools, I was involved in giving presentations and assisting the students in using the website and telescope.

For the schools in the Dublin and Wicklow area, I coordinated and ran the second sessions in both the primary and secondary schools. This involved giving a short presentation, teaching the students how to process their images, engaging with the students as they used the website, demonstrating to the teachers how they can operate the website and obtaining the feedback surveys for later analysis.

6.1 Science Outreach

'Science outreach' is the term used to describe the efforts of various institutions to promote the awareness and engagement of both the general public and students with science. Science and technology play a very important role in addressing the economic, social and environmental issues that are faced by modern society. That role needs the support and active engagement of the public who fund the work and are the ultimate beneficiaries of it.

6.1.1 Outreach to Students

Bennett and Hogarth (2009) found that interest in the physical sciences declines in students between the ages of 11 and 14 in England and Wales. Physics is perceived as a difficult subject to many students, and the desire to achieve the best possible grades leads to a decline in the number of students studying physics.

A US study showed that the 11-14 age group seems to be an important stage in the development of students' opinions towards science. This study found that students who expressed an interest in a science-based career at the age of 14 were far more likely to obtain a University science degree (*Tai et al.* 2006). This study concluded that a student of average mathematical ability who expressed an interest in a career in science had an estimated probability of obtaining a scientific degree of 34% versus 10% for a student who showed no interest in a career in science.

Maltese and Tai (2010) performed a study of the methods by which researchers and graduate students were initially engaged in science. The study found that early interest was generated by a variety of sources such as teachers, family members, self interest and specific memorable activities. 65% of those surveyed reported that their interest in science began before the age of 11.

It is important to engage these students at this formative age to encourage a greater understanding of and participation in science. Multiple previous studies have found that including a variety of activities and allowing the students to feel comfortable enough to ask questions are key factors in generating interest in science (*Muller et al.* 2013; *Tai et al.* 2006; *Royal Society* 2004). These studies motivated us to consider 5^{th} and 6^{th} class

students (10-12 years old) as part of the pilot programme.

The number of students choosing physics for the Leaving Certificate increased by 1% in 2013 over 2012, after a long decline over a number of years (*Institute of Physics* 2013), bringing the total up to 11.6% of the students sitting the Leaving Certificate. This small increase is possibly caused by the increased demand for science, technology, engineering and mathematics (STEM) students at third level.

Outreach projects such as Access All Skies can provide a very effective method of engaging students with science and generating interest among different age groups.

6.1.2 Astronomy as a Gateway to Science

Astronomy is a very popular science. This is likely due to the curiosity of the public about space and the universe as a whole. Modern astronomy involves physics, engineering, chemistry, geology, computer science, mathematics, biology and even has applications in the development of medicine. This makes astronomy very well suited for outreach as it can be used to introduce almost all of the aspects of science.

The goal of using astronomy in outreach is not just to train future astronomers, but to generate a lasting interest in science for both students and members of the public.

Unfortunately, astronomy is very poorly represented in the Irish school system. In the current primary level curriculum, astronomy is only included as a single subject strand as a part of geography (*Curriculum Committee for Social, Environmental and Scientific Education* 1999), while it is not present at all in the secondary school curriculum. Therefore, Irish school students currently have little to no formal exposure to astronomy, astrophysics and space science.

6.1.3 Robotic Telescopes in Outreach and Education

Robotic telescopes can provide a very effective avenue for student engagement with science. Their remote and autonomous nature allows students to view the night sky all around the world at any time of day or night. There are many different telescopes that are being used in outreach and education in several different ways.

Telescopes such as the NASA MicroObservatory[1] are available for public use, allowing high quality astronomical images to be easily obtained.

Some telescopes, such as the Zadko and Liverpool telescopes and those that are a member of the GLObal Robotic-telescopes Intelligent Array[2] (GLORIA), are used for outreach in conjunction with their primary research goals. These telescopes dedicate a portion of their time for schools and members of the public to use.

Other telescopes, like the BRT, have a much greater focus on outreach and are primarily used by students in primary and secondary schools. These projects provide the students with access to professional telescopes and many other astronomical resources through simple online interfaces. Granting students the ability to make their own observations, take their own images and decide for themselves what to observe means there is the potential for much greater engagement and interest in the subject of astronomy and the method of science.

6.2 The Bradford Robotic Telescope

The Bradford Robotic Telescope is a collection of telescopes and other instruments that are located at Teide Observatory on Tenerife. On board the BRT there are 3 distinct optical systems; the Galaxy camera, the Cluster camera and the Constellation camera. Each one is fitted with an eight position filter wheel and provides a different field of view (fov) for imaging a range of different sources.

[1] http://mo-www.cfa.harvard.edu/MicroObservatory/
[2] http://gloria-project.eu/en/

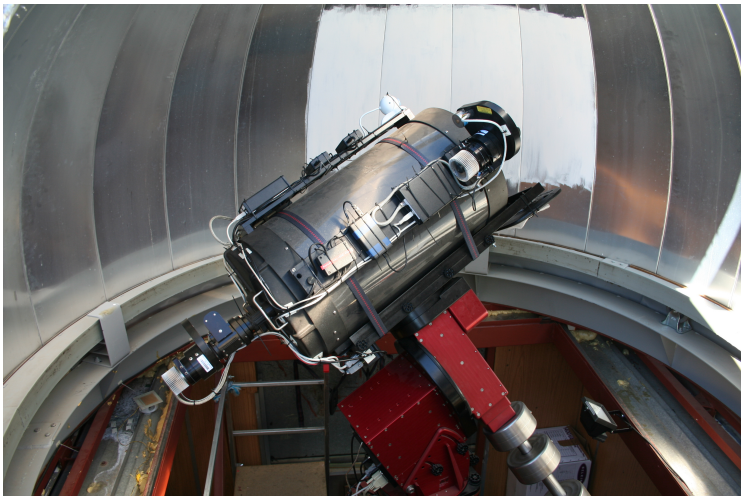

Figure 6.1: The Bradford Robotic Telescope. Photo by Dan Hedges.

The Galaxy camera is connected to a Schmidt-Cassegrain Celestron C14 optical tube, which provides a fov of $\sim$24'$\times$ 24'. As the name suggests, this camera is typically used to observe galaxies, nebula and other small sources. The Cluster camera provides a wider fov of 3°$\times$ 3° using a Nikon 200mm lens, and is used to observe globular clusters within our own galaxy. The largest fov is provided by the Constellation camera which is connected to a Nikon 16mm lens, and is capable of imaging 40°$\times$ 40° of the sky.

The primary aim of the BRT is to provide high quality astronomical observations to the public and to school students, in order to assist them in their studies and to foster an interest in science. This is done through a web interface that allows users to observe astronomical sources from a telescope at a high quality observatory site and to learn about space through games, simulations and resources, provided via the internet at www.telescope.org.

6.3 School Sessions

With the support of a BRT team member, Dr. Antonio Portas, each school that participated received two supervised sessions to familiarise them with the BRT. The minimum IT requirements for schools to participate in the project were one computer with an internet connection per pair of students and a projector/interactive whiteboard for an initial presentation.

In all of the primary schools, the students involved were in fifth or sixth class (10-12 years old). Transition year (15-16 years old) students were selected as the secondary school students, due to the greater freedom in their timetable compared to other years in secondary school. They are also an important age group in the Irish school system as they have not yet selected their subjects for the Leaving Certificate. Many students do not choose physics after the Junior Certificate due to the lack of awareness of the nature of the subject. By introducing transition year students to astronomy, one of the aims of the project was to inspire students thinking of not selecting Physics for the Leaving Certificate to change their minds.

Table 6.1 is a list of the schools that participated in the Access All Skies pilot programme.

Primary Schools	**Secondary Schools**
St. Oliver Plunkett NS, Dublin	Oatlands College, Dublin
St. Louis Infant School, Dublin	St. Killians Deutsche Schule, Dublin
Catholic University School, Dublin	Dominican College, Wicklow
Christian Brothers College Preparatory, Cork	Christian Brothers College, Cork
Scoil Nicolais, Cork	Coláiste Chríost Rí, Cork

Table 6.1: Participating schools in the Access All Skies pilot programme.

Before each session the schools' details were uploaded into the BRT database system and the accounts for the students and teachers were created. Each student account was accompanied by a unique password to ensure the students were able to work privately and make their own observation requests. In Dublin and Wicklow, 200 students took part in the pilot programme.

6.3.1 First Session

The first sessions took place during the week of 8 to 12 of October 2012. The slides for each presentation given can be found in Appendix C.

Primary Schools

The format of the first visit was designed to introduce the students to the project and to get them to engage as quickly as possible with the online quizzes and games. A short powerpoint presentation was used to introduce the students to 'BURT' (Figure 6.2), and to help them begin using the website (www.schools.telescope.org) to learn about the solar system.

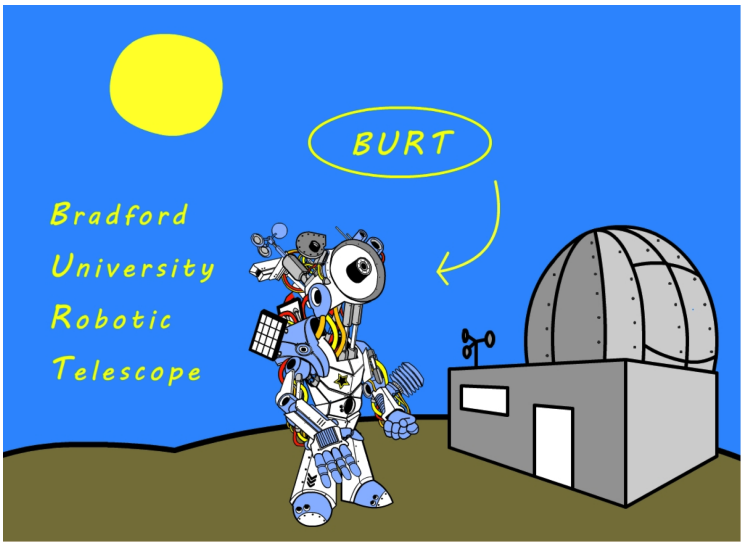

Figure 6.2: 'BURT', the Bradford University Robotic Telescope.

The students spent some time learning about the solar system before choosing objects to be observed for them by BURT. The web interface allows the students to choose between a range of different sources including galaxies, nebulae, clusters, planets and star constellations. Once the student has selected an image of a source they are interested in, the website suggests an exposure and filter for the observation and the student can place an order for the observation to be made.

Secondary Schools

The transition year students were introduced to the BRT and were guided through an experiment to calculate the age of the universe using Hubble's Law, which is the cornerstone of Big Bang Theory. This was done on the BRT website firstly by measuring the angular sizes of the galaxies. The students were able to calibrate the images in order to ascertain

the exact location of the edge of the galaxies. This was designed to show the students the subjectivity that can be involved in scientific measurements.

The students used an online tool, with provided recessional velocities, to determine the distance to the galaxies. Then, by plotting their velocities versus the calculated distance they estimated the age of the universe from the slope of the line of best fit (Figure 6.3).

Hubble's Law: The recessional velocity of galaxies is proportional to their distance from the observer.

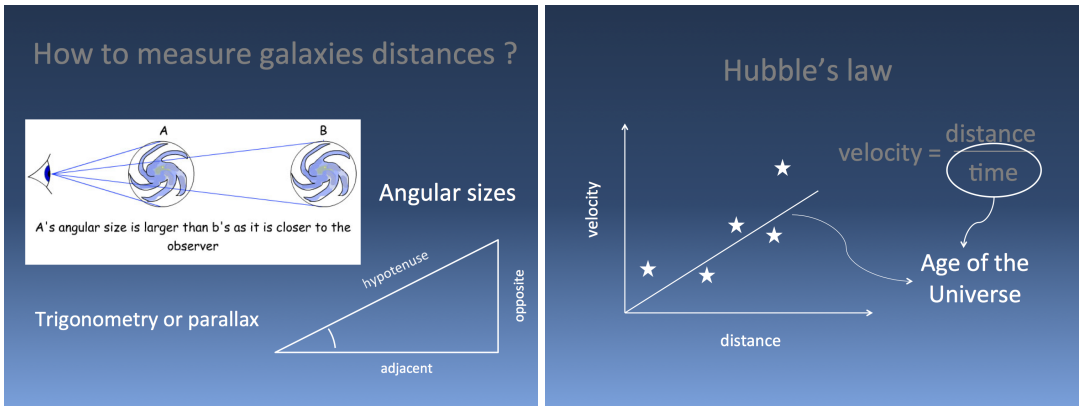

Figure 6.3: Basic method for calculating the distance to an object with the angular size (left panel). Calculating the age of the universe with Hubble's law (right panel)

Once the students had calculated an age for the universe, the students different values were averaged to arrive at a final age as calculated by the class. This demonstrated the practical application of statistics to improve the accuracy of a result. The main aim of this experiment was to show the students how the BRT could be used to perform practical experiments online, and how their own observations could be used to produce a scientific result.

The students then selected their own sources to be imaged by the BRT over the next few nights.

6.3.2 Second Session

The second session is designed to introduce the students to image reduction and analysis, and to allow them to see the results of the images that they requested in the first ses-

sion. This session typically took place within two weeks of the initial visit, to allow the telescope time to process the observation requests and take the images.

Primary Schools

In the primary schools the students were shown how to use the website to process the images and save them to an online 'scrapbook', and were given time to do so on their own. This scrapbook is designed to allow the students to save their images and print them out at a later date. During this time, the teachers were given additional online resources and shown how to use the website to provide more information and to run lessons.

After the students had spent some time producing their own images, there was a comprehensive 'questions and answers' session to allow the students to learn more about astronomy and space science by direct interaction with the astronomer.

Secondary Schools

The follow up session in the secondary schools also involved introducing the students to image processing, such as image manipulation and the concept of image calibration, in order to minimize errors in measurement.

This was followed by a discussion on the creation of the Universe and the formation of large-scale structures based on the experiment performed in the first session.

6.4 Surveys and Feedback

One of the primary metrics used by Bradford University to measure the success of the project is to monitor the continued usage of the website, both during and outside school hours after the initial sessions. The first results from the pilot programme, after two weeks of school and a week long holiday, are very similar to those from English schools.

The primary schools showed a higher level of activity than the secondary schools after the two sessions, primarily in the students' own free time. In Dublin and Wicklow, over 1,200 images were ordered by the primary students and over 1,000 images by the secondary students. The lower level of activity seen in the secondary schools is also seen in English students of a similar age.

During the second session, the students and teachers were given questionnaires to assess how successful the project was in meeting its objective. The results of this feedback for the Dublin/Wicklow schools are presented below.

Responses were on a 5 point Likert scale (*Likert* 1932) and space was available for open-ended comments. Examples of these questionnaires are given in Appendix C.

6.4.1 Primary Schools

A total of 111 primary school students took part in the pilot programme from three schools in the Dublin area. Table 6.2 shows the results of the feedback surveys that were completed by the students after completing the second session.

Primary School Questions

1. Are the images obtained from the telescope exciting for you?
2. Do you think you got an idea of what scientific work is like, from using the telescope?
3. Do you think you will continue to use the telescope on your own?
4. Has using the telescope got you more interested in science?
5. Has using the telescope got you more interested in going to University than before?

Responses	Definitely	Probably Yes	Not sure	Probably Not	Definitely Not
Question 1	65	40	5	0	1
Question 2	32	59	17	2	1
Question 3	50	40	17	3	1
Question 4	62	26	15	4	4
Question 5	44	37	13	16	1

Table 6.2: Total results for the Dublin Primary Schools feedback surveys

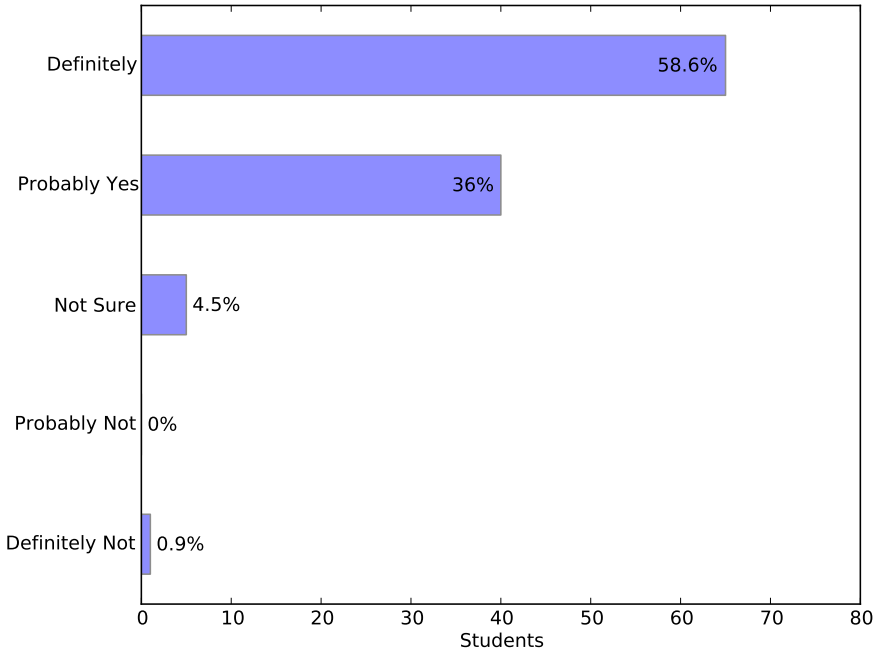

Figure 6.4: Question 1: Are the images obtained from the telescope exciting for you?

One of the objectives of scientific outreach is to demystify the world of research and to change the perspective that the public has of research. The result shown in Figure 6.5 is a good indication that the students felt like they were performing true scientific work.

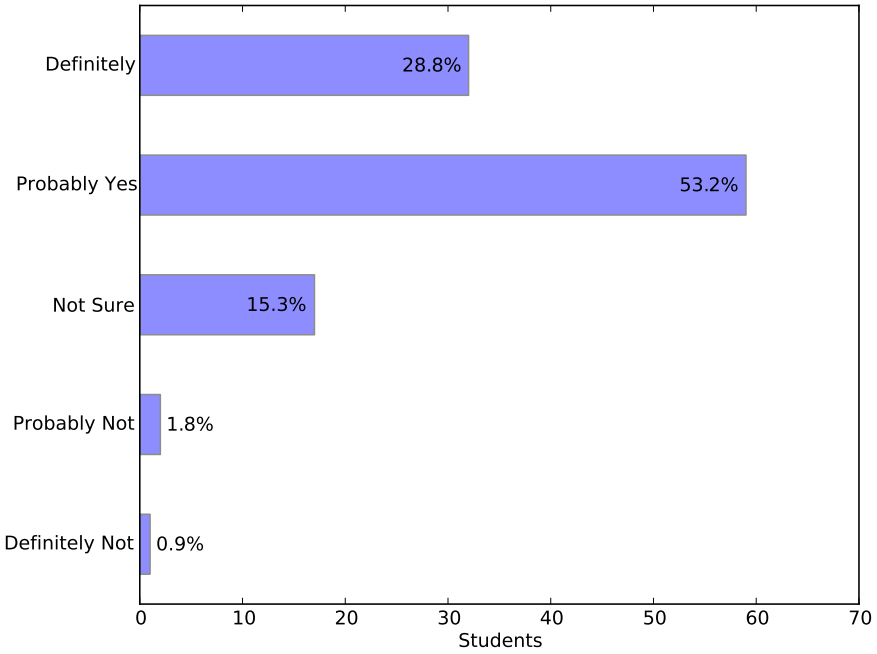

Figure 6.5: Question 2: Do you think you got an idea of what scientific work is like, from using the telescope?

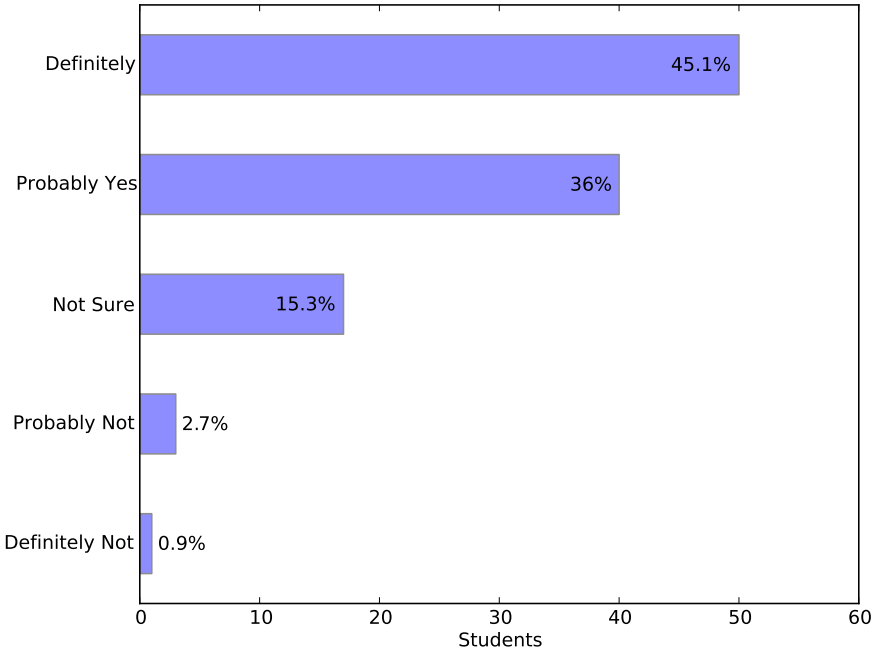

Figure 6.6: Question 3: Do you think you will continue to use the telescope on your own?

The students showed excellent engagement with the telescope and the online resources. Several of the primary students showed interaction with the online facilities up to a month after the

initial session, with the majority of the activity taking place outside of school hours. This result could be improved by engaging the teachers to a greater extent and providing more extensive resources for supporting them to integrate astronomy and space into their lesson plans.

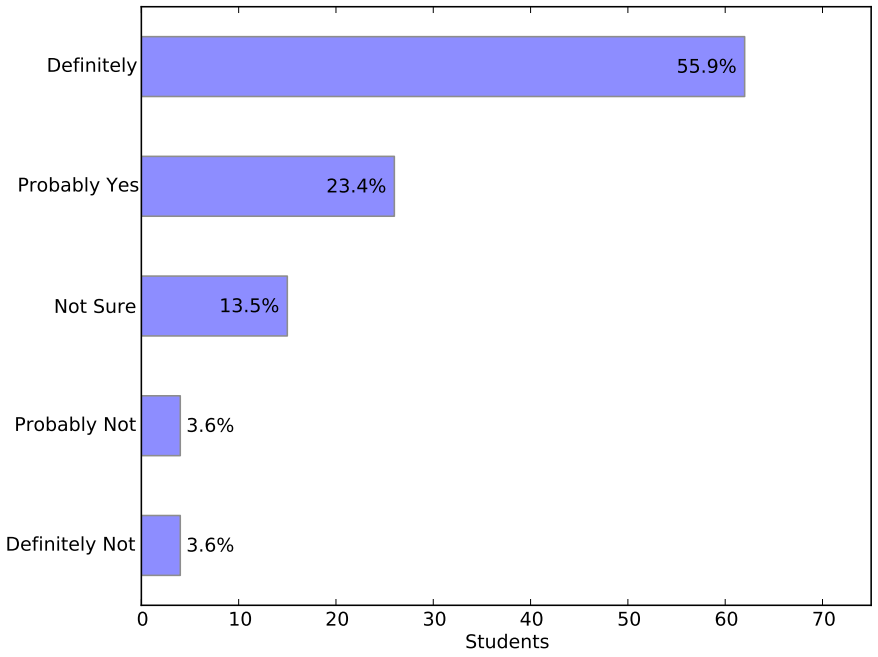

Figure 6.7: Question 4: Has using the telescope got you more interested in science?

Almost 75% of the students found that using the telescope had made them more interested in science. The comments from the students indicated that they enjoyed the entire process of using the telescope, requesting observations, seeing their own images of space and customising and analysing the images themselves.

Comments from the primary school students emphasised the content of the website and images, more than the image processing. They particularly enjoyed the games and quizzes and being able to ask a 'real' astronomer about astronomy, in the classroom.

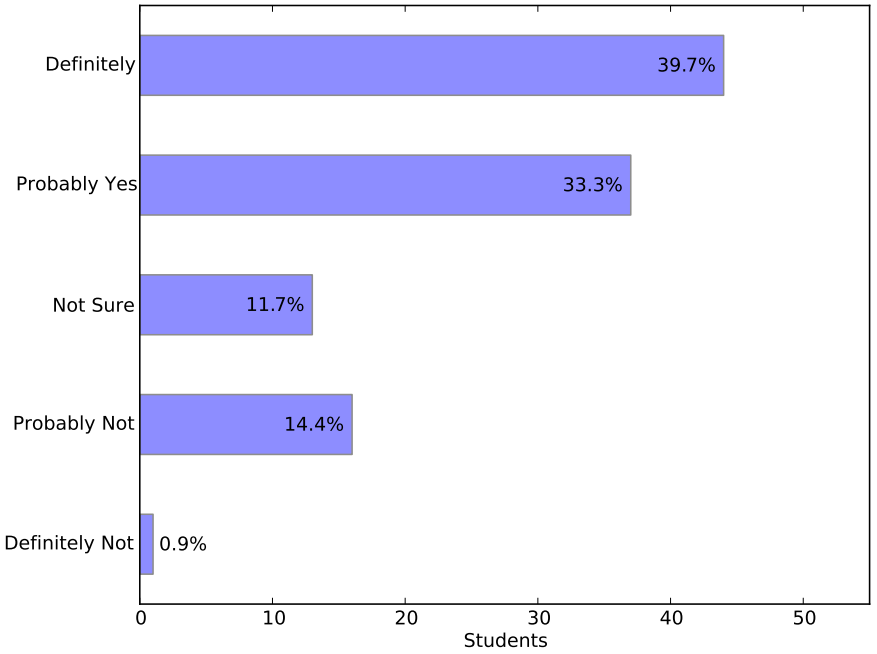

Figure 6.8: Question 5: Has using the telescope got you more interested in going to University than before?

The responses to the questionnaires provide strong evidence that the project has met its key goal, which was to inspire future scientists and engineers through the innovative use of robotic telescope technology in education.

A full listing of the free-form comments from the students is presented in Appendix C.

6.4.2 Secondary Schools

A total of 89 transition year students from three schools in the Dublin and Wicklow area took part in the pilot programme. The secondary schools that participated were diverse in background; Oatlands College is a boys' school operated by the Christian Brothers; Dominican College, Wicklow is an all girls school that is operated by the Dominican Sisters; and St. Killians German School is a multi-lingual school for boys and girls.

Secondary School Questions

1. Are the images obtained from the telescope exciting and inspirational for you?
2. Do you think you got an idea of what scientific work is like, from using the telescope?
3. Do you think you will continue to use the telescope on your own?
4. Has using the telescope got you more interested in studying Physics for the Leaving Certificate?

5. Has using the telescope got you more interested in studying science at University than before?

Table 6.3 shows the results of the feedback surveys that were completed by the students after completing the second session.

Responses	Definitely	Probably Yes	Not sure	Probably Not	Definitely Not
Question 1	31	48	9	1	0
Question 2	25	47	15	2	0
Question 3	18	22	33	9	7
Question 4	20	41	18	5	5
Question 5	22	33	21	9	4

Table 6.3: Total results for the Dublin and Wicklow Secondary Schools

The secondary school students, reflecting the experience in English schools, showed a lower level of activity than the primary schools after both of the in class sessions (Figure 6.11).

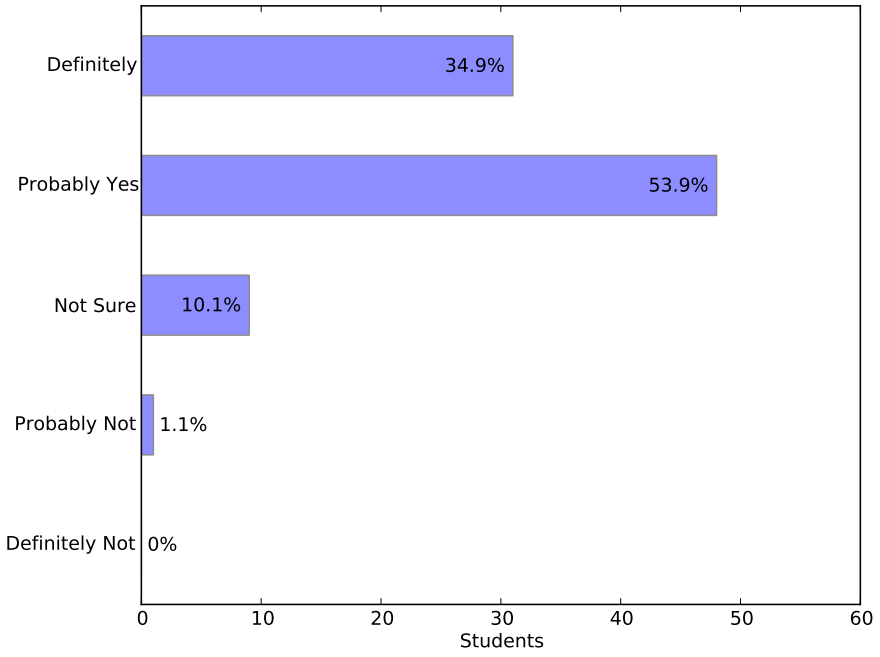

Figure 6.9: Question 1: Are the images obtained from the telescope exciting and inspirational for you?

The Access All Skies project gave the transition year students an opportunity to work with scientists, possibly for the first time. An important goal for outreach is to improve the students perception that careers in science are limited only to those who are 'gifted'. Given that, it is an

encouraging result to see that the students felt like they were completing work akin to that of research, as seen in Figure 6.10.

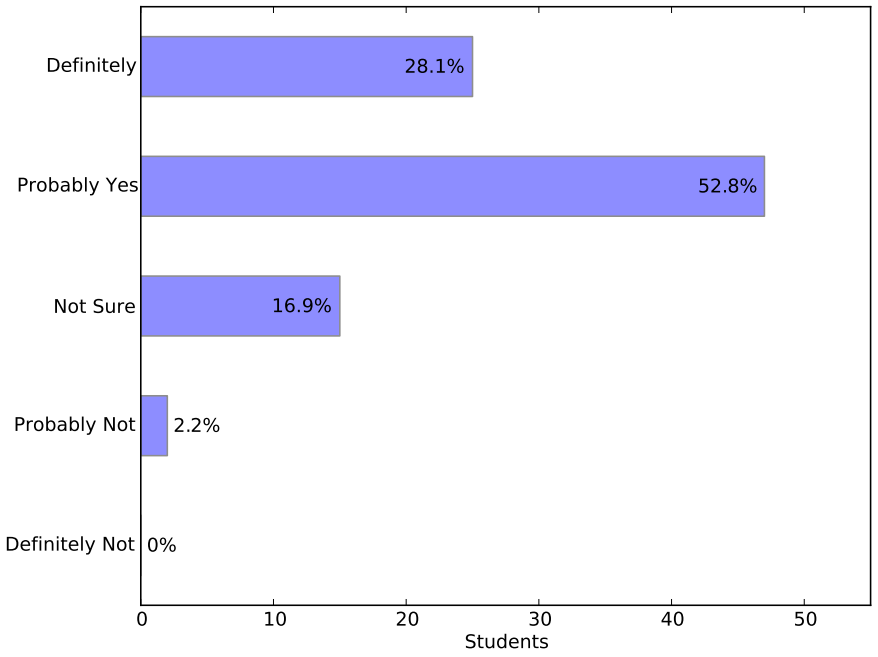

Figure 6.10: Question 2: Do you think you got an idea of what scientific work is like, from using the telescope?

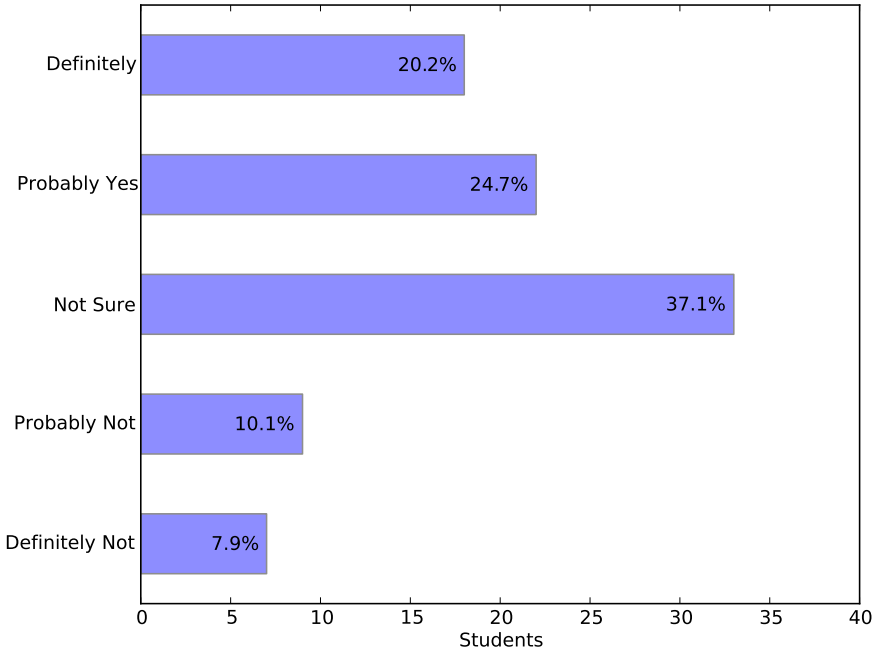

Figure 6.11: Question 3: Do you think you will continue to use the telescope on your own?

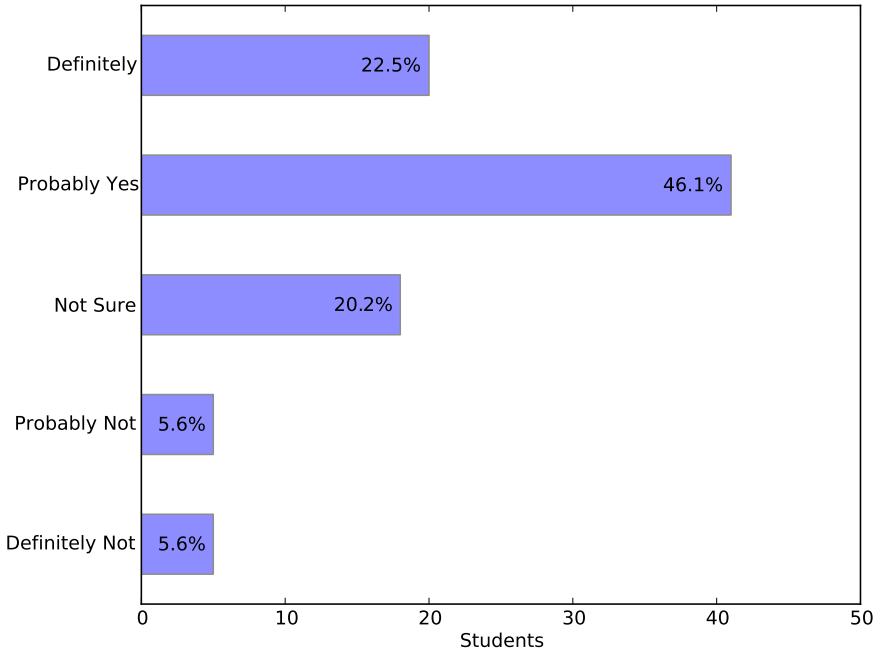

Figure 6.12: Question 4: Has using the telescope got you more interested in studying Physics for the Leaving Certificate?

Over 68% of the students who took part indicated that they were more likely to choose to study Physics for the Leaving Certificate (Figure 6.12).

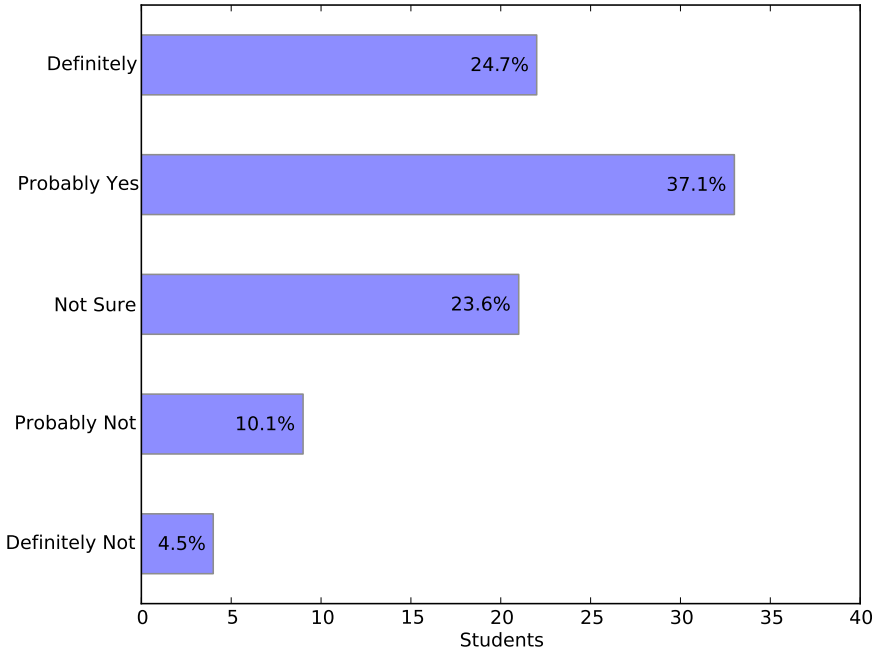

Figure 6.13: Question 5: Has using the telescope got you more interested in studying science at University than before?

Overall there was also a lower level of positivity in the feedback from the secondary school students, which is likely a result of the deterioration of attitudes towards science among this cohort, as discussed in Section 6.1.

6.4.3 Feedback from Teachers

The primary and secondary school teachers were both provided with the same questionnaires in order to ascertain their opinions of the programme. The results presented below do not include the feedback from every teacher, as some of the questionnaires were not completed.

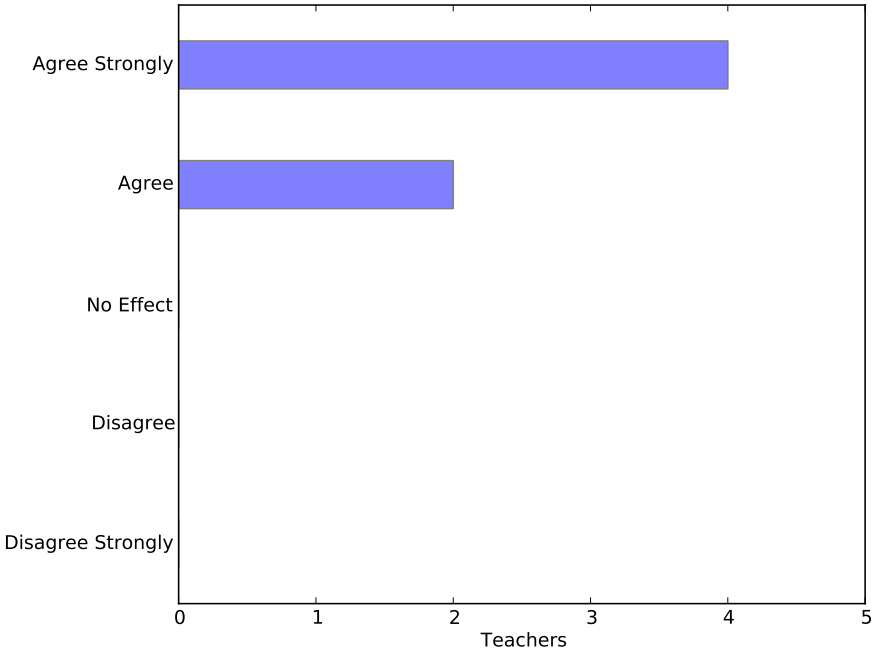

Figure 6.14: Question 1: I think that working with the telescope will encourage my students to study Science

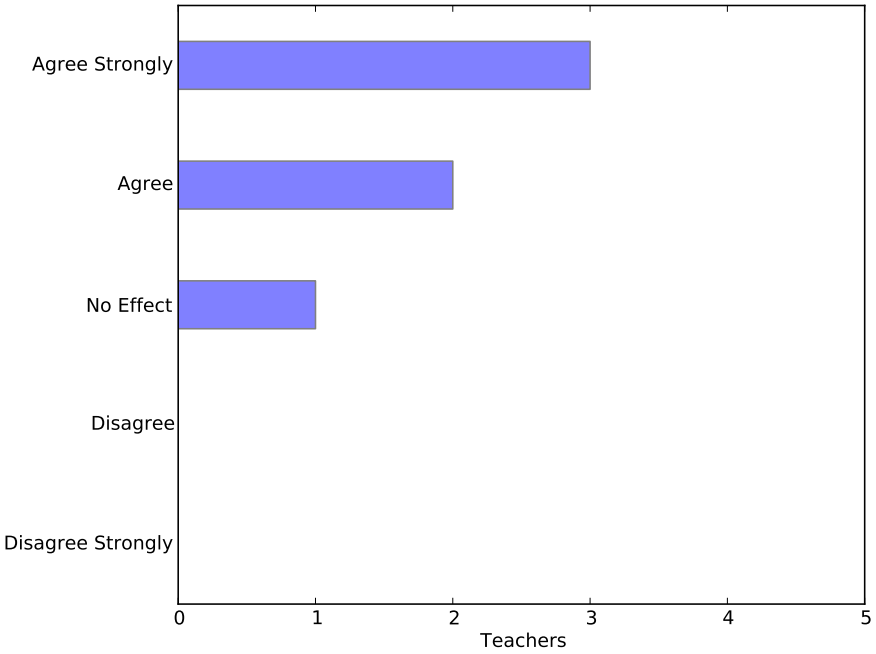

Figure 6.15: Question 2: I think that working with the telescope will encourage my pupils to think of going to University

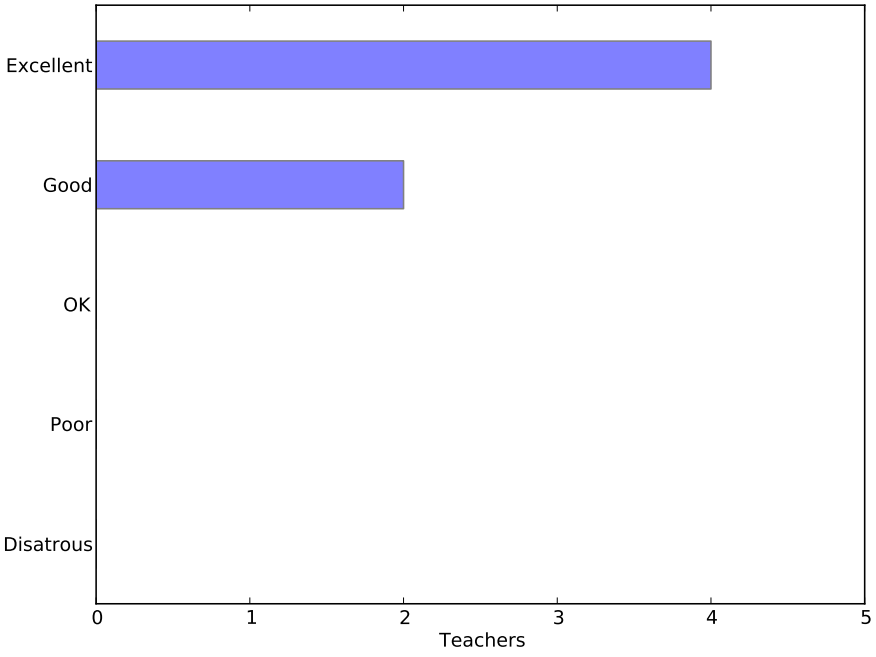

Figure 6.16: Question 3: How did you rate the session?

6.5 Discussion of Feedback

Overall the feedback from both the teachers and the students was extremely positive. Students found working with a robotic telescope interesting and exciting, and showed excellent engagement with the topics presented.

The most encouraging results of the feedback are shown in Figure 6.7 and 6.12. Almost 80% of the primary schools students stated that they were more interested in science as a result of using the telescope, and nearly 70% of the secondary school students indicated that they were more likely to study Physics for the Leaving Certificate as a result. This is a fantastic result, and one that shows the potential impact of this project on students' subject choice for the Leaving Certificate.

The feedback received from the teachers was also very positive, with many indicating that their students were more likely to study science as a result of the project. The teachers were also requested to suggest a possible pricing solution for the continued operation of the Access All Skies programme. The responses to this are included in Appendix C.

The results clearly demonstrate that the key goal of the pilot programme was met; **to inspire future scientists and engineers though the innovative use of robotic telescope technology in education.**

6.6 Roadmap for Future Projects

The success of the Access All Skies pilot project indicates that a more permanent project could be successful in inspiring more Irish students to study STEM subjects at Leaving Cert and third level. Improvements to the implementation and integration of the subject matter to the Irish curriculum could yield even better results, allowing for Astronomy and Space to have a much greater presence in the Irish classroom.

There is strong evidence that the 11 to 14 age range is the most important stage for students to become interested in science (*Muller et al.* 2013), and it is for this reason that any future outreach projects based on Access All Skies should involve a heavy focus on primary school students in their final years.

Table 6.4 shows a sample plan for a future outreach project based on using a similar resource to the BRT used in the Access All Skies programme. The proposed plan involves three sessions designed around the idea of enquiry-based learning (EBL). This method of teaching and learning

allows the students' own curiosity and questions to steer the course of the programme. It is very important in this style of learning to develop a trusting environment, in which the students are not afraid of being wrong or giving opinions. The students must be allowed to ask their own questions and investigate them for themselves (*Collier et al.* 2014).

Participation in this project would require sufficient computers for the students to work by themselves or in small groups and a reliable internet connection for the students to connect to the telescope and online resources. These requirements only pertain to the proposed second session, and for the schools that do not have the necessary resources the second session could also be completed in UCD, thus preventing schools from being excluded due to resource constraints.

1st Session *In-class*	– Short introduction to the project – What do the students know about space? – What do the students want to know about space? – How to find your own answers? – Guided experiment – Students form own investigation plan – Initial survey
2nd Session *In-class/UCD*	– Introduction to the telescope and website – Discussion of proposed plans – Guide on how to request observations – Online activities – Discussion on what we have learned so far
3rd Session *UCD*	Retrieval and processing of requested images – Discussion of uncertainty – Time to use images for investigation – Discussion of results and conclusions – Final survey

Table 6.4: Sample plan for future robotic telescopes in the classroom session

First Session

After a short introduction to the project the first session would move on to focus on discovering what the students know about space and astronomy. The students would be encouraged to ask questions and explore for themselves with some guidance. This would be followed by a discussion on how telescopes can be used to investigate and explore these topics.

A sample investigation could be used to guide the students through the process of asking a question, developing a method of answering the questions asked and finally, making an evidence

based conclusion. This exercise lends itself well to having the students work in small groups. Once the students are familiar with this method, they can begin to form their own questions to be answered.

It would be important, at this stage to give the students a questionnaire about their current view of science and astronomy, to better understand the effect that this programme has on their views.

Second Session

The second session would revisit the questions asked by the students, and how to use the telescope to gather the evidence to answer these questions. The students would then require time to make the observation requests.

This session would also provide a good opportunity to introduce the students to online activities and learning resources available on the website. The results of the Access All Skies pilot programme showed that the students from both levels enjoyed the online games, quizzes and facts that were available for them to learn.

Towards the end of the session, time would be dedicated to the discussion of what has been learned so far, and if any new questions have arisen.

Third Session

The final session would be focussed on the results of the student enquiries. The first stage of this would be to introduce the idea of calibrating the images in order increase the accuracy of any measurements to be made. This would involve a discussion about any errors involved in their measurements and how to go about minimizing them.

The students can then present what they have learned and any conclusions that can be made based on their experiment. Emphasis should be made at this point that the students can continue to investigate and learn with the online resources in their own time.

Before the end of the final session it would be important to have the students answer another questionnaire in order to track how their views of science and astronomy have been changed by the project.

Teacher Support

To support teachers who would like to encourage their students to continue using the telescope, a number of workshops dedicated to teachers would be held at centres around the country according to demand.

6.7 Conclusion

The pilot programme has indicated that robotic telescopes in a guided-enquiry classroom setting could have a significant positive impact on primary students engagement with science and the uptake of Physics at Leaving Certificate for secondary students.

Chapter 7

Conclusions

The primary objective of this thesis is to observe southern hemisphere blazars with the Watcher robotic telescope as part of a new monitoring campaign. The results of these observations, made during the austral winter of 2013, are presented. The secondary objective of this thesis is to present the 'Access All Skies' outreach and education pilot programme that was coordinated by UCD during October 2012. The method and results of this programme are presented in Chapter 6.

A study of the two blazars PKS 2005-489 and PKS 2155-304 (Chapter 4) was conducted in the I, R and V filters. The main results of this study are:

- Variability was detected on 10 out of 56 nights of observing between July and October 2013 in PKS 2005-489. The variations observed were similar to those seen in previous studies of PKS 2005-489 in a low state.

- There was no significant detection of variability in PKS 2155-304 out of 68 nights of observations during the monitoring period. Some activity was seen in the 100 MeV – 300 GeV energy range by the LAT on board the Fermi satellite, however. The lack of variability at both wavelengths could indicate that the source of the VHE emission may be hadronic in nature, significant further analysis would be required to investigate this fully.

- Simulations were used to investigate the reliability of the C-statistic and F-test statistical tools for verifying variability. The results of these simulations indicated that the C-statistic is not ideally suited for small sample sizes ($<$10 images). The F-test was found to be less influenced by the number of data points used.

The aim of the 'Access All Skies' programme was run by UCD in collaboration with Blackrock Castle Observatory, Bradford Robotic Telescope and Dublin City of Science 2012. This pro-

gramme included 10 schools in Dublin, Wicklow and Cork. This thesis reports on the programme in the Dublin and Wicklow schools:

- The 'Access All Skies' programme included 3 primary and 3 secondary schools in the Dublin and Wicklow area. The schools were chosen to include a wide range of backgrounds and environments. Several classes were visited, on two occasions, in each school.
- In the first visit, the students were introduced to the programme and used an online interface to request their own images with the Bradford Robotic Telescope. The second visit focussed on the calibration and processing of the students own images, and the discussion of topics within astronomy.
- Both the students and teachers involved completed feedback surveys based on their experience in the programme. The results of this feedback was extremely positive. The students showed excellent engagement with the subject matter and indicated that they enjoyed using a telescope for themselves.
- The success of the pilot programme indicated that there is a strong desire for a project of this nature to be a more permanent feature in the Irish education system. A plan for a future outreach project is proposed in Section 6.6.

Bibliography

Abdo, A. A., et al. (2010), The spectral energy distribution of fermi bright blazars, *Astrophys. J.*, *716*, 30–70, doi:10.1088/0004-637X/716/1/30.

Ackermann, M., et al. (2011), The second catalog of active galactic nuclei detected by the fermi large area telescope, *Astrophys. J.*, *743*, doi:10.1088/0004-637X/743/2/171.

Agudo, I., et al. (2011), Location of γ-ray flare emission in the jet of the bl lacertae object oj287 more than 14 pc from the central engine, *Astrophys. J., Lett.*, *726*, L13, doi:10.1088/2041-8205/726/1/L13.

Aharonian, F., et al. (2005a), Discovery of vhe gamma rays from pks 2005-489, *Astronomy & Astrophysics*, *436*, L17–L20, doi:10.1051/0004-6361:200500113.

Aharonian, F., et al. (2005b), H.e.s.s. observations of pks 2155-304, *Astronomy & Astrophysics*, *430*, 865–875, doi:10.1051/0004-6361:20041853.

Aharonian, F., et al. (2005c), Multi-wavelength observations of pks 2155-304 with hess, *Astronomy & Astrophysics*, *442*, 895–907, doi:10.1051/0004-6361:20053353.

Aharonian, F., et al. (2007), An exceptional very high energy gamma-ray flare of pks 2155-304, *Astrophys. J., Lett.*, *664*, L71–L74, doi:10.1086/520635.

Aharonian, F., et al. (2009), Simultaneous observations of pks 2155-304 with hess, fermi, rxte, and atom: Spectral energy distributions and variability in a low state, *Astrophys. J., Lett.*, *696*, L150–L155, doi:10.1088/0004-637X/696/2/L150.

Alfvén, H., and N. Herlofson (1950), Cosmic Radiation and Radio Stars, *Physical Review*, *78*(5), 616–616.

Andruchow, I., G. E. Romero, and S. A. Cellone (2005), Polarization microvariability of bl lacertae objects, *Astronomy & Astrophysics*, *442*, 97–107, doi:10.1051/0004-6361:20053325.

Antonucci, R. R. J., and J. S. Miller (1985), Spectropolarimetry and the nature of NGC 1068, *Astrophysical Journal*, *297*, 621–632.

Baade, W., and R. Minkowski (1954), Identification of the Radio Sources in Cassiopeia, Cygnus A, and Puppis A., *Astrophysical Journal*, *119*, 206.

Bahcall, J. N., and E. E. Salpeter (1965), On the Interaction of Radiation from Distant Sources with the Intervening Medium., *Astrophysical Journal*, *142*, 1677–1680.

Barthel, P. D. (1989), Is every quasar beamed?, *Astrophysical Journal*, *336*, 606–611.

Barthel, P. D. (1994), Unified Schemes of FR2 Radio Galaxies and Quasars, *The First Stromlo Symposium: The Physics of Active Galaxies. ASP Conference Series*, *54*, 175.

Beckmann, V., and C. Shrader (2012), The agn phenomenon: open issues, in *Proceedings of "An INTEGRAL view of the high-energy sky (the first 10 years)" - 9th INTEGRAL Workshop*.

Bennett, J., and S. Hogarth (2009), Would you want to talk to a scientist at a party? high school students' attitudes to school science and to science, *International Journal of Science Education*, *31*(14), 1975–1998, doi:10.1080/09500690802425581.

Berry, R., and J. Burnell (2005), *The Handbook of Astronomical Image Processing*, CWillmann-Bell, Inc.

Biraud, F., and P. Veron (1968), VRO 42 22 01: a Variable Source with Circular Polarization, *Nature*, *219*(5), 254–255.

Bolton, J. G., and G. J. Stanley (1948), Variable Source of Radio Frequency Radiation in the Constellation of Cygnus, *Nature*, *161*, 312–313.

Bolton, J. G., G. J. Stanley, and O. B. Slee (1948), Positions of Three Discrete Sources of Galactic Radio-Frequency Radiation, *Nature*, *164*, 101–102.

Bonning, E., C. M. Urry, C. Bailyn, M. Buxton, R. Chatterjee, P. Coppi, G. Fossati, J. Isler, and L. Maraschi (2012), Smarts optical and infrared monitoring of 12 gamma-ray bright blazars, *Astrophys. J.*, *756*, 13, doi:10.1088/0004-637X/756/1/13.

Böttcher, M. (2005), A hadronic synchrotron mirror model for the "orphan" tev flare in 1es 1959+650, *Astrophys. J.*, *621*, 176–180, doi:10.1086/427430.

Burbidge, E. M., C. R. Lynds, and G. R. Burbidge (1966), On the Measurement and Interpretation of Absorption Features in the Spectrum of the Quasi-Stellar Object 3C 191, *Astrophysical Journal*, *144*, 447.

Chadwick, P. M., K. Lyons, T. J. L. McComb, K. J. Orford, J. L. Osborne, S. M. Rayner, S. E. Shaw, K. E. Turver, and G. J. Wieczorek (1999), Very high energy gamma rays from pks 2155-304, *Astrophys. J.*, *513*, 161–167, doi:10.1086/306862.

Chatterjee, R., et al. (2008), Correlated multi-wave band variability in the blazar 3c 279 from 1996 to 2007, *Astrophys. J.*, *689*, 79–94, doi:10.1086/592598.

Chatterjee, R., C. D. Bailyn, E. W. Bonning, M. Buxton, P. Coppi, G. Fossati, J. Isler, L. Maraschi, and C. M. Urry (2012), Similarity of the optical-infrared and γ-ray time variability of fermi blazars, *Astrophys. J.*, *749*, 191, doi:10.1088/0004-637X/749/2/191.

Chernyakova, M., et al. (2014), Multiwavelength observations of the binary system psr b1259-63/ls 2883 around the 2010-2011 periastron passage, *Mon. Not. R. Astron. Soc.*, *439*, 432–445, doi:10.1093/mnras/stu021.

Chiappetti, L., et al. (1999), Spectral evolution of pks 2155-304 observed with bepposax during an active gamma-ray phase, *Astrophys. J.*, *521*, 552–560, doi:10.1086/307577.

Colla, G., C. Fanti, R. Fanti, I. Gioia, C. Lari, J. Lequeux, R. Lucas, and M. H. Ulrich (1975), A complete sample of radio sources identified with elliptical galaxies - Radio luminosity function and other properties, *Astronomy and Astrophysics*, *38*, 209–223.

Collier, C., J. Johnson, L. Nyberg, and V. Lockwood (2014), Learning science through inquiry, Available at http://www.learner.org/workshops/inquiry/resources/faq.html, [accessed 28-August-2014].

Curriculum Committee for Social, Environmental and Scientific Education (1999), *Primary School Curriculum - Geography*, The Stationery Office.

de Diego, J. A. (2010), Testing tests on active galactic nucleus microvariability, *The Astronomical Journal*, *139*, 1269–1282, doi:10.1088/0004-6256/139/3/1269.

Disney, M. J., B. A. Peterson, and A. W. Rodgers (1974), The redshift and composite nature of AP Librae /PKS 1514-24 , *Astrophysical Journal*, *194*, L79–L82.

Falomo, R., L. Maraschi, A. Treves, and E. G. Tanzi (1987), The redshift of the bl lacertae object pks 2005-489, *Astrophys. J., Lett.*, *318*, L39–L41, doi:10.1086/184933.

Fanaroff, B. L., and J. M. Riley (1974), The morphology of extragalactic radio sources of high and low luminosity, *Monthly Notices of the Royal Astronomical Society*, *167*, 31P–36P.

Fath, E. A. (1909), The spectra of some spiral nebulae and globular star clusters, *Lick Observatory bulletin ; no. 149; Lick Observatory bulletins ; no. 149.*, *5*, 71–77.

Ferrero, A., et al. (2010), The photometry pipeline of the watcher robotic telescope, in *Peer-reviewed Proceedings of the First Workshop on "Robotic Autonomous Astronomical Observatories"*, vol. 2010, pp. 131–135, doi:10.1155/2010/715237.

Flynn, C. (2005), Synchrotron radiation, Available at http://www.astro.utu.fi/ cflynn/astroII/synch.gif, [accessed 15-July-2014].

French, J., L. Hanlon, B. McBreen, S. McBreen, L. Moran, N. Smith, A. Giltinan, P. Meintjes, and M. Hoffman (2004), Watcher: A telescope for rapid gamma-ray burst follow-up observations, in *Gamma-Ray Bursts: 30 Years of Discovery*, *American Institute of Physics Conference Series*, vol. 727, edited by E. Fenimore and M. Galassi, pp. 741–744, doi:10.1063/1.1810948.

Gaur, H., et al. (2012), Optical flux and spectral variability of blazars, *Mon. Not. R. Astron. Soc.*, *425*, 3002–3023, doi:10.1111/j.1365-2966.2012.21583.x.

Greenstein, J. L., and T. A. Matthews (1963), Red-Shift of the Unusual Radio Source: 3C 48, *Nature*, *197*, 1041.

Greenstein, J. L., and M. Schmidt (1964), The Quasi-Stellar Radio Sources 3C 48 and 3C 273., *Astrophysical Journal*, *140*, 1.

Griffiths, R. E., U. Briel, L. Chaisson, and S. Tapia (1979), Optical and x-ray properties of the newly discovered bl lacertae object pks 2155-304 /= h2155-304/, *Astrophys. J.*, *234*, 810–817, doi:10.1086/157560.

Gupta, A. C., et al. (2008), Multicolor near-infrared intra-day and short-term variability of the blazar s5 0716+714, *The Astronomical Journal*, *136*, 2359–2366, doi:10.1088/0004-6256/136/6/2359.

Gupta, S. P., U. S. Pandey, K. Singh, B. Rani, J. Pan, J. H. Fan, and A. C. Gupta (2012), Optical intra-day variability timescales and black hole mass of the blazars, *New Astronomy*, *17*, 8–17, doi:10.1016/j.newast.2011.05.005.

Hamuy, M., and J. Maza (1989), Ubvri photoelectric photometry in the fields of fifteen active galaxies, *The Astronomical Journal*, *97*, 720–725, doi:10.1086/115017.

Hartman, R. C., et al. (1999), The third egret catalog of high-energy gamma-ray sources, *Astrophys. J., Suppl.*, *123*, 79–202, doi:10.1086/313231.

Hazard, C., M. B. Mackey, and A. J. Shimmins (1963), Investigation of the Radio Source 3C 273 By The Method of Lunar Occultations, *Nature*, *197*, 1037.

H.E.S.S. Collaboration, et al. (2010), Pks 2005-489 at vhe: four years of monitoring with hess and simultaneous multi-wavelength observations, *Astronomy & Astrophysics*, *511*, A52, doi:10.1051/0004-6361/200913073.

H.E.S.S. Collaboration, et al. (2011), Simultaneous multi-wavelength campaign on pks 2005-489 in a high state, *Astronomy & Astrophysics*, *533*, A110, doi:10.1051/0004-6361/201016170.

H.E.S.S. Collaboration, et al. (2012), A multiwavelength view of the flaring state of pks 2155-304 in 2006, *Astronomy & Astrophysics*, *539*, A149, doi:10.1051/0004-6361/201117509.

Hey, J. S., S. J. Parsons, and P. J. W (1947), Fluctuations in Cosmic Radiation at Radio-Frequencies, *Nature*, *158*, 234.

Hoffmeister, C. (1929), 354 neue Veränderliche, *Astronomische Nachrichten*, *236*, 233.

Howell, S. B. (1989), Two-dimensional aperture photometry - signal-to-noise ratio of point-source observations and optimal data-extraction techniques, *Publications of the Astronomical Society of the Pacific*, *101*, 616–622, doi:10.1086/132477.

Howell, S. B., A. Warnock, III, and K. J. Mitchell (1988), Statistical error analysis in ccd time-resolved photometry with applications to variable stars and quasars, *The Astronomical Journal*, *95*, 247–256, doi:10.1086/114634.

Hubble, E. P. (1926), Extragalactic nebulae., *Astrophysical Journal*, *64*, 321–369.

Hudec, R. (2010), The role of ground-based robotic observatories in satellite projects, *Advances in Astronomy*, doi:10.1155/2010/594854.

Institute of Physics (2013), Welcome rise in leaving certificate physics but it's not enough, Available at http://www.iopireland.org/news/13/aug/page_60885.html, [accessed 05-July-2014].

Jang, M., and H. R. Miller (1997), The microvariability of selected radio-quiet and radio-loud qsos., *The Astronomical Journal*, *114*, 565–574, doi:10.1086/118493.

Johnson, H. L., and W. W. Morgan (1953), Fundamental stellar photometry for standards of spectral type on the revised system of the yerkes spectral atlas, *Astrophys. J.*, *117*, 313, doi:10.1086/145697.

Kaufmann, S., et al. (2009), Broadband multi-wavelength campaign on pks 2005-489, *ArXiv e-prints*.

Kiepenheuer, K. O. (1950), Cosmic Rays as the Source of General Galactic Radio Emission, *Physical Review*, *79*(4), 738–739.

Kisaka, S., and Y. Kojima (2011), Multi-wavelength emission region of gamma-ray pulsars, *2011 Fermi Symposium proceedings*.

Kristian, J. (1973), Quasars as Events in the Nuclei of Galaxies: the Evidence from Direct Photographs, *Astrophysical Journal*, *179*, L61.

Lenain, J.-P., et al. (2008), Pks 2155-304 in july 2006: H.e.s.s. results and simultaneous multi-wavelength observations, in *American Institute of Physics Conference Series*, *American Institute of Physics Conference Series*, vol. 1085, edited by F. A. Aharonian, W. Hofmann, and F. Rieger, pp. 415–418, doi:10.1063/1.3076696.

Likert, R. (1932), A technique for the measurement of attitudes., *Archives of psychology*.

Longair, S. M. (2011), *High Energy Astrophysics*, Cambridge University Press.

Maltese, A. V., and R. H. Tai (2010), Eyeballs in the fridge: Sources of early interest in science, *International Journal of Science Education*, *32*(5), 669–685, doi:10.1080/09500690902792385.

Marscher, A. P. (1996), Variability of the non-thermal emission in the jets of blazars, in *Blazar Continuum Variability*, *Astronomical Society of the Pacific Conference Series*, vol. 110, edited by H. R. Miller, J. R. Webb, and J. C. Noble, p. 248.

Matthews, T. A., and A. R. Sandage (1963), Optical Identification of 3C 48, 3C 196, and 3C 286 with Stellar Objects., *Astrophysical Journal*, *138*, 30.

Matthews, T. A., J. G. Bolton, J. L. Greenstein, M. G, and A. R. Sandage (1961), American Astronomical Society Meeting, New York, *Sky and Telescope*, *21*, 148.

Monet, D. e. a. (1998), A catalogue of astrometric standards., *VizieR Online Data Catalog*, *1252*, 0.

Morris, D., H. P. Palmer, and A. R. Thompson (1957), Five radio sources of small angular diameter, *The Observatory*, *77*, 103–106.

Muller, C. L., et al. (2013), The blue marble: a model for primary school stem outreach, *Physics Education*, *48*(2), 176.

Nishijima, K. (2002), Very high energy gamma-ray observations of agn with cangaroo, *Publications of the Astronomical Society of Australia*, *19*, 26–28, doi:10.1071/AS01089.

Oke, J. B. (1963), Absolute Energy Distribution in the Optical Spectrum of 3C 273, *Nature*, *197*, 1040–1041.

Paltani, S., T. J.-L. Courvoisier, A. Blecha, and P. Bratschi (1997), Very rapid optical variability of pks 2155-304., *Astronomy & Astrophysics*, *327*, 539–549.

Patiño-Álvarez, V., A. Carramiñana, L. Carrasco, and V. Chavushyan (2013), A multiwavelength cross-correlation variability study of fermi-lat blazars, *2012 Fermi Symposium Proceedings*.

Pearson Education, Inc. (2008), Synchrotron radiation, Available at http://pages.uoregon.edu/jimbrau/BrauImNew/Chap24/6th/24_35Figurea-F.jpg, [accessed 15-July-2014].

Perlman, E. S., G. Madejski, J. T. Stocke, and T. A. Rector (1999), X-ray spectral variability of pks 2005-489 during the spectacular 1998 november flare, *Astrophys. J., Lett.*, *523*, L11–L15, doi:10.1086/312260.

Pohl, M., and R. Schlickeiser (2000), On the conversion of blast wave energy into radiation in active galactic nuclei and gamma-ray bursts, *Astronomy & Astrophysics*, *354*, 395–410.

Rector, T. A., and E. S. Perlman (2003), A search for intraday variability in the blazar pks 2005-489, *The Astronomical Journal*, *126*, 47–52, doi:10.1086/375644.

Royal Society (2004), *Taking a Leading Role: A Good Practice Guide for All Those Involved in Role Model Schemes Aiming to Inspire Young People about Science, Engineering and Technology*, Royal Society.

Rutledge, R. E. (1998), The astronomer's telegram: A web-based short-notice publication system for the professional astronomical community, *The Publications of the Astronomical Society of the Pacific*, *110*, 754–756, doi:10.1086/316184.

Ryle, M., F. G. Smith, and B. Elsmore (1950), A preliminary survey of the radio stars in the Northern Hemisphere, *Monthly Notices of the Royal Astronomical Society*, *110*, 508.

Sandage, A. (1965), The Existence of a Major New Constituent of the Universe: the Quasistellar Galaxies., *Astrophysical Journal*, *141*, 1560.

Schmidt, M. (1963), The Quasar Enigma Solved, *Nature*, *197*, 1040–1041.

Schmitt, J. L. (1968), BL Lac identified as a Radio Source, *Nature*, *218*(5), 663.

Seyfert, C. K. (1943), Nuclear Emission in Spiral Nebulae., *Astrophysical Journal*, *97*, 28.

Slipher, V. M. (1917), The spectrum and velocity of the nebula N.G.C. 1068 (M 77), *Lowell Observatory Bulletin*, *3*, 59–62.

Smith, F. G. (1951), An Accurate Determination of the Positions of Four Radio Stars, *Nature*, *168*(4274), 555–555.

Stalin, C. S., Gopal-Krishna, R. Sagar, and P. J. Wiita (2004), Intranight optical variability of radio-quiet and radio lobe-dominated quasars, *Mon. Not. R. Astron. Soc.*, *350*, 175–188, doi:10.1111/j.1365-2966.2004.07631.x.

Stein, W. A., S. L. Odell, and P. A. Strittmatter (1976), The BL Lacertae objects, *In: Annual review of Astronomy and Astrophysics. Volume 14. (A76-46826 24-90) Palo Alto*, *14*, 173–195.

Strittmatter, P. A., K. Serkowski, R. Carswell, W. A. Stein, K. M. Merrill, and E. M. Burbidge (1972), Compact Extragalactic Nonthermal Sources, *Astrophysical Journal*, *175*, L7.

Strómgren, B. (1956), Two-dimensional spectral classification of f stars through photoelectric photometry with interference filters, *Vistas in Astronomy*, *2*, 1336–1346, doi:10.1016/0083-6656(56)90060-5.

Tai, R. H., C. Qi Liu, A. V. Maltese, and X. Fan (2006), Career choice. Planning early for careers in science., *Science (New York, N.Y.)*, *312*(5777), 1143–4, doi:10.1126/science.1128690.

Tody, D. (1993), Iraf in the nineties, *stronomical Data Analysis Software and Systems II, A.S.P. Conference Series*, *52*, 173.

Torres, D. F., and L. A. Anchordoqui (2004), Astrophysical Origins of Ultrahigh Energy Cosmic Rays, *arXiv.org*, *astro-ph*.

Urry, C. M. (1996), An overview of blazar variability, in *Blazar Continuum Variability*, *Astronomical Society of the Pacific Conference Series*, vol. 110, edited by H. R. Miller, J. R. Webb, and J. C. Noble, p. 391.

Urry, C. M. (1998), Multiwavelength properties of blazars, *Advances in Space Research*, *21*, 89–100, doi:10.1016/S0273-1177(97)00619-4.

Urry, C. M., and P. Padovani (1995), Unified Schemes for Radio-Loud Active Galactic Nuclei, *Publications of the Astronomical Society of the Pacific*, *astro-ph*, 803.

Vestrand, W. T., J. G. Stacy, and P. Sreekumar (1995), High-energy gamma rays from the bl lacertae object pks 2155-304, *Astrophys. J., Lett.*, *454*, L93, doi:10.1086/309790.

Villforth, C., et al. (2010), Variability and stability in blazar jets on timescales of years: optical polarization monitoring of oj287 in 2005-2009, *Monthly Notices of the Royal Astronomical Society*, *402*(3), 2087–2111, doi:10.1111/j.1365-2966.2009.16133.x.

Wall, J. V., A. J. Shimmins, and J. G. Bolton (1975), The parkes 2700 mhz survey (ninth part): Supplementary catalogue for the declination zone -45^o to -65^o, *Australian Journal of Physics Astrophysical Supplement*, *34*, 55.

Zhang, Y. H., et al. (2002), Four years of monitoring blazar pks 2155-304 with bepposax: Probing the dynamics of the jet, *Astrophys. J.*, *572*, 762–785, doi:10.1086/340349.

Zwicky, F. (1966), Compact Galaxies and Compact Parts of Galaxies. II, *Astrophysical Journal*, *143*, 192.

List of Publications

A. Martin-Carrillo, L. Hanlon, M. Topinka, +20 authors (P. Tisdall 10th) – "GRB 120711A: an intense INTEGRAL burst with long-lasting soft γ-ray emission and a powerful optical flash" – *Astronomy and Astrophysics*, vol. 567:A84

M. Topinka, S. Meehan, L. Hanlon, +6 authors (P. Tisdall 1st) "Status update of the Watcher Robotic Telescope" – *EAS Publications Series*, vol. 61:487

M. Topinka, L. Hanlon, P. Tisdall, et al. – "GRB 130427A, watcher afterglow detection" – *GRB Coordinates Network*, vol. 14598:1

P. Tisdall, L. Hanlon, D. Murphy, et al. – "Blazar Monitoring with the Watcher Robotic Telescope"– *Third Workshop on Robotic Autonomous Observatories (2013)*

Appendix A

A.1 PKS 2005-489

Date	Filter	Number of Images	Observed C-Test	Observed F-Test	F Critical Value
12/07/13	I	100	3.277	2.003	1.873
	R	99	2.806	1.889	1.880
	V	92	2.123	1.276	1.926
18/07/13	I	12	1.878	2.315	7.761
	R	14	1.175	1.931	6.409
20/07/13	I	159	2.294	2.071	1.640
	R	158	2.673	1.832	1.643
	V	131	1.466	1.361	1.727
22/07/13	I	14	1.960	1.394	6.409
	R	11	1.863	1.989	8.754
	V	9	1.295	0.878	12.046
23/07/13	I	27	2.396	5.010	3.532
	R	25	2.254	4.596	3.735
	V	27	2.113	5.031	3.532
25/07/13	I	36	2.562	2.966	2.934
	R	36	2.316	2.729	2.934
	V	31	2.319	3.019	3.217
26/07/13	I	86	2.857	4.135	1.971
	R	86	1.373	1.330	1.971
	V	78	2.287	1.832	2.042
31/07/13	I	53	3.204	2.667	2.398

Date	Filter	Number of Images	Observed C-Test	Observed F-Test	F Critical Value
	R	54	2.256	1.076	2.377
	V	54	3.011	1.637	2.377
02/08/13	I	88	3.649	2.980	1.955
	R	90	3.551	1.547	1.940
	V	81	1.970	1.207	2.014
03/08/13	I	26	1.904	0.949	3.629
	R	26	2.314	1.229	3.629
	V	25	2.530	0.905	3.735
08/08/13	I	4	4.767	22.027	141.108
	R	4	3.543	26.979	141.108
	V	4	3.623	9.991	141.108
11/08/13	I	89	1.981	1.503	1.948
	R	90	3.426	1.167	1.940
	V	86	2.952	1.155	1.971
13/08/13	I	171	2.493	1.797	1.611
	R	175	2.814	1.648	1.602
	V	151	2.357	1.249	1.662
14/08/13	I	149	2.285	0.774	1.668
	R	169	2.341	1.075	1.616
	V	150	2.323	0.973	1.665
15/08/13	I	130	1.789	1.364	1.731
	R	131	2.340	1.520	1.727
	V	130	1.661	1.305	1.731
16/08/13	I	192	2.759	2.031	1.568
	R	191	2.927	1.571	1.570
	V	180	1.366	1.188	1.591
17/08/13	I	169	2.858	2.118	1.616
	R	167	2.783	1.347	1.620
	V	143	2.324	1.231	1.686
19/08/13	I	125	2.467	1.690	1.750
	R	124	2.307	1.227	1.754

Date	Filter	Number of Images	Observed C-Test	Observed F-Test	F Critical Value
	V	115	1.971	0.809	1.794
20/08/13	I	113	2.749	2.197	1.803
	R	109	2.433	2.010	1.823
	V	87	1.893	0.943	1.963
21/08/13	I	138	2.776	1.758	1.702
	R	138	1.965	1.567	1.702
	V	128	2.054	1.676	1.738
22/08/13	I	160	2.514	2.662	1.638
	R	160	3.244	2.399	1.638
	V	144	2.462	2.014	1.683
23/08/13	I	186	1.608	0.697	1.579
	R	183	2.525	0.882	1.585
	V	172	1.500	0.903	1.609
24/08/13	I	174	2.289	1.085	1.604
	R	173	1.833	1.060	1.607
	V	162	1.477	1.083	1.633
25/08/13	I	64	1.575	1.021	2.207
	R	71	1.903	1.053	2.117
	V	44	1.094	1.325	2.627
26/08/13	I	3	4.598	4.838	999.000
	R	4	1.883	2.000	141.108
	V	3	4.031	3.799	999.000
05/09/13	I	16	2.269	1.891	5.535
	R	16	2.286	1.148	5.535
	V	15	1.693	1.041	5.930
06/09/13	I	25	2.634	1.023	3.735
	R	25	0.787	0.788	3.735
	V	21	2.290	0.841	4.290
08/09/13	I	4	4.084	1.791	141.108
	V	4	7.917	1.433	141.108
09/09/13	I	12	1.436	1.141	7.761

Date	Filter	Number of Images	Observed C-Test	Observed F-Test	F Critical Value
	R	10	1.606	0.609	10.107
	V	11	1.450	0.973	8.754
13/09/13	I	15	1.304	0.690	5.930
	R	18	1.552	0.689	4.924
	V	14	0.992	0.787	6.409
17/09/13	I	26	2.443	2.232	3.629
	R	26	2.633	2.974	3.629
	V	21	1.531	1.172	4.290
18/09/13	I	32	1.416	0.827	3.152
	R	29	2.939	0.963	3.362
	V	27	1.395	0.971	3.532
25/09/13	I	18	2.836	1.038	4.924
	R	17	3.303	0.951	5.205
	V	17	1.938	1.038	5.205
27/09/13	I	37	3.400	1.991	2.888
	R	37	3.437	1.552	2.888
	V	35	3.171	1.466	2.983
28/09/13	I	38	3.202	1.233	2.844
	R	37	3.690	1.441	2.888
	V	37	2.696	1.109	2.888
29/09/13	I	37	2.196	0.828	2.888
	R	38	1.914	0.730	2.844
	V	36	1.728	0.889	2.934
30/09/13	I	38	3.846	3.805	2.844
	R	38	2.744	3.147	2.844
	V	37	4.058	5.600	2.888
01/10/13	I	37	3.357	4.944	2.888
	R	38	3.755	4.506	2.844
	V	38	2.018	3.666	2.844
02/10/13	I	18	2.082	1.339	4.924
	R	18	2.794	1.845	4.924

Date	Filter	Number of Images	Observed C-Test	Observed F-Test	F Critical Value
	V	18	1.472	1.551	4.924
03/10/13	I	17	2.502	3.948	5.205
	R	17	3.272	1.999	5.205
	V	16	2.503	3.423	5.535
04/10/13	I	39	2.839	4.055	2.803
	R	38	2.991	3.804	2.844
	V	37	1.718	4.933	2.888
06/10/13	I	27	2.494	0.859	3.532
	R	31	2.270	1.088	3.217
	V	29	1.242	1.121	3.362
07/10/13	I	35	1.888	2.285	2.983
	R	35	4.191	7.779	2.983
	V	33	1.968	3.475	3.092
09/10/13	I	17	2.282	4.209	5.205
	R	17	3.049	6.732	5.205
	V	14	1.653	1.643	6.409
10/10/13	I	17	2.809	2.655	5.205
	R	18	3.619	3.791	4.924
	V	16	1.666	2.389	5.535
12/10/13	I	9	0.965	1.055	12.046
	R	12	1.810	2.467	7.761
	V	6	2.722	3.924	29.752
13/10/13	I	23	3.080	4.265	3.983
	R	23	2.895	3.899	3.983
	V	20	1.860	3.393	4.474
14/10/13	I	25	2.039	2.015	3.735
	R	24	1.947	1.620	3.853
	V	23	2.957	2.655	3.983
15/10/13	I	28	2.805	2.637	3.443
	R	25	2.191	3.324	3.735
	V	27	1.895	1.728	3.532

Date	Filter	Number of Images	Observed C-Test	Observed F-Test	F Critical Value
16/10/13	I	38	2.031	3.860	2.844
	R	36	1.681	2.104	2.934
	V	36	1.896	2.604	2.934
17/10/13	I	20	3.195	7.871	4.474
	R	23	2.539	5.106	3.983
	V	24	1.729	2.292	3.853
18/10/13	I	11	2.344	0.552	8.754
	R	13	2.109	0.780	7.005
	V	10	2.458	0.416	10.107
22/10/13	I	18	2.824	4.819	4.924
	R	18	2.696	3.305	4.924
	V	18	2.369	4.505	4.924

A.2 PKS 2155-304

Date	Filter	Number of Images	Observed C-Test	Observed F Test	F Critical Value
11/07/13	I	124	2.515	0.910	1.754
	R	129	2.331	0.953	1.735
	V	126	1.925	0.973	1.746
16/07/13	I	10	1.400	1.367	10.107
	R	9	0.686	0.093	12.046
	V	9	0.656	0.109	12.046
17/07/13	I	5	2.635	1.186	53.436
	R	6	2.535	0.779	29.752
	V	5	1.019	0.753	53.436
18/07/13	I	66	2.245	1.092	2.179
	R	65	1.843	0.838	2.193
	V	55	2.355	0.967	2.357
21/07/13	I	73	1.414	0.774	2.094
	R	72	1.781	0.686	2.105
	V	71	1.687	0.881	2.117
23/07/13	I	60	1.559	1.054	2.268
	R	59	1.472	1.240	2.285
	V	52	1.711	1.069	2.419
24/07/13	I	75	1.740	1.262	2.072
	R	73	1.779	0.687	2.094
	V	70	1.877	0.518	2.128
25/07/13	I	67	1.423	0.516	2.166
	R	64	1.183	0.491	2.207
	V	63	1.694	0.616	2.222
26/07/13	I	78	1.560	0.629	2.042
	R	73	1.401	0.568	2.094
	V	73	1.312	1.062	2.094
31/07/13	I	111	1.499	1.139	1.813
	R	114	1.651	1.223	1.798
	V	112	1.370	1.306	1.808

Date	Filter	Number of Images	Observed C-Test	Observed F Test	F Critical Value
02/08/13	I	104	1.580	0.550	1.850
	R	102	0.969	0.708	1.862
	V	104	1.384	0.913	1.850
03/08/13	I	97	1.205	1.009	1.892
	R	93	1.126	0.914	1.919
	V	94	1.285	1.019	1.912
08/08/13	I	15	4.057	0.887	5.930
	R	16	3.406	0.936	5.535
	V	14	2.383	0.955	6.409
20/08/13	I	7	1.996	0.855	20.030
	R	7	2.331	1.982	20.030
	V	7	2.131	2.179	20.030
22/08/13	I	9	1.354	1.697	12.046
	R	9	0.725	0.933	12.046
	V	9	1.183	1.115	12.046
24/08/13	I	6	1.763	1.506	29.752
	R	7	2.141	0.733	20.030
	V	6	2.308	0.648	29.752
25/08/13	I	10	2.619	1.339	10.107
	R	9	1.661	1.246	12.046
	V	9	1.918	0.833	12.046
26/08/13	I	8	2.198	1.806	15.019
	R	8	1.630	1.464	15.019
	V	5	3.837	0.217	53.436
27/08/13	I	36	1.574	0.859	2.934
	R	36	2.405	0.958	2.934
	V	34	2.126	0.965	3.036
28/08/13	I	40	1.834	1.119	2.764
	R	38	1.477	0.883	2.844
	V	37	1.245	1.043	2.888
29/08/13	I	33	1.141	1.152	3.092

Date	Filter	Number of Images	Observed C-Test	Observed F Test	F Critical Value
	R	35	1.616	1.367	2.983
	V	21	1.691	1.234	4.290
30/08/13	I	29	1.601	0.960	3.362
	R	29	1.335	1.035	3.362
	V	23	2.711	0.908	3.983
31/08/13	I	38	2.163	0.448	2.844
	R	38	1.747	1.024	2.844
	V	39	2.257	0.926	2.803
04/09/13	I	39	1.595	0.831	2.803
	R	36	1.469	0.871	2.934
	V	36	1.247	0.933	2.934
05/09/13	I	70	1.160	1.331	2.128
	R	69	1.209	1.161	2.141
	V	69	1.169	1.132	2.141
06/09/13	I	30	0.832	1.611	3.287
	R	28	2.151	1.263	3.443
	V	27	1.779	1.193	3.532
07/09/13	I	57	1.662	0.904	2.320
	R	59	1.171	1.009	2.285
	V	42	1.381	1.004	2.692
08/09/13	I	63	1.248	0.962	2.222
	R	62	2.030	1.007	2.237
	V	61	1.234	1.026	2.252
09/09/13	I	19	1.387	0.878	4.683
	R	21	3.424	1.090	4.290
	V	17	3.368	1.006	5.205
10/09/13	I	40	1.786	1.014	2.764
	R	42	2.257	0.920	2.692
	V	32	1.397	1.007	3.152
11/09/13	I	7	1.796	1.111	20.030
	R	8	1.220	0.921	15.019

Date	Filter	Number of Images	Observed C-Test	Observed F Test	F Critical Value
	V	8	1.278	0.905	15.019
13/09/13	I	84	1.952	0.910	1.988
	R	84	1.815	0.943	1.988
	V	75	1.597	0.932	2.072
15/09/13	I	85	2.174	0.712	1.979
	R	83	1.555	0.853	1.996
	V	82	1.431	0.827	2.005
17/09/13	I	58	1.093	1.069	2.302
	R	55	1.428	0.945	2.357
	V	55	1.523	0.996	2.357
18/09/13	I	61	1.411	1.261	2.252
	R	61	1.389	0.987	2.252
	V	38	1.728	1.480	2.844
25/09/13	I	18	3.157	0.976	4.924
	R	20	2.213	1.048	4.474
	V	17	2.079	0.989	5.205
27/09/13	I	105	0.936	0.814	1.844
	R	105	2.174	1.025	1.844
	V	103	1.376	0.880	1.856
28/09/13	I	107	1.693	0.899	1.834
	R	107	1.927	0.859	1.834
	V	106	1.053	0.958	1.839
29/09/13	I	48	1.851	1.163	2.514
	R	48	1.253	1.200	2.514
	V	48	1.351	1.194	2.514
30/09/13	I	48	1.315	0.941	2.514
	R	48	1.125	0.916	2.514
	V	47	1.239	0.900	2.540
01/10/13	I	29	1.666	0.182	3.362
	R	28	1.825	0.239	3.443
	V	28	1.209	0.187	3.443

Date	Filter	Number of Images	Observed C-Test	Observed F Test	F Critical Value
03/10/13	I	47	1.591	0.320	2.540
	R	46	1.364	0.348	2.568
	V	46	1.817	0.280	2.568
04/10/13	I	28	1.509	0.410	3.443
	R	29	1.644	0.309	3.362
	V	29	1.274	0.482	3.362
06/10/13	I	14	0.593	1.253	6.409
	R	16	0.779	1.042	5.535
	V	11	0.645	0.973	8.754
07/10/13	I	28	1.434	0.444	3.443
	R	28	1.247	0.766	3.443
	V	29	1.536	1.843	3.362
08/10/13	I	20	1.218	1.784	4.474
	R	19	1.677	1.050	4.683
	V	19	0.806	1.066	4.683
09/10/13	I	48	1.293	0.189	2.514
	R	48	0.886	0.284	2.514
	V	47	1.815	0.676	2.540
10/10/13	I	36	1.749	0.711	2.934
	R	34	2.217	0.881	3.036
11/10/13	I	14	1.922	1.089	6.409
	R	13	1.747	1.098	7.005
	V	13	1.446	1.023	7.005
12/10/13	I	24	1.609	0.987	3.853
	R	24	1.308	0.974	3.853
	V	21	1.508	0.912	4.290
13/10/13	I	27	1.711	0.438	3.532
	R	28	1.240	0.442	3.443
	V	27	0.994	0.513	3.532
14/10/13	I	27	1.796	0.863	3.532
	R	27	1.448	0.844	3.532

Date	Filter	Number of Images	Observed C-Test	Observed F Test	F Critical Value
	V	27	1.214	0.611	3.532
15/10/13	I	28	2.510	0.773	3.443
	R	29	1.698	0.865	3.362
	V	29	1.726	1.054	3.362
16/10/13	I	20	2.126	3.326	4.474
	R	19	1.621	2.937	4.683
	V	18	1.973	3.993	4.924
17/10/13	I	19	1.787	0.776	4.683
	V	17	2.133	0.819	5.205
18/10/13	I	6	0.687	1.071	29.752
	R	6	0.552	3.031	29.752
	V	3	1.656	5.476	999.000
22/10/13	I	16	2.774	1.370	5.535
	R	19	2.371	1.973	4.683
	V	15	1.467	1.165	5.930
23/10/13	I	46	1.819	0.241	2.568
	R	46	2.647	0.533	2.568
	V	44	1.444	0.376	2.627
30/10/13	I	21	0.979	0.914	4.290
	V	16	1.623	1.121	5.535
01/11/13	I	10	1.131	0.393	10.107
	R	9	1.745	0.925	12.046
	V	9	1.099	1.613	12.046
02/11/13	I	19	2.834	1.086	4.683
	R	23	0.970	1.165	3.983
	V	16	1.235	0.769	5.535
03/11/13	I	17	2.283	1.661	5.205
	R	18	1.302	0.341	4.924
	V	16	1.339	0.334	5.535
07/11/13	I	10	2.062	5.114	10.107
	R	10	2.375	0.123	10.107

Date	Filter	Number of Images	Observed C-Test	Observed F Test	F Critical Value
	V	9	1.454	0.882	12.046
08/11/13	I	8	1.815	0.632	15.019
	V	9	1.606	1.482	12.046
09/11/13	I	10	2.738	0.626	10.107
	R	9	1.172	0.523	12.046
	V	9	1.607	0.456	12.046
10/11/13	I	8	2.424	0.544	15.019
	R	9	1.197	0.749	12.046
	V	9	1.131	2.153	12.046
11/11/13	I	17	1.882	1.188	5.205
	R	17	1.718	0.980	5.205
	V	16	2.937	0.950	5.535
12/11/13	I	17	2.770	1.070	5.205
	R	18	2.058	0.924	4.924
	V	17	1.952	1.142	5.205

Appendix B

The full database of nightly lightcurves for PKS 2005-489 and PKS 2155-304 can be found at www.watchertelescope.ie/files/petetisdall/AppendixB.pdf

B.1 PKS 2005-489

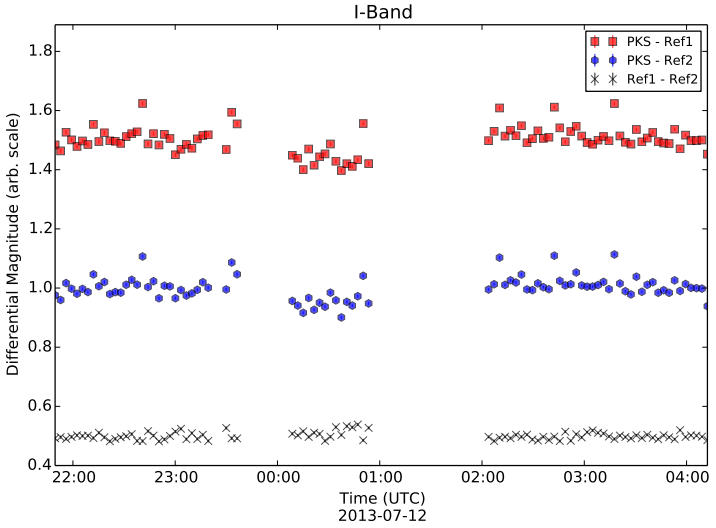

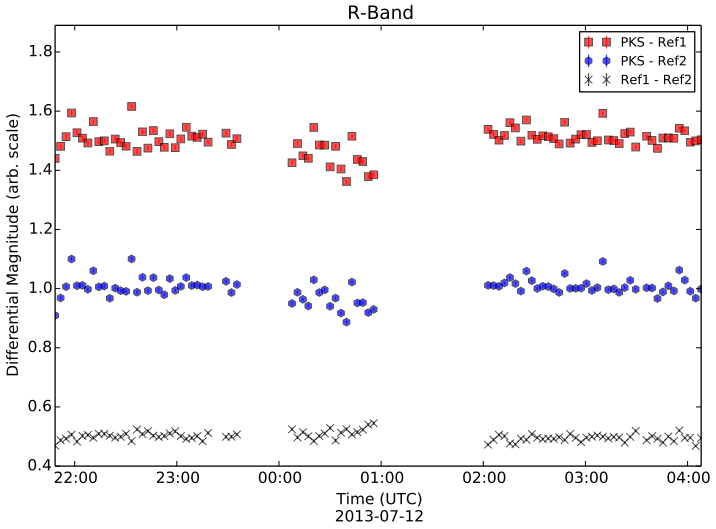

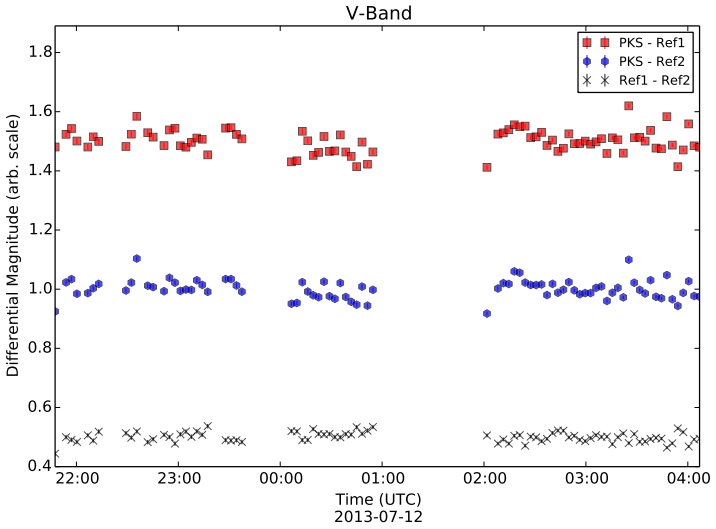

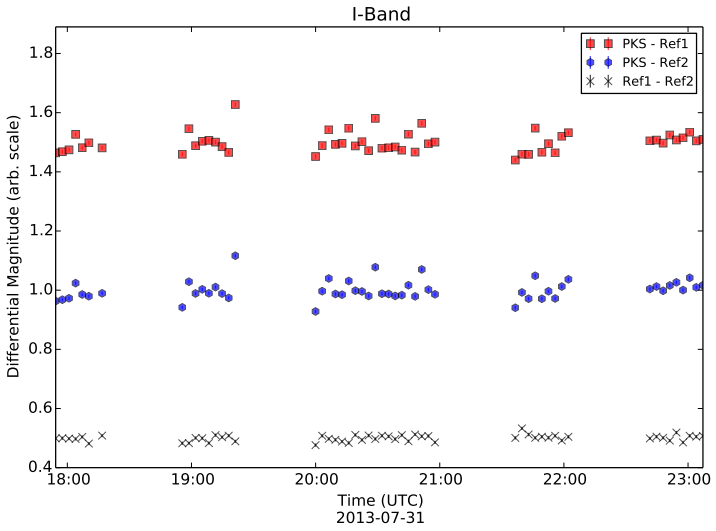
I-Band
PKS - Ref1
PKS - Ref2
Ref1 - Ref2
Differential Magnitude (arb. scale)
1.8
1.6
1.4
1.2
1.0
0.8
0.6
0.4
18:00
19:00
20:00
21:00
22:00
23:00
Time (UTC)
2013-07-31

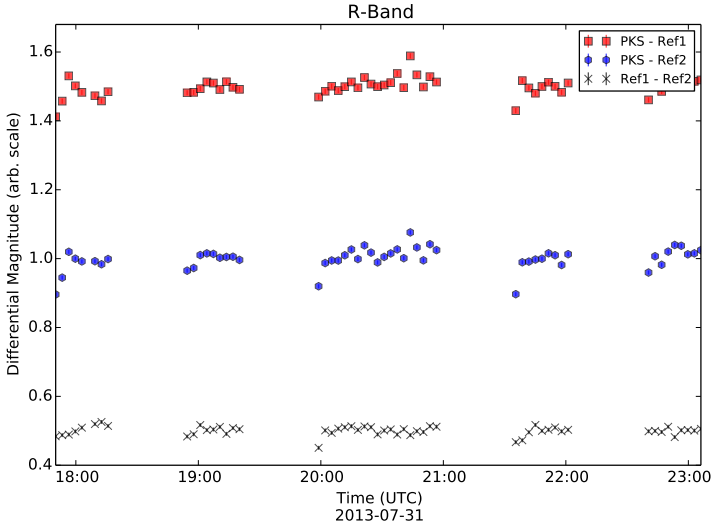
R-Band
PKS - Ref1
PKS - Ref2
Ref1 - Ref2
Differential Magnitude (arb. scale)
1.6
1.4
1.2
1.0
0.8
0.6
0.4
18:00
19:00
20:00
21:00
22:00
23:00
Time (UTC)
2013-07-31

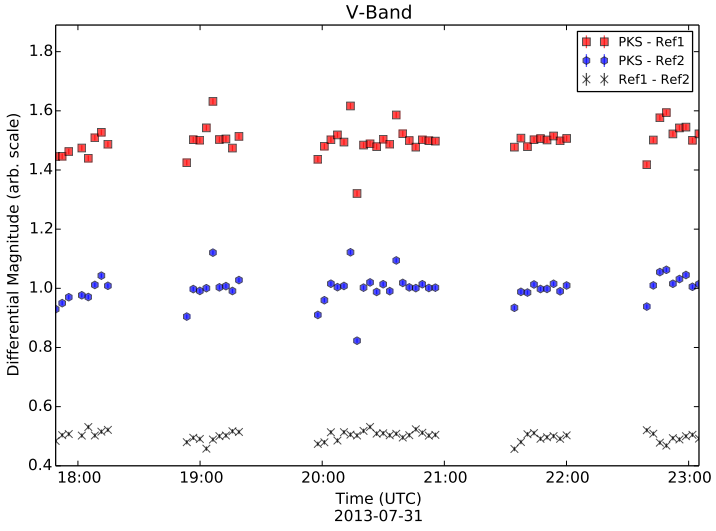
V-Band
PKS - Ref1
PKS - Ref2
Ref1 - Ref2
Differential Magnitude (arb. scale)
1.8
1.6
1.4
1.2
1.0
0.8
0.6
0.4
18:00
19:00
20:00
21:00
22:00
23:00
Time (UTC)
2013-07-31

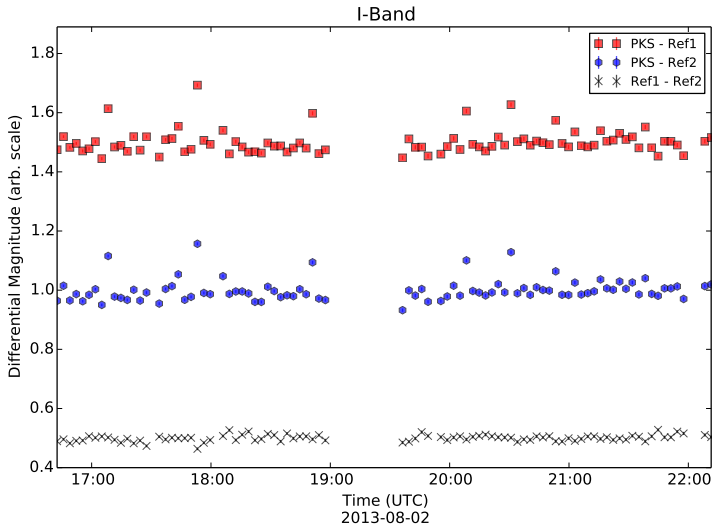
I-Band
PKS - Ref1
PKS - Ref2
Ref1 - Ref2
Differential Magnitude (arb. scale)
1.8
1.6
1.4
1.2
1.0
0.8
0.6
0.4
17:00
18:00
19:00
20:00
21:00
22:00
Time (UTC)
2013-08-02

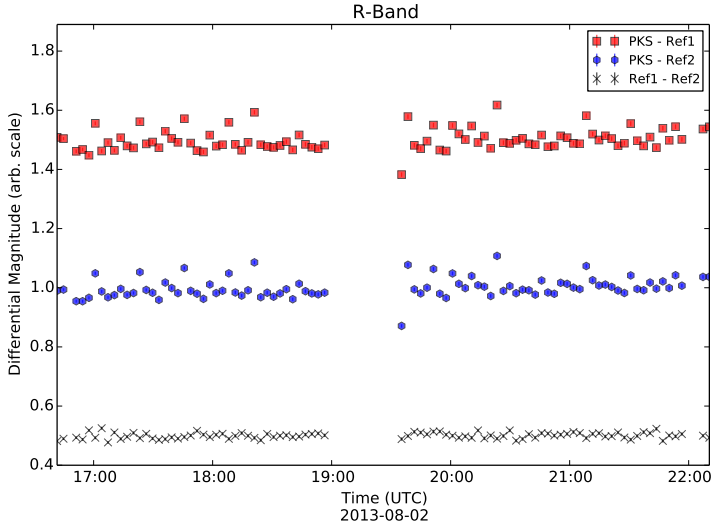
R-Band
PKS - Ref1
PKS - Ref2
Ref1 - Ref2
Differential Magnitude (arb. scale)
1.8
1.6
1.4
1.2
1.0
0.8
0.6
0.4
17:00
18:00
19:00
20:00
21:00
22:00
Time (UTC)
2013-08-02

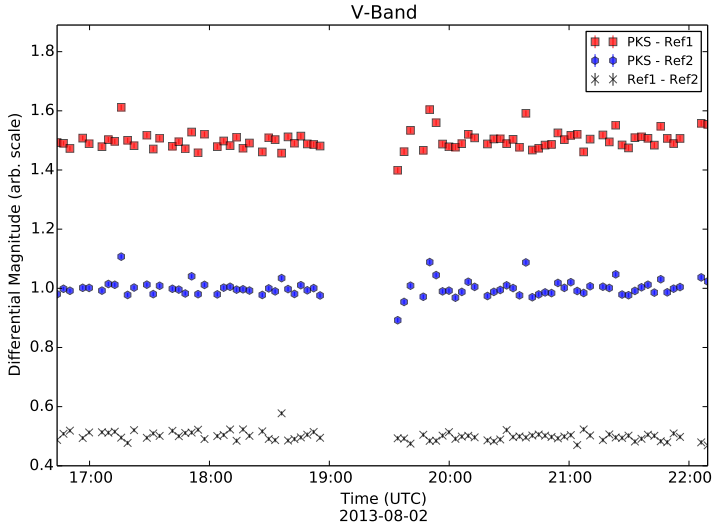
V-Band
PKS - Ref1
PKS - Ref2
Ref1 - Ref2
Differential Magnitude (arb. scale)
1.8
1.6
1.4
1.2
1.0
0.8
0.6
0.4
17:00
18:00
19:00
20:00
21:00
22:00
Time (UTC)
2013-08-02

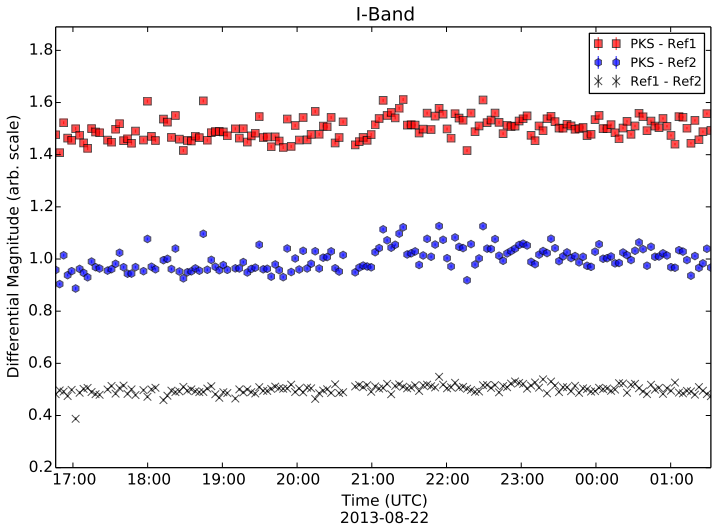
I-Band
PKS - Ref1
PKS - Ref2
Ref1 - Ref2
Differential Magnitude (arb. scale)
1.8
1.6
1.4
1.2
1.0
0.8
0.6
0.4
0.2
17:00
18:00
19:00
20:00
21:00
22:00
23:00
00:00
01:00
Time (UTC)
2013-08-22

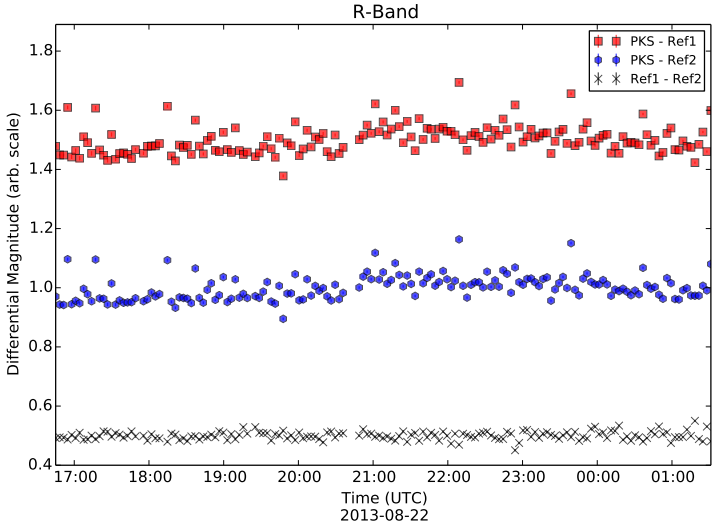
R-Band
PKS - Ref1
PKS - Ref2
Ref1 - Ref2
Differential Magnitude (arb. scale)
1.8
1.6
1.4
1.2
1.0
0.8
0.6
0.4
17:00
18:00
19:00
20:00
21:00
22:00
23:00
00:00
01:00
Time (UTC)
2013-08-22

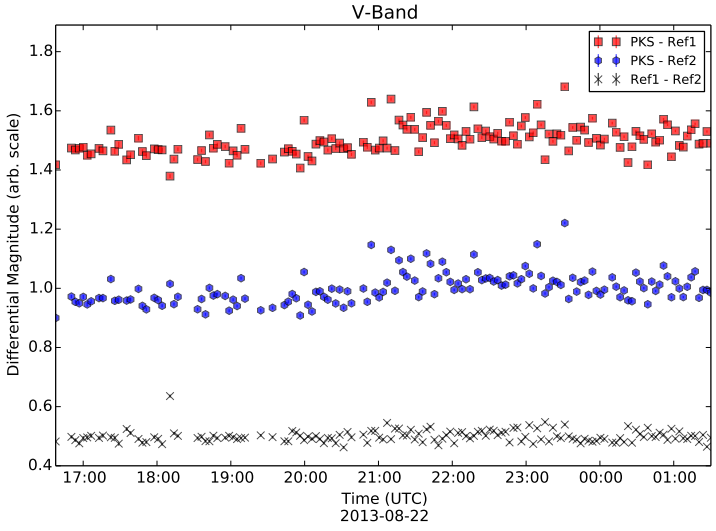
V-Band
PKS - Ref1
PKS - Ref2
Ref1 - Ref2
Differential Magnitude (arb. scale)
1.8
1.6
1.4
1.2
1.0
0.8
0.6
0.4
17:00
18:00
19:00
20:00
21:00
22:00
23:00
00:00
01:00
Time (UTC)
2013-08-22

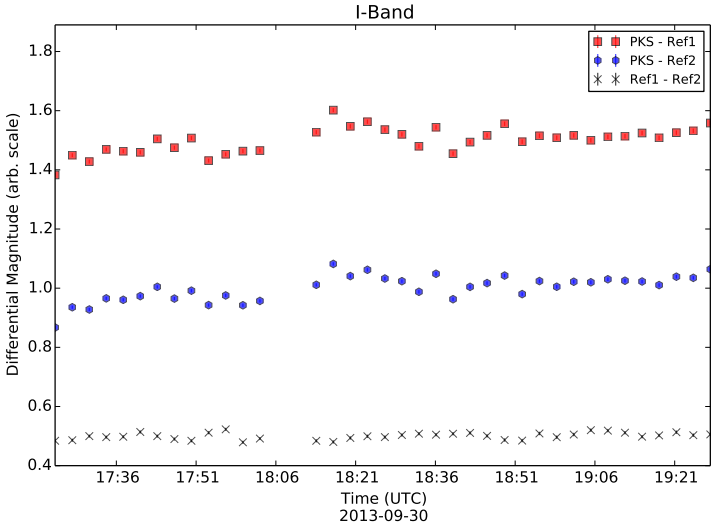
I-Band
PKS - Ref1
PKS - Ref2
Ref1 - Ref2
Differential Magnitude (arb. scale)
1.8
1.6
1.4
1.2
1.0
0.8
0.6
0.4
17:36
17:51
18:06
18:21
18:36
18:51
19:06
19:21
Time (UTC)
2013-09-30

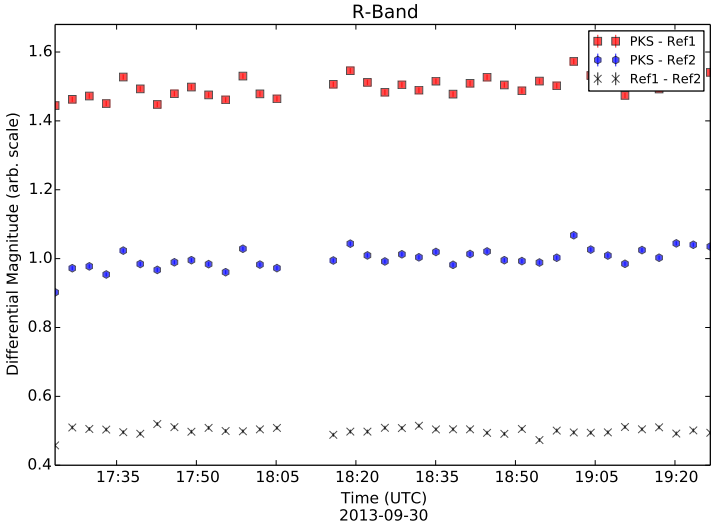
R-Band
PKS - Ref1
PKS - Ref2
Ref1 - Ref2
Differential Magnitude (arb. scale)
1.6
1.4
1.2
1.0
0.8
0.6
0.4
17:35
17:50
18:05
18:20
18:35
18:50
19:05
19:20
Time (UTC)
2013-09-30

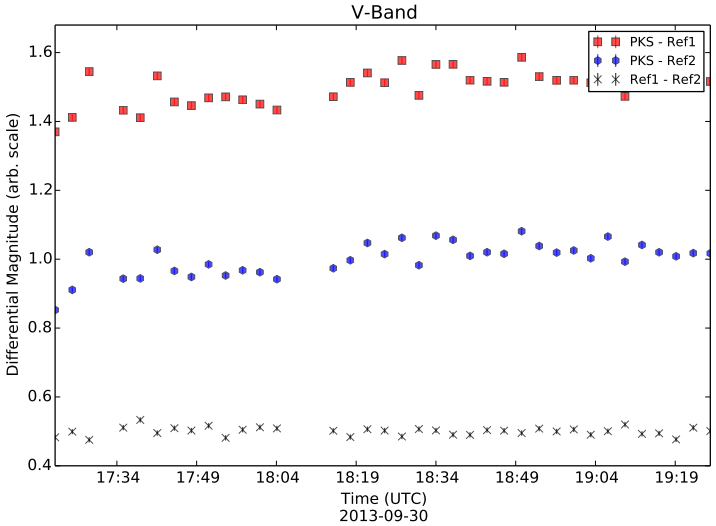
V-Band
PKS - Ref1
PKS - Ref2
Ref1 - Ref2
Differential Magnitude (arb. scale)
1.6
1.4
1.2
1.0
0.8
0.6
0.4
17:34
17:49
18:04
18:19
18:34
18:49
19:04
19:19
Time (UTC)
2013-09-30

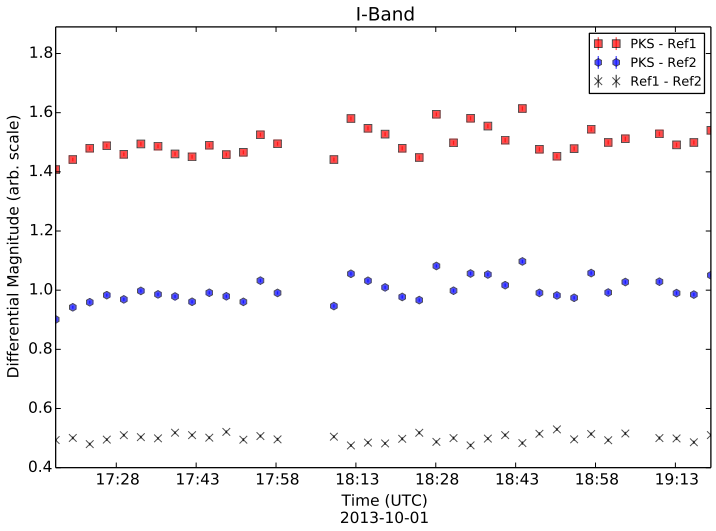
I-Band
PKS - Ref1
PKS - Ref2
Ref1 - Ref2
Differential Magnitude (arb. scale)
1.8
1.6
1.4
1.2
1.0
0.8
0.6
0.4
17:28
17:43
17:58
18:13
18:28
18:43
18:58
19:13
Time (UTC)
2013-10-01

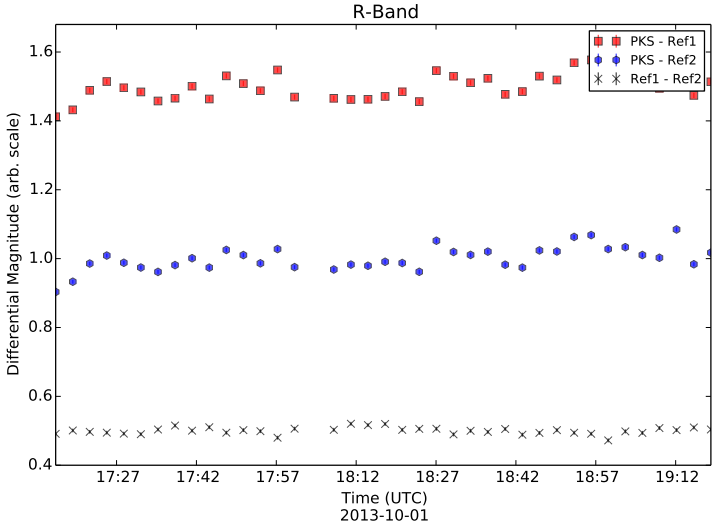
R-Band
PKS - Ref1
PKS - Ref2
Ref1 - Ref2
Differential Magnitude (arb. scale)
1.6
1.4
1.2
1.0
0.8
0.6
0.4
17:27
17:42
17:57
18:12
18:27
18:42
18:57
19:12
Time (UTC)
2013-10-01

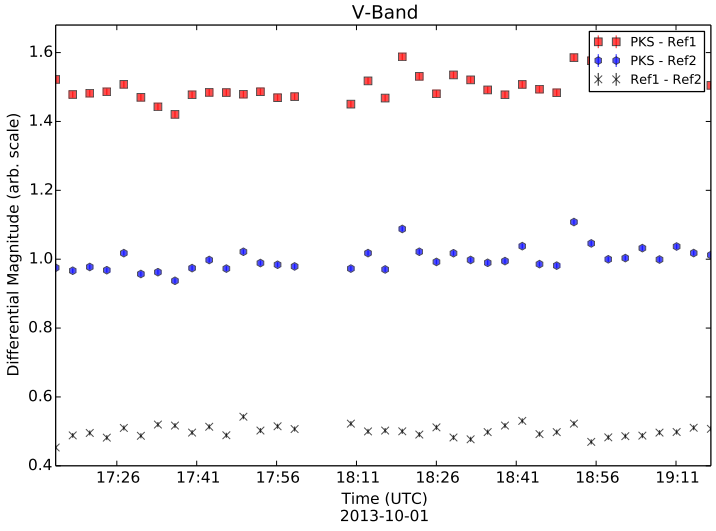
V-Band
PKS - Ref1
PKS - Ref2
Ref1 - Ref2
Differential Magnitude (arb. scale)
1.6
1.4
1.2
1.0
0.8
0.6
0.4
17:26
17:41
17:56
18:11
18:26
18:41
18:56
19:11
Time (UTC)
2013-10-01

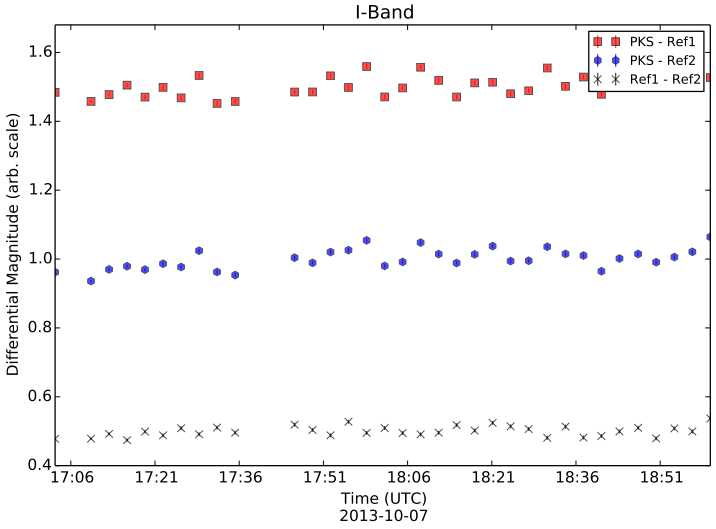
I-Band
PKS - Ref1
PKS - Ref2
Ref1 - Ref2
Differential Magnitude (arb. scale)
1.6
1.4
1.2
1.0
0.8
0.6
0.4
17:06
17:21
17:36
17:51
18:06
18:21
18:36
18:51
Time (UTC)
2013-10-07

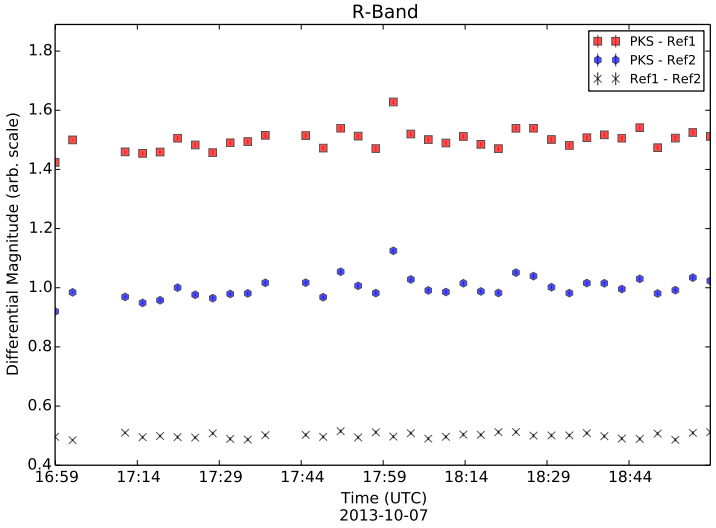
R-Band
PKS - Ref1
PKS - Ref2
Ref1 - Ref2
Differential Magnitude (arb. scale)
1.8
1.6
1.4
1.2
1.0
0.8
0.6
0.4
16:59
17:14
17:29
17:44
17:59
18:14
18:29
18:44
Time (UTC)
2013-10-07

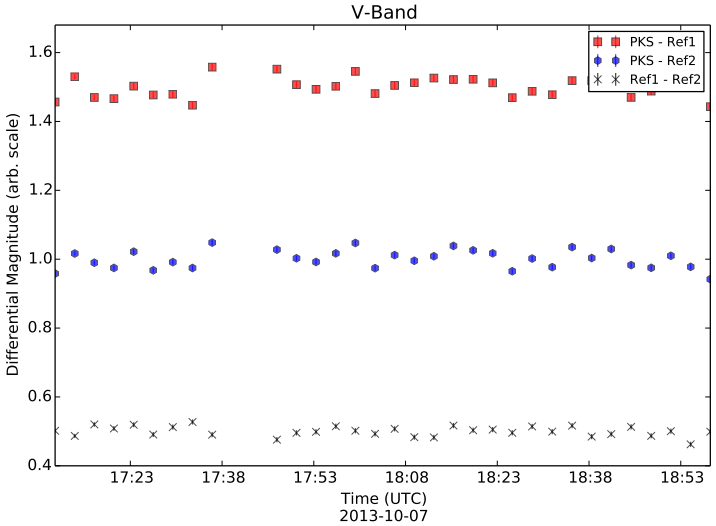
V-Band
PKS - Ref1
PKS - Ref2
Ref1 - Ref2
Differential Magnitude (arb. scale)
1.6
1.4
1.2
1.0
0.8
0.6
0.4
17:23
17:38
17:53
18:08
18:23
18:38
18:53
Time (UTC)
2013-10-07

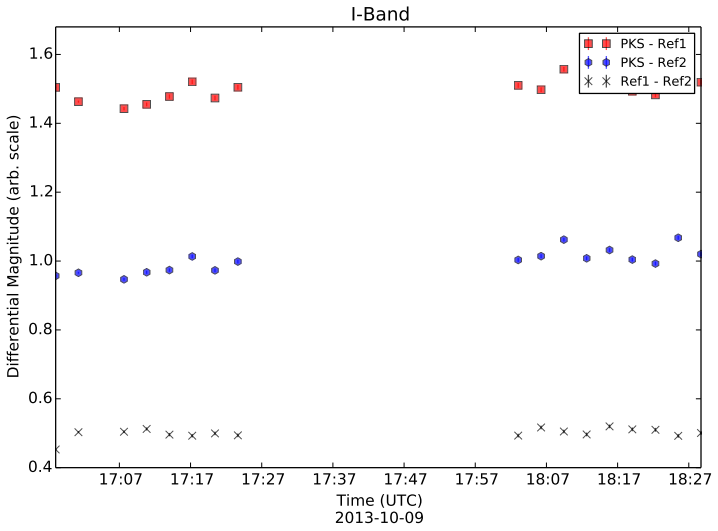
I-Band
PKS - Ref1
PKS - Ref2
Ref1 - Ref2
Differential Magnitude (arb. scale)
1.6
1.4
1.2
1.0
0.8
0.6
0.4
17:07
17:17
17:27
17:37
17:47
17:57
18:07
18:17
18:27
Time (UTC)
2013-10-09

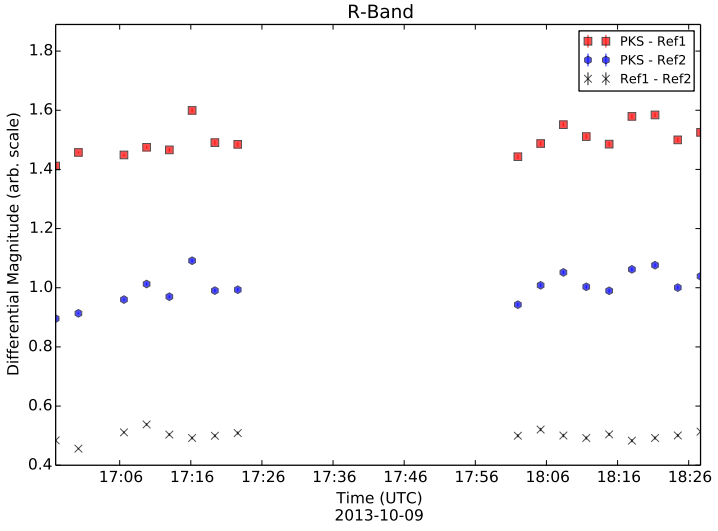
R-Band
PKS - Ref1
PKS - Ref2
Ref1 - Ref2
Differential Magnitude (arb. scale)
1.8
1.6
1.4
1.2
1.0
0.8
0.6
0.4
17:06
17:16
17:26
17:36
17:46
17:56
18:06
18:16
18:26
Time (UTC)
2013-10-09

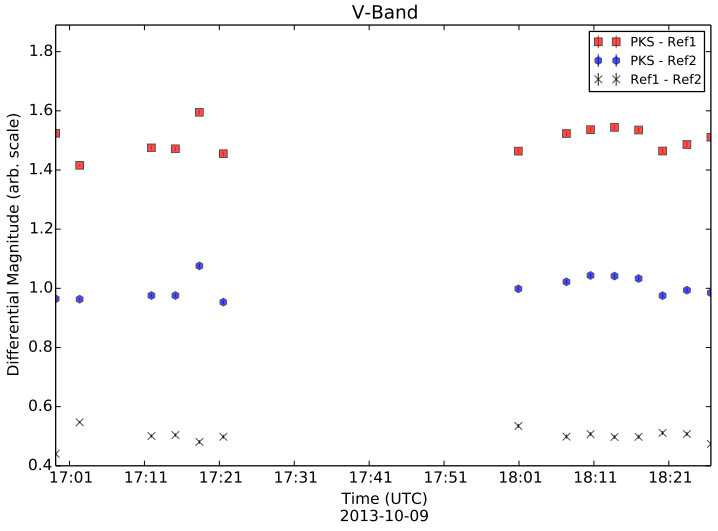
V-Band
PKS - Ref1
PKS - Ref2
Ref1 - Ref2
Differential Magnitude (arb. scale)
1.8
1.6
1.4
1.2
1.0
0.8
0.6
0.4
17:01
17:11
17:21
17:31
17:41
17:51
18:01
18:11
18:21
Time (UTC)
2013-10-09

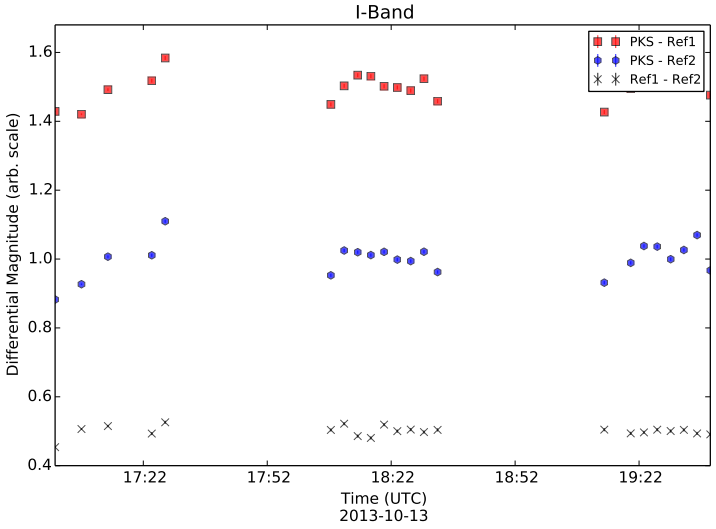
I-Band
PKS - Ref1
PKS - Ref2
Ref1 - Ref2
Differential Magnitude (arb. scale)
1.6
1.4
1.2
1.0
0.8
0.6
0.4
17:22
17:52
18:22
18:52
19:22
Time (UTC)
2013-10-13

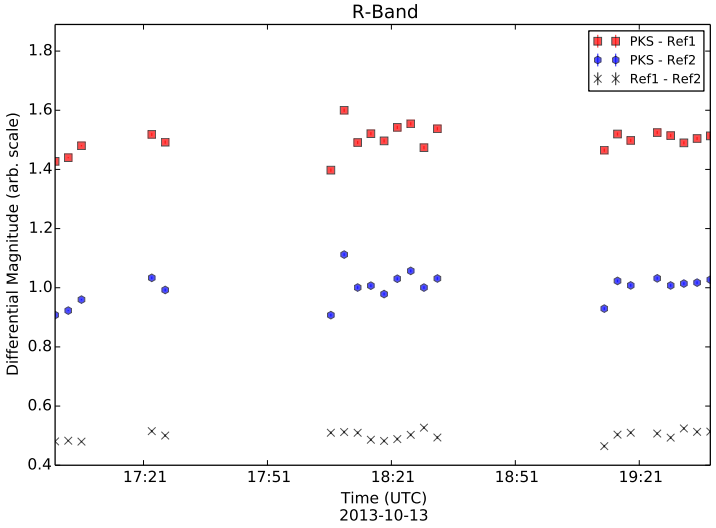
R-Band
PKS - Ref1
PKS - Ref2
Ref1 - Ref2
Differential Magnitude (arb. scale)
1.8
1.6
1.4
1.2
1.0
0.8
0.6
0.4
17:21
17:51
18:21
18:51
19:21
Time (UTC)
2013-10-13

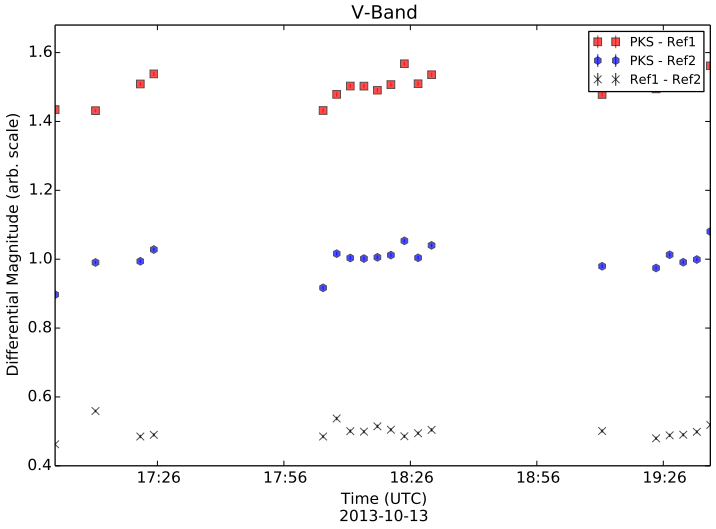
V-Band
PKS - Ref1
PKS - Ref2
Ref1 - Ref2
Differential Magnitude (arb. scale)
1.6
1.4
1.2
1.0
0.8
0.6
0.4
17:26
17:56
18:26
18:56
19:26
Time (UTC)
2013-10-13

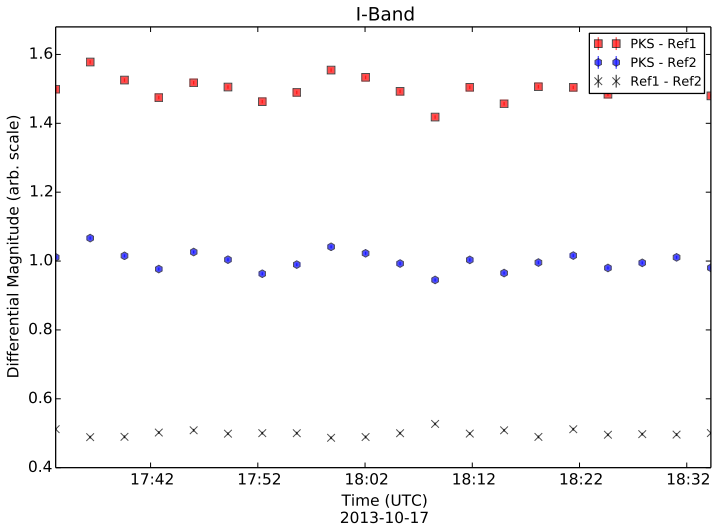
I-Band
PKS - Ref1
PKS - Ref2
Ref1 - Ref2
Differential Magnitude (arb. scale)
1.6
1.4
1.2
1.0
0.8
0.6
0.4
17:42
17:52
18:02
18:12
18:22
18:32
Time (UTC)
2013-10-17

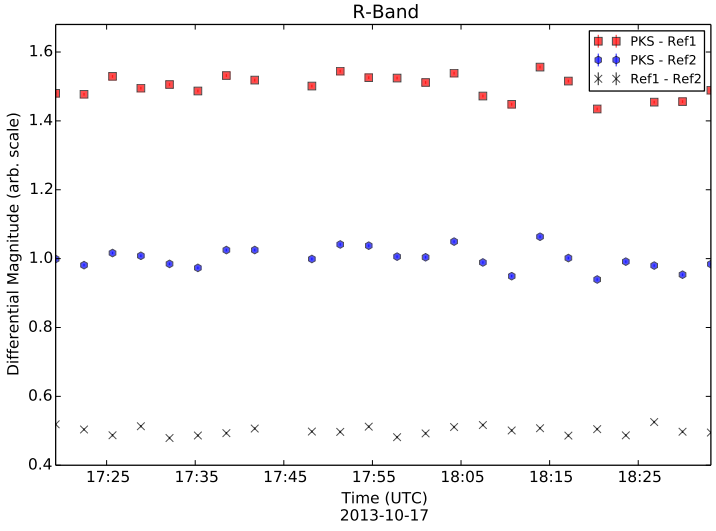
R-Band
PKS - Ref1
PKS - Ref2
Ref1 - Ref2
Differential Magnitude (arb. scale)
1.6
1.4
1.2
1.0
0.8
0.6
0.4
17:25
17:35
17:45
17:55
18:05
18:15
18:25
Time (UTC)
2013-10-17

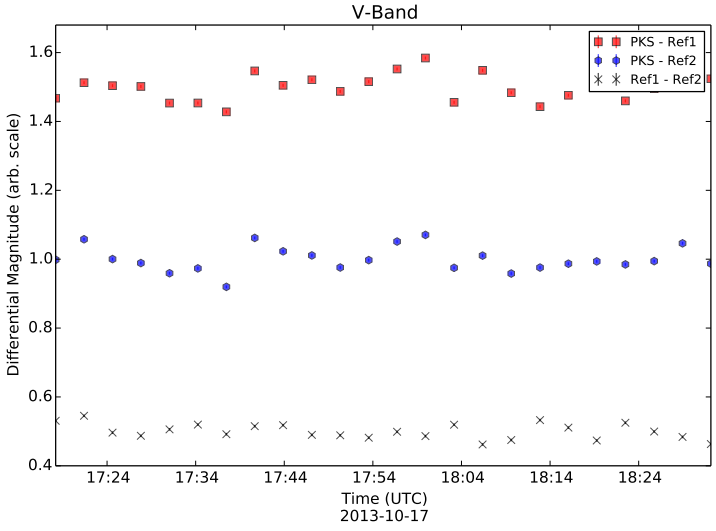
V-Band
PKS - Ref1
PKS - Ref2
Ref1 - Ref2
Differential Magnitude (arb. scale)
1.6
1.4
1.2
1.0
0.8
0.6
0.4
17:24
17:34
17:44
17:54
18:04
18:14
18:24
Time (UTC)
2013-10-17

B.2 PKS 2155-304

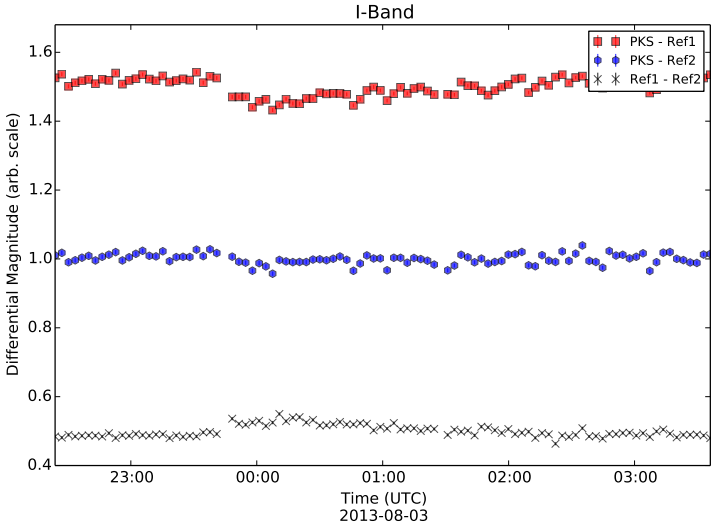

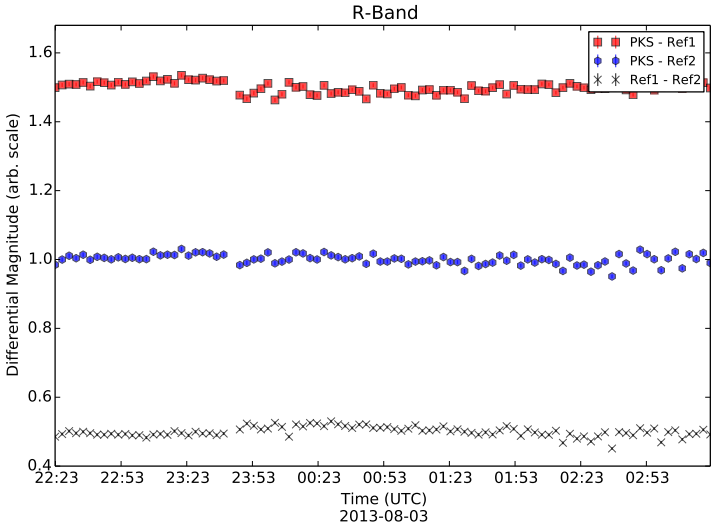

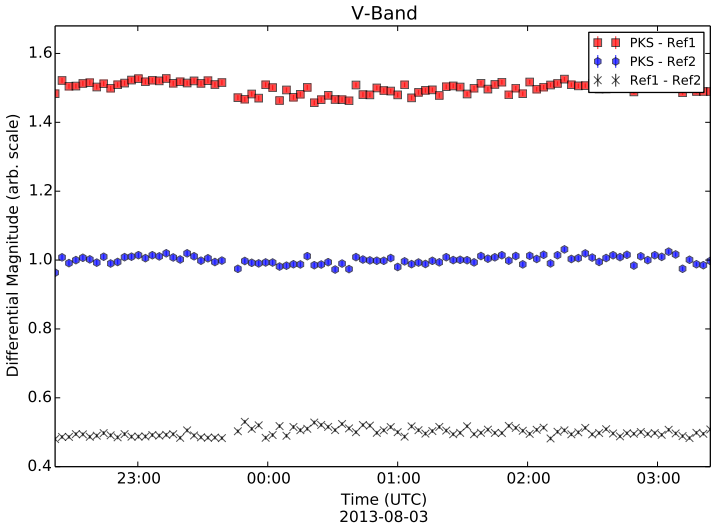

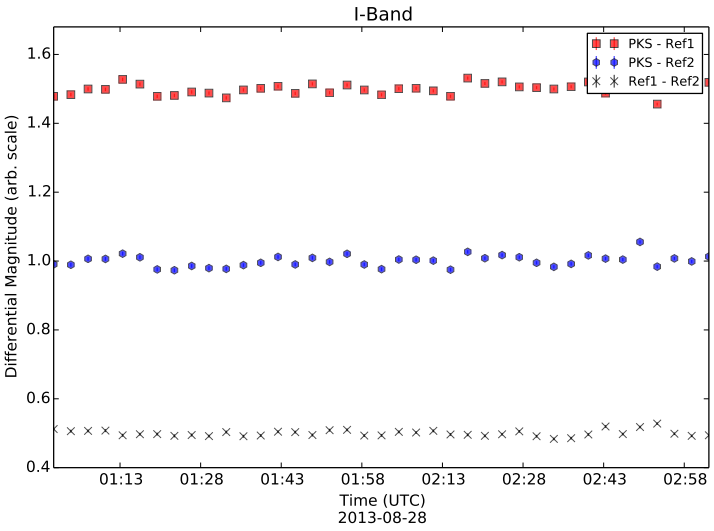
I-Band
PKS - Ref1
PKS - Ref2
Ref1 - Ref2
Differential Magnitude (arb. scale)
1.6
1.4
1.2
1.0
0.8
0.6
0.4
01:13
01:28
01:43
01:58
02:13
02:28
02:43
02:58
Time (UTC)
2013-08-28

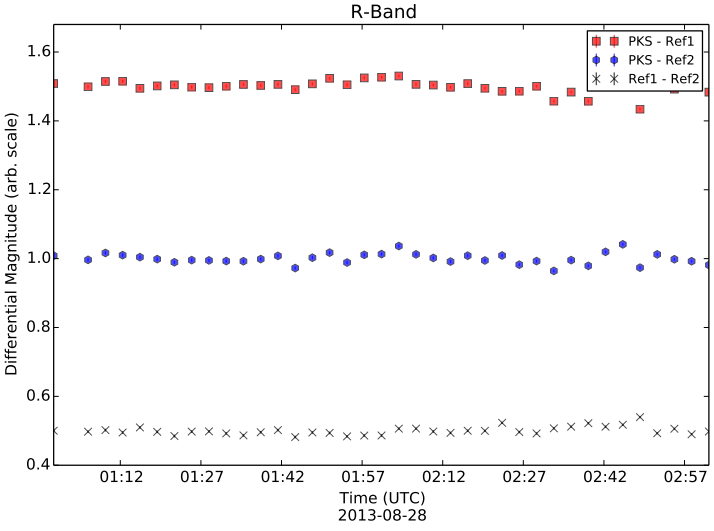
R-Band
PKS - Ref1
PKS - Ref2
Ref1 - Ref2
Differential Magnitude (arb. scale)
1.6
1.4
1.2
1.0
0.8
0.6
0.4
01:12
01:27
01:42
01:57
02:12
02:27
02:42
02:57
Time (UTC)
2013-08-28

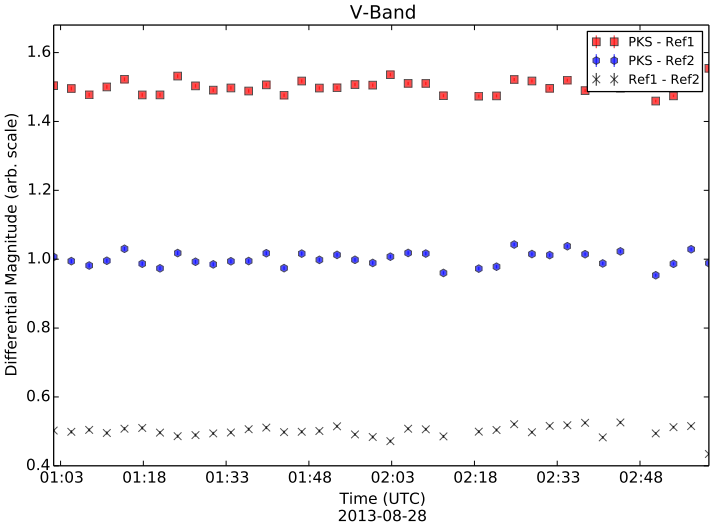
V-Band
PKS - Ref1
PKS - Ref2
Ref1 - Ref2
Differential Magnitude (arb. scale)
1.6
1.4
1.2
1.0
0.8
0.6
0.4
01:03
01:18
01:33
01:48
02:03
02:18
02:33
02:48
Time (UTC)
2013-08-28

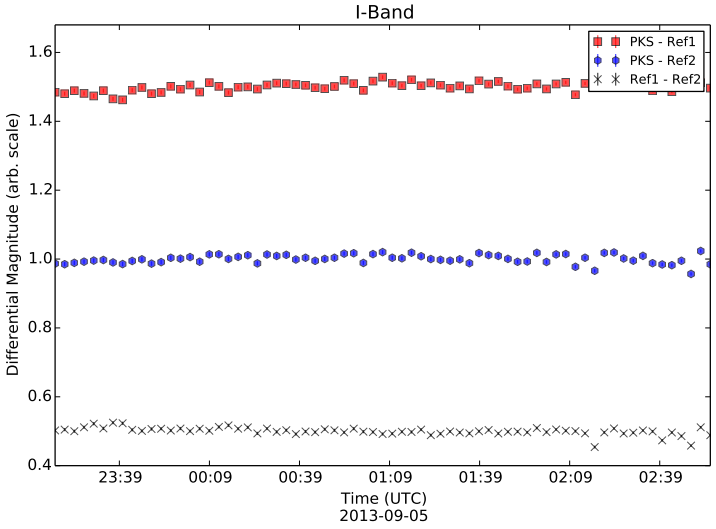
I-Band
PKS - Ref1
PKS - Ref2
Ref1 - Ref2
Differential Magnitude (arb. scale)
1.6
1.4
1.2
1.0
0.8
0.6
0.4
23:39
00:09
00:39
01:09
01:39
02:09
02:39
Time (UTC)
2013-09-05

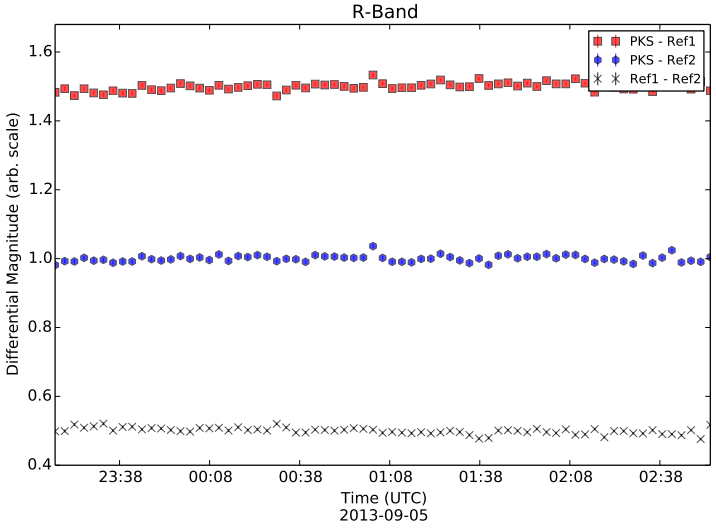
R-Band
PKS - Ref1
PKS - Ref2
Ref1 - Ref2
Differential Magnitude (arb. scale)
1.6
1.4
1.2
1.0
0.8
0.6
0.4
23:38
00:08
00:38
01:08
01:38
02:08
02:38
Time (UTC)
2013-09-05

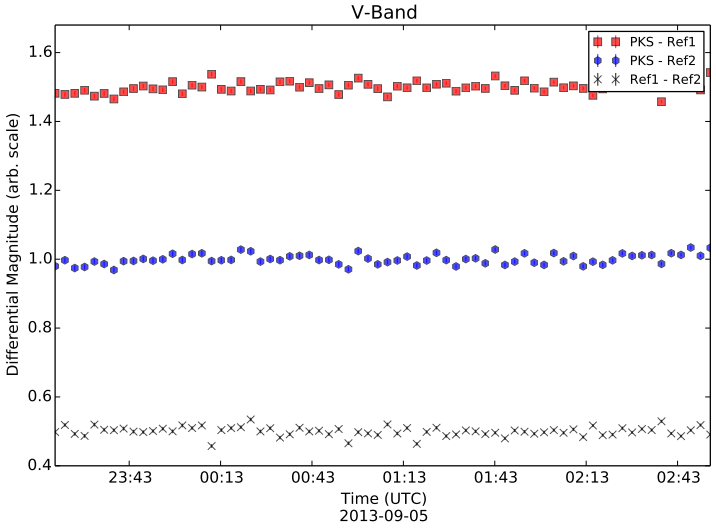
V-Band
PKS - Ref1
PKS - Ref2
Ref1 - Ref2
Differential Magnitude (arb. scale)
1.6
1.4
1.2
1.0
0.8
0.6
0.4
23:43
00:13
00:43
01:13
01:43
02:13
02:43
Time (UTC)
2013-09-05

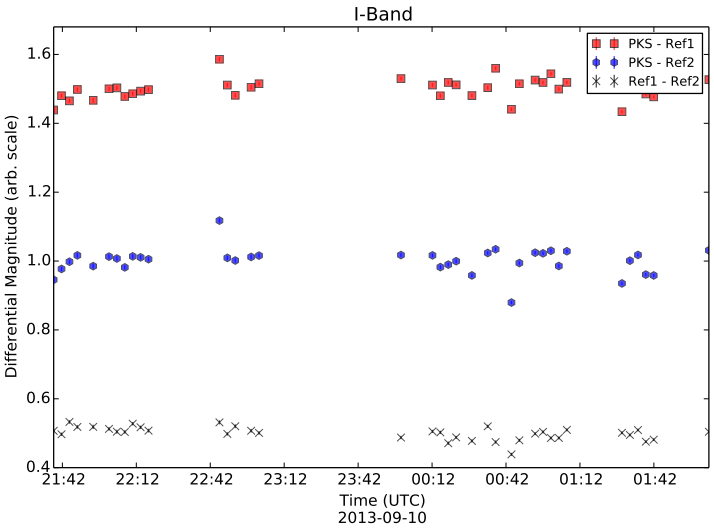
I-Band
PKS - Ref1
PKS - Ref2
Ref1 - Ref2
Differential Magnitude (arb. scale)
1.6
1.4
1.2
1.0
0.8
0.6
0.4
21:42
22:12
22:42
23:12
23:42
00:12
00:42
01:12
01:42
Time (UTC)
2013-09-10

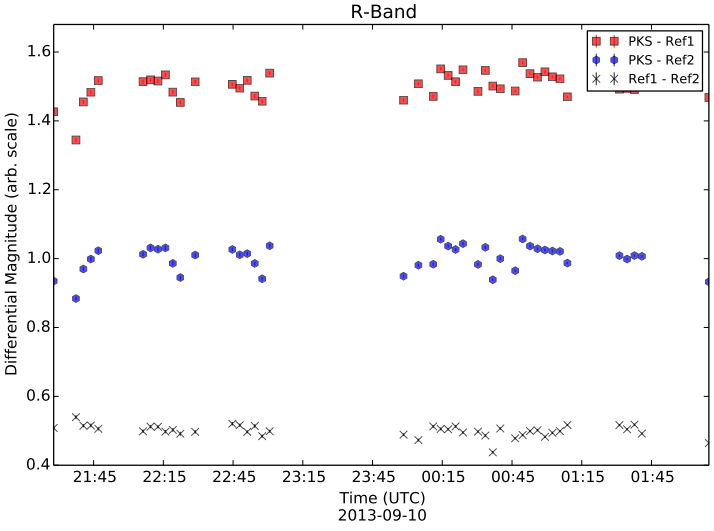
R-Band
PKS - Ref1
PKS - Ref2
Ref1 - Ref2
Differential Magnitude (arb. scale)
1.6
1.4
1.2
1.0
0.8
0.6
0.4
21:45
22:15
22:45
23:15
23:45
00:15
00:45
01:15
01:45
Time (UTC)
2013-09-10

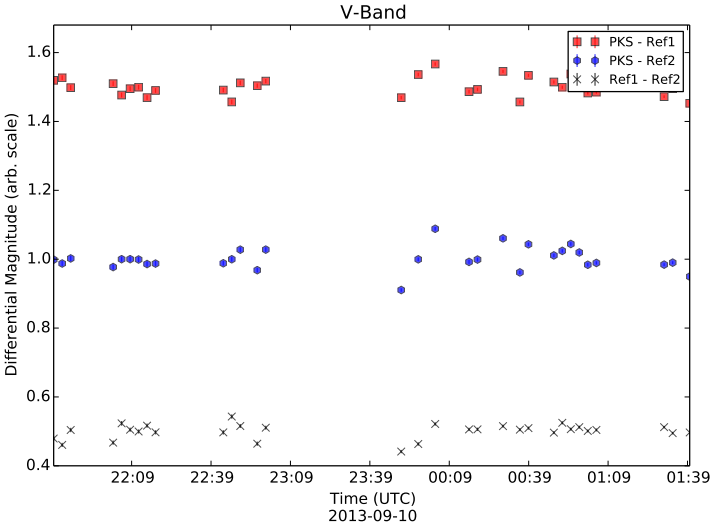
V-Band
PKS - Ref1
PKS - Ref2
Ref1 - Ref2
Differential Magnitude (arb. scale)
1.6
1.4
1.2
1.0
0.8
0.6
0.4
22:09
22:39
23:09
23:39
00:09
00:39
01:09
01:39
Time (UTC)
2013-09-10

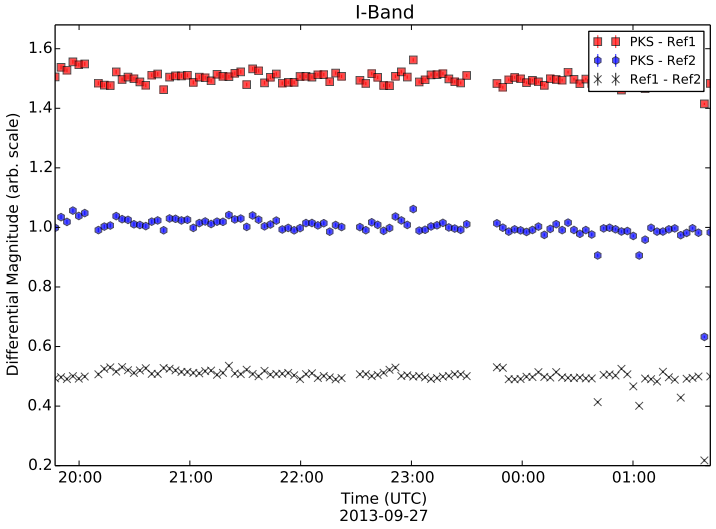
I-Band
PKS - Ref1
PKS - Ref2
Ref1 - Ref2
Differential Magnitude (arb. scale)
1.6
1.4
1.2
1.0
0.8
0.6
0.4
0.2
20:00
21:00
22:00
23:00
00:00
01:00
Time (UTC)
2013-09-27

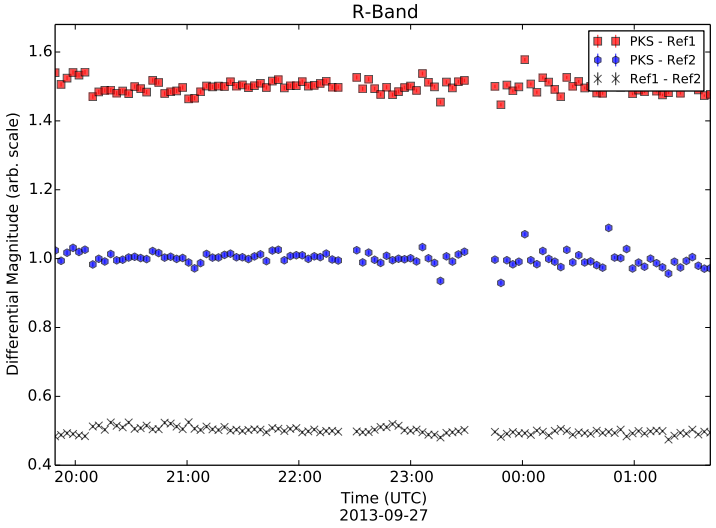
R-Band
PKS - Ref1
PKS - Ref2
Ref1 - Ref2
Differential Magnitude (arb. scale)
1.6
1.4
1.2
1.0
0.8
0.6
0.4
20:00
21:00
22:00
23:00
00:00
01:00
Time (UTC)
2013-09-27

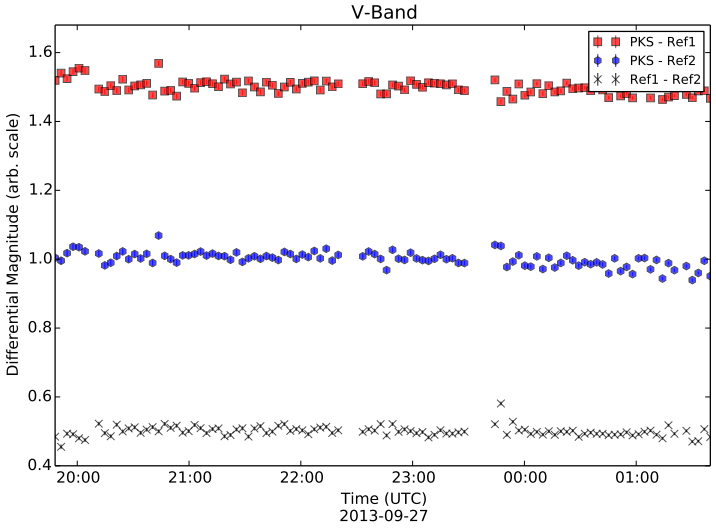
V-Band
PKS - Ref1
PKS - Ref2
Ref1 - Ref2
Differential Magnitude (arb. scale)
1.6
1.4
1.2
1.0
0.8
0.6
0.4
20:00
21:00
22:00
23:00
00:00
01:00
Time (UTC)
2013-09-27

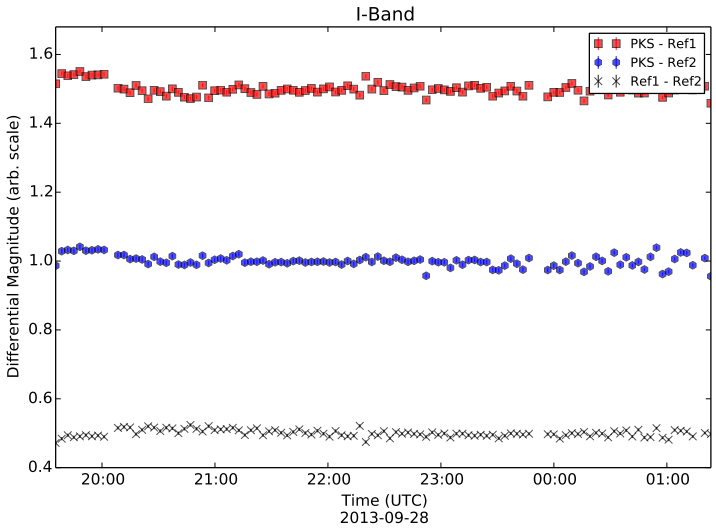
I-Band
PKS - Ref1
PKS - Ref2
Ref1 - Ref2
Differential Magnitude (arb. scale)
1.6
1.4
1.2
1.0
0.8
0.6
0.4
20:00
21:00
22:00
23:00
00:00
01:00
Time (UTC)
2013-09-28

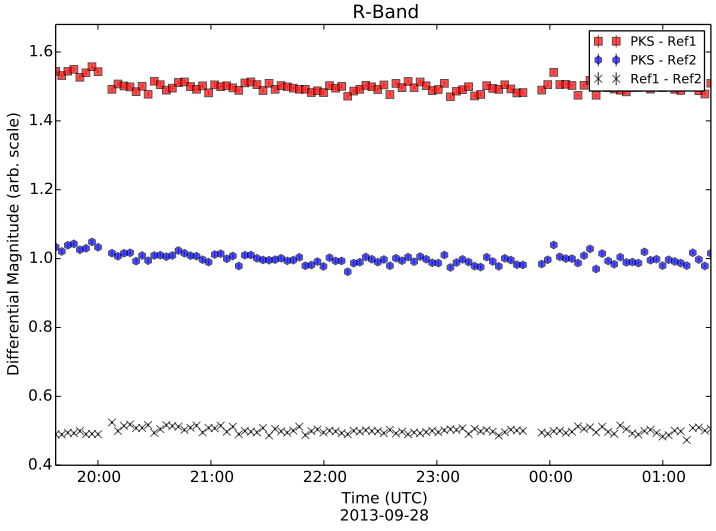
R-Band
PKS - Ref1
PKS - Ref2
Ref1 - Ref2
Differential Magnitude (arb. scale)
1.6
1.4
1.2
1.0
0.8
0.6
0.4
20:00
21:00
22:00
23:00
00:00
01:00
Time (UTC)
2013-09-28

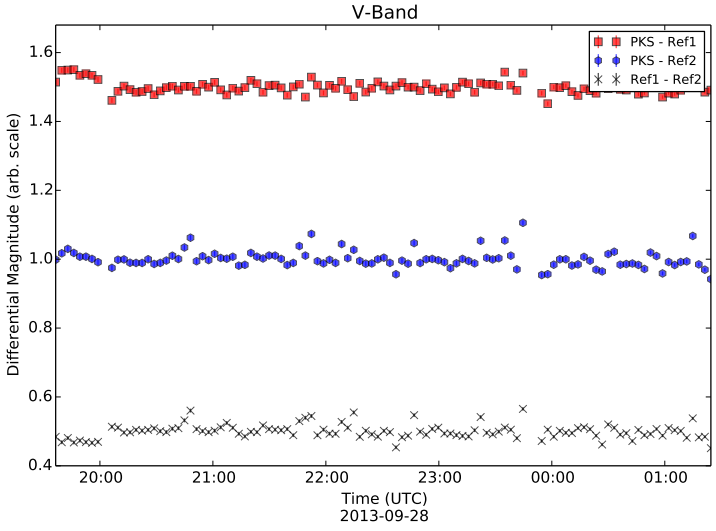
V-Band
PKS - Ref1
PKS - Ref2
Ref1 - Ref2
Differential Magnitude (arb. scale)
1.6
1.4
1.2
1.0
0.8
0.6
0.4
20:00
21:00
22:00
23:00
00:00
01:00
Time (UTC)
2013-09-28

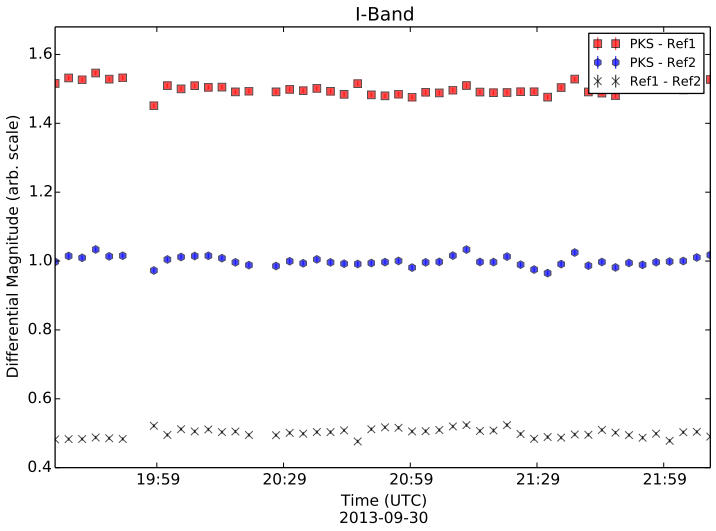
I-Band
PKS - Ref1
PKS - Ref2
Ref1 - Ref2
Differential Magnitude (arb. scale)
1.6
1.4
1.2
1.0
0.8
0.6
0.4
19:59
20:29
20:59
21:29
21:59
Time (UTC)
2013-09-30

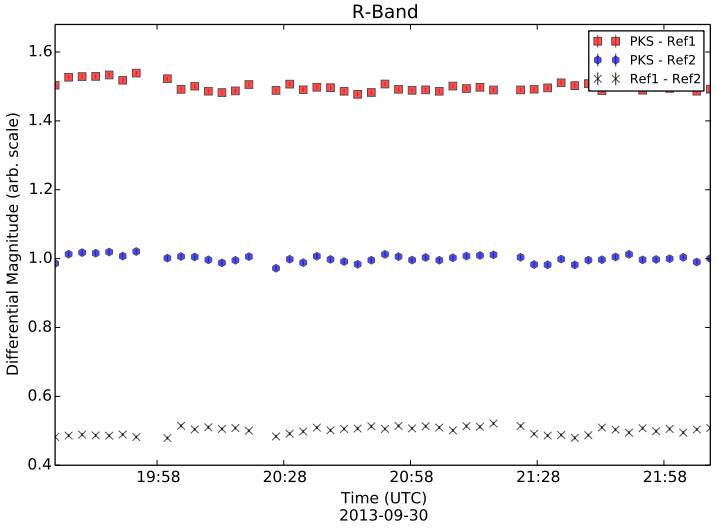
R-Band
PKS - Ref1
PKS - Ref2
Ref1 - Ref2
Differential Magnitude (arb. scale)
1.6
1.4
1.2
1.0
0.8
0.6
0.4
19:58
20:28
20:58
21:28
21:58
Time (UTC)
2013-09-30

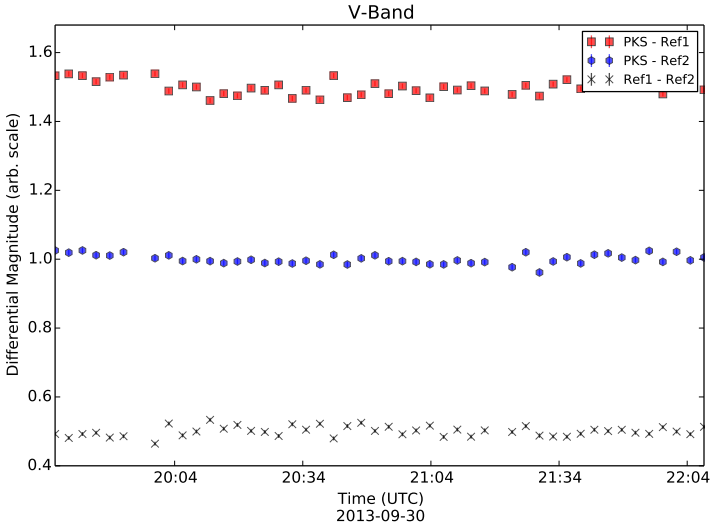
V-Band
PKS - Ref1
PKS - Ref2
Ref1 - Ref2
Differential Magnitude (arb. scale)
1.6
1.4
1.2
1.0
0.8
0.6
0.4
20:04
20:34
21:04
21:34
22:04
Time (UTC)
2013-09-30

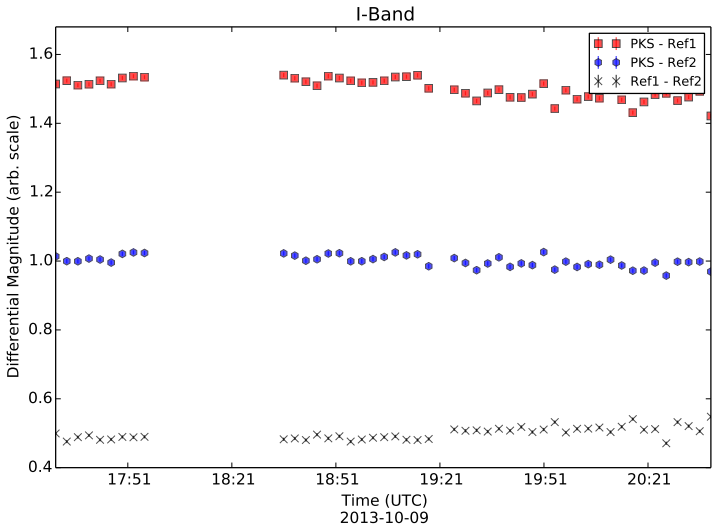
I-Band
PKS - Ref1
PKS - Ref2
Ref1 - Ref2
Differential Magnitude (arb. scale)
1.6
1.4
1.2
1.0
0.8
0.6
0.4
17:51
18:21
18:51
19:21
19:51
20:21
Time (UTC)
2013-10-09

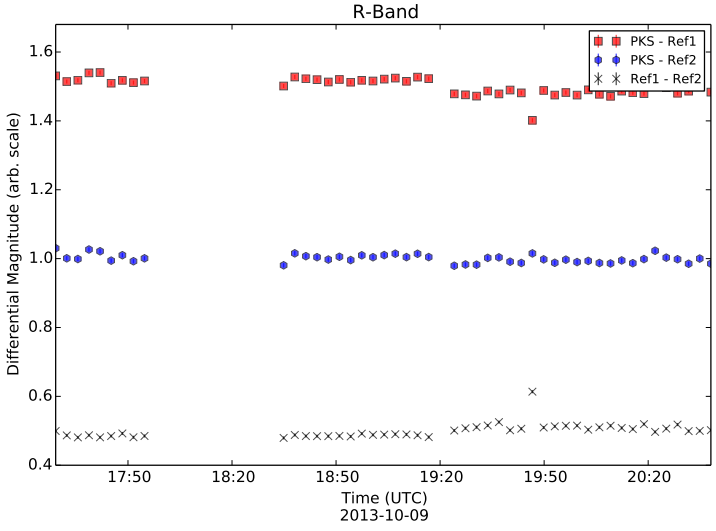
R-Band
PKS - Ref1
PKS - Ref2
Ref1 - Ref2
Differential Magnitude (arb. scale)
1.6
1.4
1.2
1.0
0.8
0.6
0.4
17:50
18:20
18:50
19:20
19:50
20:20
Time (UTC)
2013-10-09

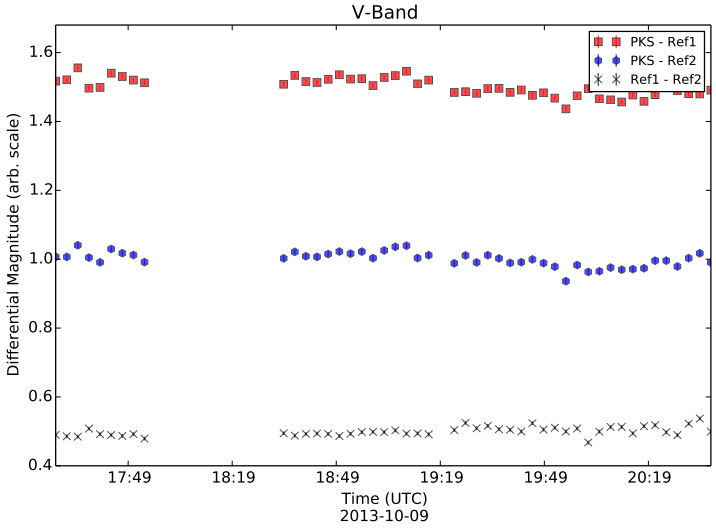
V-Band
PKS - Ref1
PKS - Ref2
Ref1 - Ref2
Differential Magnitude (arb. scale)
1.6
1.4
1.2
1.0
0.8
0.6
0.4
17:49
18:19
18:49
19:19
19:49
20:19
Time (UTC)
2013-10-09

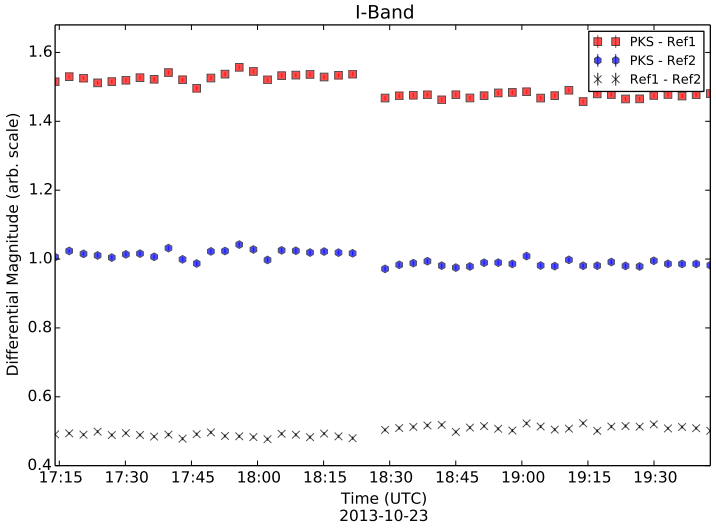
I-Band
PKS - Ref1
PKS - Ref2
Ref1 - Ref2
Differential Magnitude (arb. scale)
1.6
1.4
1.2
1.0
0.8
0.6
0.4
17:15
17:30
17:45
18:00
18:15
18:30
18:45
19:00
19:15
19:30
Time (UTC)
2013-10-23

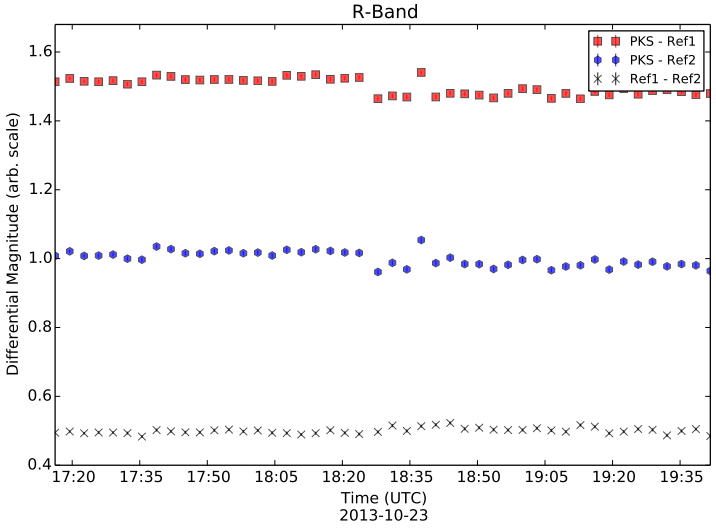
R-Band
PKS - Ref1
PKS - Ref2
Ref1 - Ref2
Differential Magnitude (arb. scale)
1.6
1.4
1.2
1.0
0.8
0.6
0.4
17:20
17:35
17:50
18:05
18:20
18:35
18:50
19:05
19:20
19:35
Time (UTC)
2013-10-23

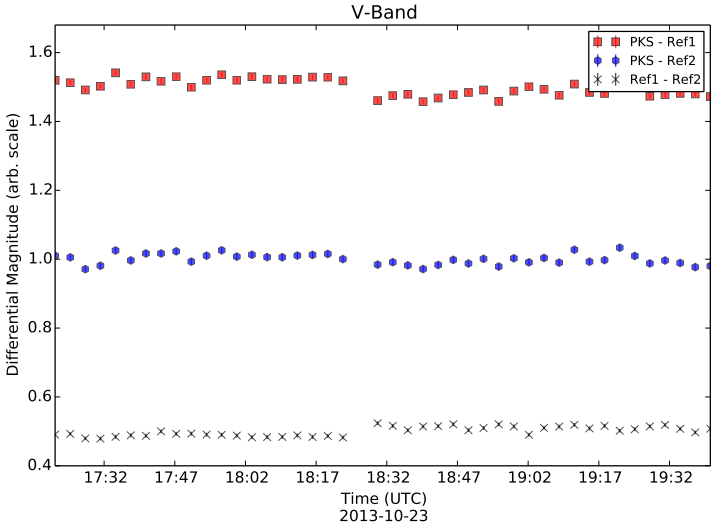
V-Band
PKS - Ref1
PKS - Ref2
Ref1 - Ref2
Differential Magnitude (arb. scale)
1.6
1.4
1.2
1.0
0.8
0.6
0.4
17:32
17:47
18:02
18:17
18:32
18:47
19:02
19:17
19:32
Time (UTC)
2013-10-23

Appendix C

C.1 Primary Schools

Catholic University School Feedback

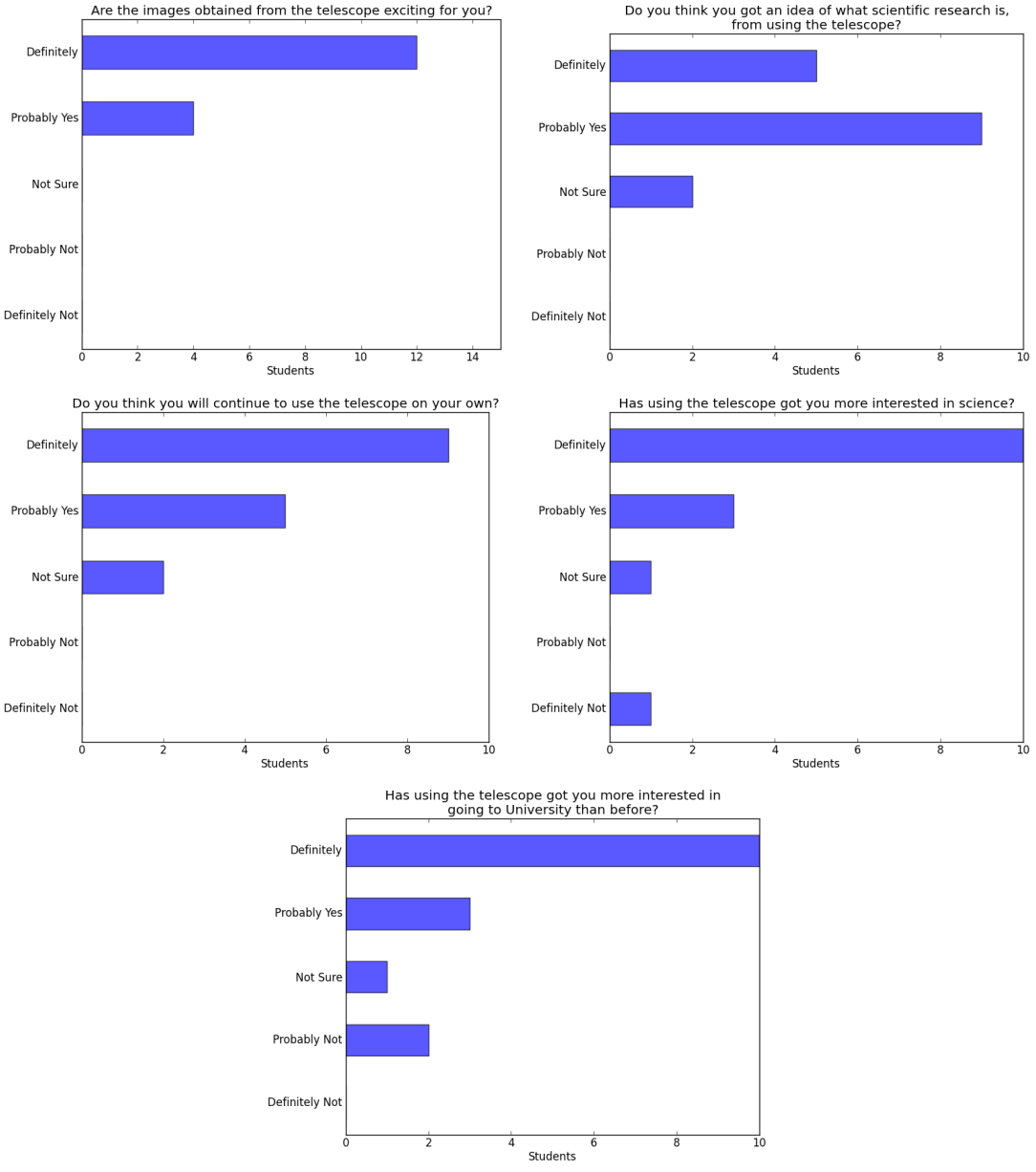

Figure C.1: Catholic University School Prep. feedback results

Question 6: What did you enjoy most about the telescope lessons?

"Being able to do quizzes and print pictures"

"Editing the images"

"They teach a lot about science and space and it makes me learn more about the universe"

"I most enjoy the time you first see your image"

"That space is so diverse"

"The way we could take pictures"

"Taking pictures and looking at them"

"The way it takes pictures"

"I played games"

"Looking at the pictures"

"Printing the pictures"

"The editing of the pictures"

"The facts"

"I enjoyed looking at all of the planets"

"Looking at the planets"

Question 7: What would you like to have done more of?

"Games"

"More editing images"

"Taking the pictures and doing more tests"

"Options on which pictures to take"

"Looking at more of the amazing pictures"

"Taking more pictures"

"I would like if you could look around in the telescope"

"Taking pictures of planets"

"Move the telescope and have a live feed"

"The quiz"

"Printing the pictures"

"Learn about space stations"

"YES!!!!"

"I don't know"

"Taking tests"

Question 8: Any other feedback?

"No"

"No"

"Not really, just the username and password is hard to learn and know how to spell"

"Not really"

"Not really"

"Yes. I really like the way we could zoom in on the pictures we took and I really enjoyed it"

"Not really no, the site is really fun though"

"No"

"I enjoyed it"

"No"

"More games!"

"No"

"NO!"

"No. Beast!"

"No"

St. Louis Infant School Feedback

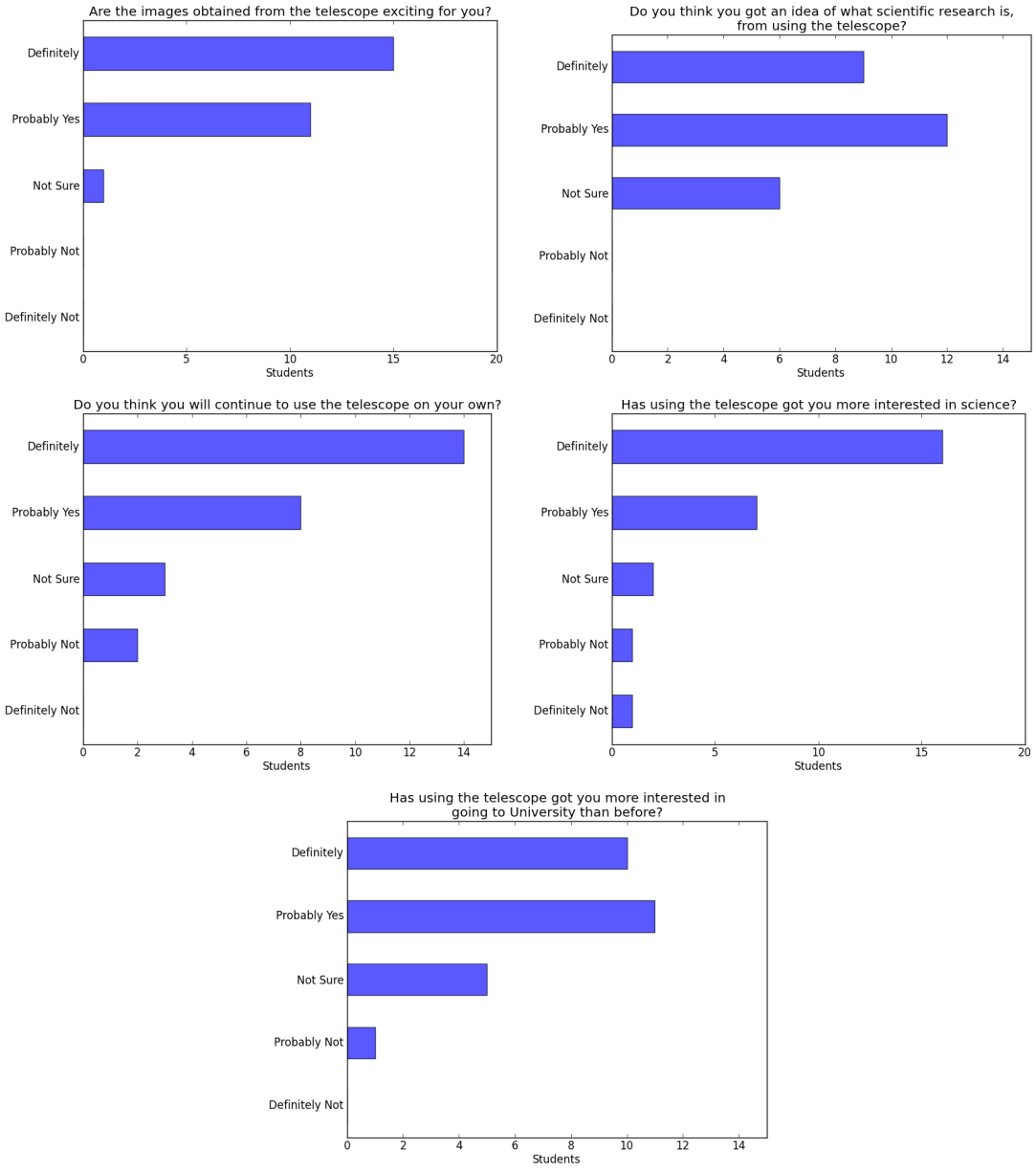

Figure C.2: St. Louis Infant School feedback results

Question 6: What did you enjoy most about the telescope lessons?

"The way it made me get more interested in something new"

"Looking at planets and finding facts"

"I enjoyed when Pete was telling us all about the telescope"

"Using the telescope"

"I enjoyed doing the tests"

"I enjoy watching the objects, stars and planets and learning about it"

"Learning about new planets"

"Learning about stars and planets"

"About the galaxies"

"The galaxies"

"The games"

"About Watcher"

"The games"

"Getting to take pictures"

"I learned so much that I didn't know"

"It has many different"

"The images"

"When we get them back, how we get to change them"

"About what Pete does and the robotic telescope"

"I enjoyed learning about what else is in space"

"Activities"

"I enjoy the telescope lessons because it is very interesting"

"I enjoyed changing the pictures"

"I enjoyed the beautiful pictures of the galaxy and planets"

"I enjoyed going on the PC"

"I loved all of the amazing pictures and the colours"

Question 7: What would you like to have done more of?

"Pete coming and telling us more"

"Going to UCD and discovering about stars"

"Learning more about space"

"Taking pictures"

“I would like to see the telescope”

“Learn about new planets”

“Using the telescope”

“I would like to work at UCD”

“Pictures with Pete because he explained it well”

“I would like to go to UCD”

“About Watcher”

“More pictures of the real telescope”

“Nothing”

“Seeing it for real. A school trip going to UCD and seeing the machines”

“No”

“I would like if Pete explained a bit more about it”

“Learning about what Pete does”

“learning about galaxies”

“I would like to know some names of stars”

“Yes!!”

“The activities”

“To discover everything about what is in the black space”

“I would like to learn more about the sun, and the outside of the universe”

Question 8: Any other feedback?

“We have the best pictures of the solar system”

“Pete is a very good astronomy”

“No”

“I really enjoyed it, I would like to study Astronomy”

“No :P”

“I guess I want to work in Astronomy”

“no”

“I loved it”

“no”

“It was COOL”

“no”

“no”

“no”

“I am really grateful and learned lots. Thanks.”

“no”

“Can we go to UCD?”

“no”

“I really enjoyed learning about space! Thank you”

“THANK YOU! I am looking forward to coming!! :)”

“no”

“Sun is a star and the only one closest to us. About Venus and Mercury”

“I really enjoyed all of it and had amazing fun so thank you”

St. Oliver Plunketts Feedback

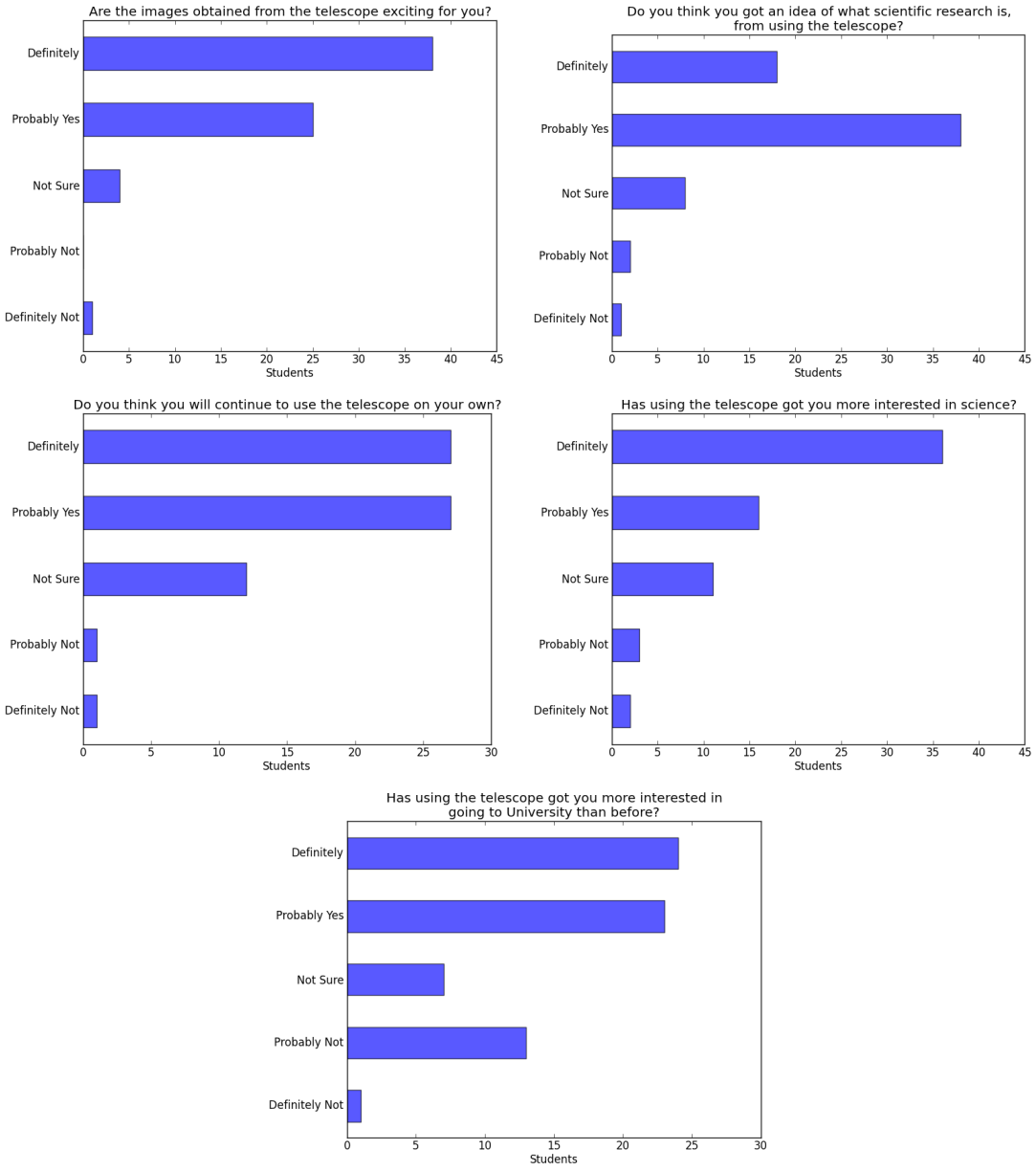

Figure C.3: St. Oliver Plunkett N.S. feedback results

Question 6: What did you enjoy most about the telescope lessons?

"I enjoyed the games and the pictures. I enjoyed the game."

"The Game"

"Images"

"I liked coming on and seeing a new picture that was done and I liked the high scores."

“You got to take pictures of things in space and design it. I enjoyed the activities”

“That you get to look at all of the cool pictures.”

“Images.”

“Doing the activities.”

“I enjoyed seeing what is really in space.”

“I enjoyed editing the photos.”

“The Constellations!”

“Constellations”

“Doing up the photos and making them bright and colourful.”

“I liked the photos.”

“Designing the images.”

“I enjoyed the first lesson when we took the pictures”

“I enjoyed looking at the pictures.”

“The pictures”

“The pictures.”

“I like the way they thought us. It was very good and the pictures were great and the games.”

“I liked the pictures that we got.”

“Doing the quiz.”

“I enjoyed editing the photos, and changing the colour.”

“Looking at all the different images after we processed them. I loved that.”

“I mostly enjoyed learning about BURT and how he takes pictures and its like a real person but he is a robot. Thanks.”

“I enjoyed quizzes and taking photos of planets, then putting them into my space scrapbook.”

“Processing the pics!”

“I enjoyed processing the images the most.”

“Looking at the stars.”

“I loved it all especially the photos.”

“I enjoyed taking the tests.”

“All of the stuff that we learned and the cool pictures we got.”

“Processing the images.”

“The good and detailed explanation on BURT and everything else to do with space.”

“The thing I enjoyed most was changing the brightness and darkness in the image.”

“I liked when we got the pictures and we zoomed in on them.”

“Looking at all the cool photos.”

“I enjoyed the fact that you can choose what pictures you want BURT to take.”

“I enjoyed looking at the pictures that I made.”

“I loved zooming in on the photos and seeing photos of space I’ve never seen before.”

“I enjoyed the pictures.”

“I learned that there are billions of galaxies.”

“Seeing the pictures on the computer.”

“I enjoyed looking at the pictures.”

“The quiz and the pictures.”

“Getting to use the telescope.”

“Seeing the stars and galaxies.”

“The using of the telescope.”

“I enjoyed looking at all of the different pictures on the computer by BURT.”

“The pictures.”

“Learning about planets and stuff.”

“I enjoyed looking at the photos and processing them.”

“Learning about the different planets and clusters etc.”

“Looking at all the different planets and galaxies.”

“Good.”

“I enjoyed the interesting facts that we were told and looking at all kinds of things.”

“I enjoyed looking at the galaxies.”

"I loved all of the pictures of space."

"Seeing all the cool stuff."

"That you can take photos of what you want."

"To see more worlds"

"I enjoyed the first lesson when we were able to zoom in so far and we could see stars."

"Seeing the results and the amazing quality of the pictures."

"Playing the games."

"Looking at the pictures."

"The images and analysing them."

"When you get to see the pictures."

Question 7: What would you like to have done more of?

"Maybe the games."

"More fun games."

"Nothing"

"Nothing"

"I'd like to more of planets."

"Playing games."

"Nothing."

"More activities."

"Get loads more pictures of the moon and gases."

"I would have enjoyed more games/activities."

"Maybe more of what it's like to be an astronomer."

"I would have liked to do activities."

"Activities"

"Videos."

"Using the colours"

"Nothing."

“Games.”

“The activities.”

“Would have liked to be able to more challenges.”

“I would have liked more quizzes.”

“Looking at the galaxy.”

“Editing the photos. I would like to know more about the Seven Sisters.”

“I think probably learning how to change the colours of images and a little bit more of the images.”

“I would like to have done more games and quizzes.”

“Quiz”

“Learning about the sun and Earth.”

“Talk about Galaxies.”

“Constellations”

“I would have liked to do more games.”

“Probably fixing up the pictures and making them look better.”

“Nebulas.”

“I think everything was well explained but would have liked them to talk about more stuff.”

“I would have liked to have done more about the science to do with astronomy and would have liked to learn where you find it out and how.”

“I think the lesson was fine, so I have no answer to that questions.”

“See a little bit more clearer photos.”

“The pictures.”

“I would have liked to learn more about BURT.”

“I would liked to have learned more about the planets.”

“No, I did loads and learned loads.”

“Learning about stars.”

“See one of the telescope.”

“I would like to see more of the telescopes and where they are.”

"More about space in general."

"Stars."

"I would have liked to take more pictures."

"I would like to take more pictures."

"I would have liked to do more quizzes."

"Quests."

"Seeing exploding stars and stuff."

"I would have liked to do more of the quiz."

"I thought everything was fine."

"I don't, no."

"More of the quizzes."

"Look closer into the moon."

"I would have liked to maybe go there with my family."

"Nothing."

"More stuff about the planets or stars."

"Nothing."

"Talk more about human life on different planets."

"Talking about certain constellations, galaxies and so on."

"The telescope."

"More pictures and a different quiz system."

"Maybe learn more about the planets."

Question 8: Any other feedback?

"No, but I had a great time, thank you!"

"No."

"No."

"No"

"No, it's really good."

“No.”

“No.”

“No.”

“Peter is really good at telling us about gases, stars and the moon.”

“Overall, I enjoyed it.”

“I think something explaining how to spot the constellations in the sky”

“No.”

“No, only thank you.”

“Nope.”

“No.”

“No”

“No, but thanks for teaching me about astronomy, planets and stars.”

“No.”

“No.”

“I would like if there was a fact page.”

“You should make a sign up for you website so like you can sign up and login.”

“Thank You. I really enjoyed it and was greatly inspired by it to go on and do astronomy”

“It really was brilliant and interesting and I think you only need to change very, very few things. I think also that on the quiz, its a bit hard to remember to pull up the stars for points.”

“I think there should be more things to do on the website like more games, quizzes, activities and more planets to order pictures from.”

“You were very good at explaining things!”

“I also enjoyed learning about BURT.”

“No.”

“It was a good experience.”

“It was very enjoyable and interesting.”

“No, thanks.”

“No.”

“I really enjoyed it and would like if they came back.”

“It was fantastic! I really enjoyed it and I would recommend it to anyone.”

“I think you should have a live camera videoing things at night and you can look at the saved clips at daytime.”

“No”

“At the start brilliant but the best pictures that you can get on the projector so it might make the children a lot more excited.”

“I think the website is very well laid out and explained and it is inspiring and has definitely inspired e.”

“I think that there should have been more on the planets but other than that it was amazing.”

“No, it was an amazing experience.”

“No.”

“Keep going with Project Gloria.”

“Great work with Gloria.”

“It was interesting and fun.”

“Yes. It was really fun and interesting.”

“Yes. It’s the best fun on computers.”

“No.”

“No.”

“It was really interesting.”

“No.”

“No.”

“No.”

“No.”

“No, thank you very much.”

“No.”

“No.”

“No.”

“No.”

“No.”

“No, not really.”

“It was a fun thing to do and I think a great way to encourage children to take an interest in astronomy.”

“It was fun.”

“Amazing website, bits can be a bit childish though.”

“Not really.”

C.2 Secondary Schools

Dominican College Wicklow Feedback

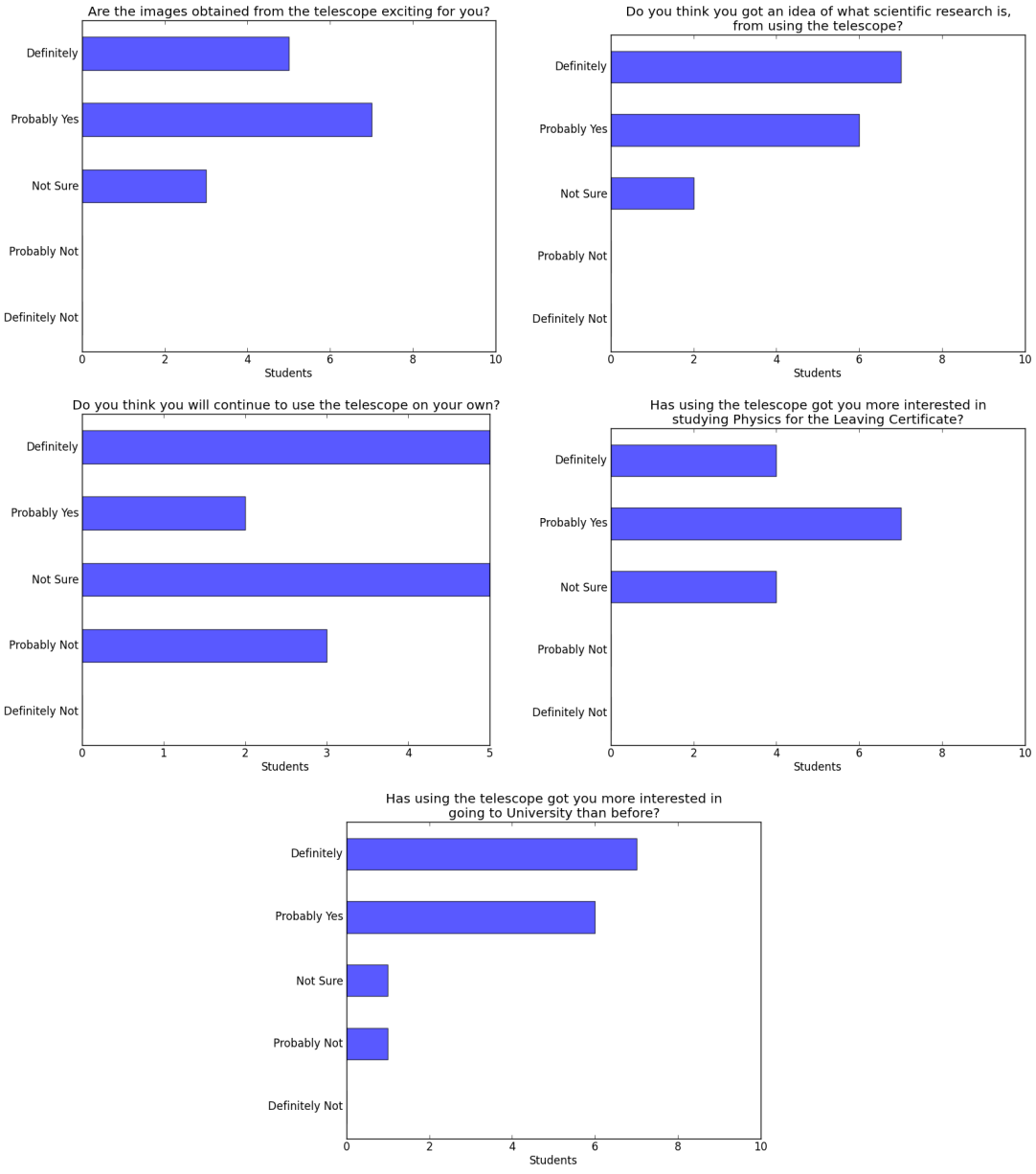

Figure C.4: Dominican College Wicklow feedback results

Question 6: What did you enjoy most about the telescope lessons?

"It was interesting because we got to get pictures that we wouldn't otherwise get to have."

"Taking pictures (especially of nebulas) and learning about space and planets."

ed us to see interesting images."

"It was really awesome when I got to see space from a computer."

"Learning about how physics and science are used in real life."

"Taking pictures of space."

"Yeah"

"Seeing cool images."

"That I could take my own photos of objects in space, and the photos were very interesting."

"The pictures were interesting."

"Looking at the stars and galaxies."

"It was unusual and interesting to learn about what is out there."

"Processing the image."

"I got a better look at what space is really like."

"Processing the images."

"Everything."

Question 7: What would you like to have done more of?

"More classes."

"Learning a bit more about astrology. More lessons."

"More research of our own."

"Go closer to the different images."

"Learned more about the background of it all."

"Learn more theory about it."

"Yes"

"Nothing."

"Nothing."

"Learning about what you do in astronomy in college."

"Taking pictures."

"To learn about galaxies etc. and what they do and they form."

"Take more pictures."

“Process more images.”

“Process more different images.”

“Nothing.”

Question 8: Any other feedback?

“Thanks for coming.”

“No.”

“Nope.”

“No!”

“It was fun, thanks.”

“No.”

“No.”

“Nope.”

“Thank you!”

“Good instructor, fun and interesting.”

“Good instructor. Pretty pictures.”

“Good instructor. ”

“No.”

St. Killians German School Feedback

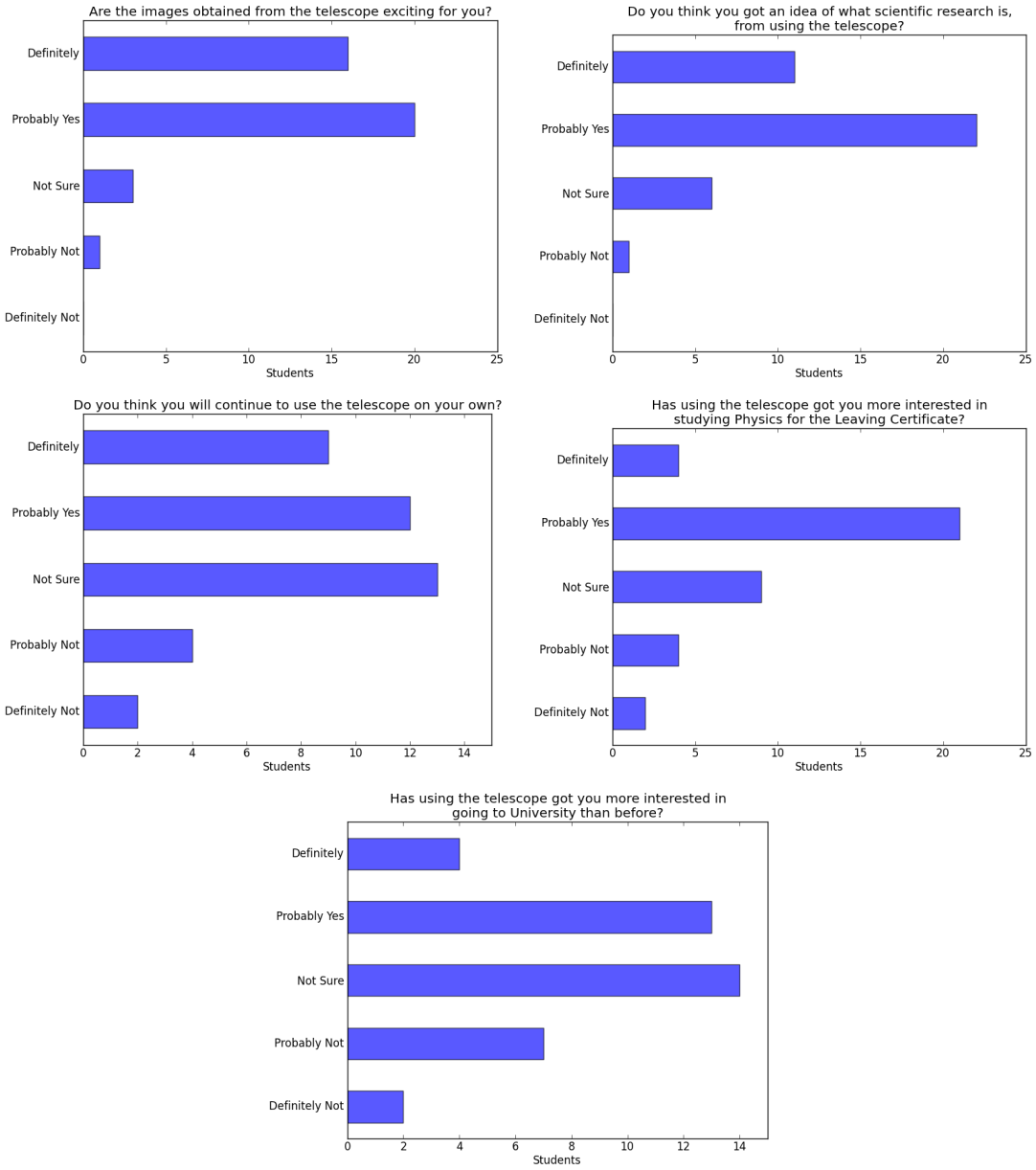

Figure C.5: St. Killians German School feedback results

Question 6: What did you enjoy most about the telescope lessons?

"The pictures"

"The cool images."

"Seeing the images and modifying them so we could see the objects better."

"The image processing programme."

“Processing the images of the talks.”

“The adventure”

“Taking pictures of the Sombrero Galaxy.”

“Looking at the planets , especially looking at the moon.”

“Taking pictures with the telescopes and processing images.”

“Customising the pictures.”

“Working with the telescope”

“Looking at all the different galaxies”

“Processing the Image”

“The pictures were very good and fun. Interesting topics.”

“Looking at different galaxies and discovering different things.”

“I really enjoyed getting to take our own pictures and seeing them after they were processes.”

“Taking pictures and looking at pictures.”

“Seeing the pictures and then processing them.”

“Seeing the different pictures with the telescope.”

“Seeing the different pictures with the telescope.”

“Looking at the nebulas”

“Seeing all the different pictures.”

“Seeing how the pictures turned out.”

“The ability to have a very accurate view of certain objects.”

“Learning about the Big Bang and our Universe.”

“Finding the images and processing them.”

“Seeing all the images, which were amazing. Also, just the fact of how the talk made me think ne think about what’s actually out there and how big it is.”

“The images”

“I enjoyed the section on the Big Bang.”

“Studying pictures of galaxies.”

“The information was useful.”

“Understanding the way of space.”

“It was cool to take pictures of space.”

“The processing.”

“The pictures.”

“Galaxies”

“Learning about our galaxy.”

“Being able to choose what you wanted nand then looking at them and adjusting the effects to be able to see the photos.”

“It’s really interesting as I haven’t looked through a telescope before and its cool being able to get the pictures from your computer from a real telescope.”

Question 7: What would you like to have done more of?

“More pictures.”

“Activities”

“Learned more about the universe.”

“Teach more about the universe.”

“The Big Bang.”

“Look at more nebulas.”

“Hunting aliens with science.”

“I don’t know”

“Talking about aliens and Mars landing.”

“More time to actually do it in school.”

“Talking about the Big Bang.”

“Take pictures.”

“Taking pictures.”

“Looking and taking pictures.”

“I missed the 1st lesson.”

"I missed the first lesson."

"More telescope research."

"More telescope research."

"Missed the first session - but I thought it was enough."

"Nothing."

"No."

"Talk more pictures, but I'll do that at home, so no."

"Get images printed in class."

"Discussing extraterrestrial life forms."

"Studied some other things (e.g planets)"

"Universe theory."

"Taking pictures."

"More pictures."

"Processing."

"More pictures."

"Life on other planets."

"Finding photos of galaxies."

"Taking pictures of planets."

Question 8: Any other feedback?

"No."

"No, liked it."

"Very interesting project/idea."

"No, it was delightful."

"Nope."

"I loved it."

"N/A"

"Using the telescope is fun."

“No”

“It was a good class.”

“It was great.”

“I really enjoyed the talks and they were well explained.”

“I enjoyed it and it was very well explained.”

“Very well explained, the pictures are good.”

“None.”

“N/A”

“The powerpoint was very good.”

“Very interesting, would gladly do something like this again.”

“Really interesting. Easy to understand.”

“No.”

“No.”

“Nope.”

Oatlands College Feedback

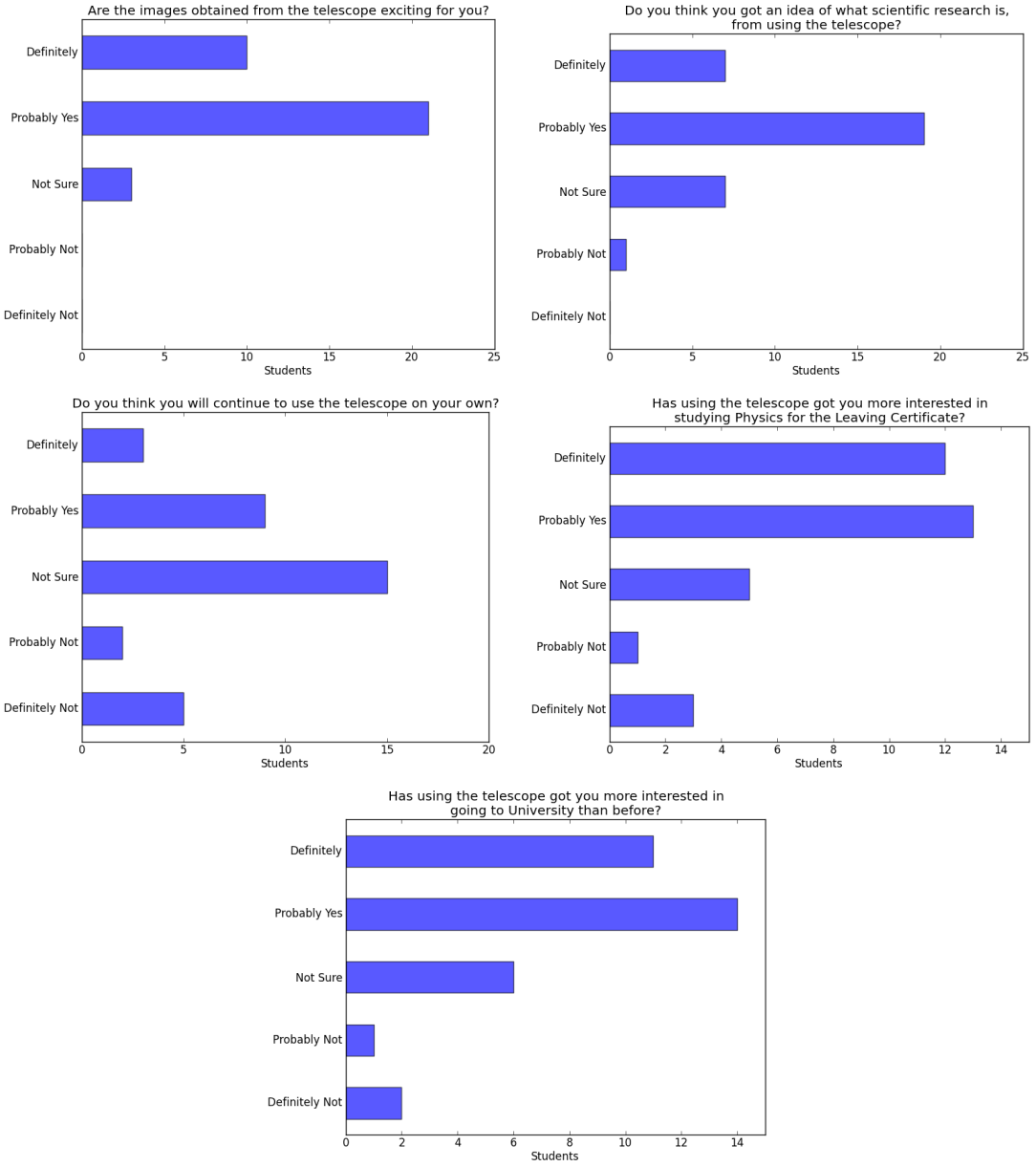

Figure C.6: Oatlands College feedback results

Question 6: What did you enjoy most about the telescope lessons?

"Pictures"

"Taking personal images of galaxies"

"Taking pictures."

"Looking at the galaxies and the nebulas"

“Talking about the universe.”

“Getting back the pictures”

“Looking at the images.”

“Looking at things that are millions of miles away.”

“Looking at the pictures of planets and discussion of the Big Bang.”

“Doing the activities”

“The Images”

“The activities”

“Pictures”

“The part when you see different images of the galaxies”

“Looking at the images of the galaxies and changing the brightness.”

“The visual picture of other galaxies.”

“Looking at galaxies.”

“Editing the pictures with brightness and colour.”

“Seeing the galaxies”

“Editing the colours of the galaxy.”

“Learning about the Big Bang Theory and images.”

“The images we got back.”

“Adjusting the lights on the planets’ images.”

“Viewing the different galaxies”

“The pictures of different galaxies.”

“Seeing different planets and orbits.”

“The images because you can draw on them.”

“I taught it was amazing that I could take pictures of galaxies over the computer.”

“Using the telescope”

“The moon.”

“I don’t know.”

“Looking at the images.”

“Seeing out into space.”

“The pictures.”

Question 7: What would you like to have done more of?

“Processing Pictures”

“More visual demonstrations of the Big Bang Theory.”

“Talking.”

“Take more photos.”

“Equations”

“More research”

“Processing pictures.”

“Fiddling around with the pictures”

“More explanation of the galaxy pictures. More activities.”

“More visual pictures.”

“Taking pictures.”

“Take a closer look at the planets like Google Earth.”

“Other galaxies locations in relevance to ours.”

“Talking about Big Bang.”

“Different telescopes and why they’re used and videos.”

“Learn about the theories of the big bang.”

“Nothing, we did everything to answer my questions.”

“Play more games on the computer.”

“Sun and moon.”

“More about how the world was made.”

“Question.”

“I don’t know.”

“Nothing really.”

“More pictures.”

Question 8: Any other feedback?

“Teachers were very helpful.”

“Website was boring.”

“No”

“No.”

“Cool to mess around with the pictures.”

“Show videos on the Big Bang Theory.”

“Thank you”

“No.”

“Needs short videos and links.”

“Very enjoyable course.”

“It was very interesting.”

“No.”

“No.”

“No.”

Presentation Slides

Primary Schools

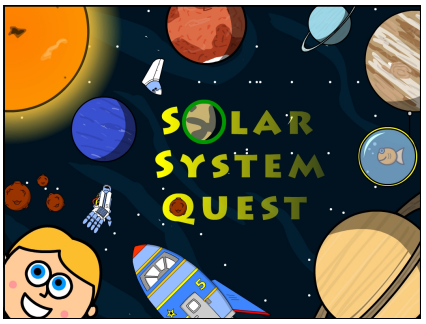

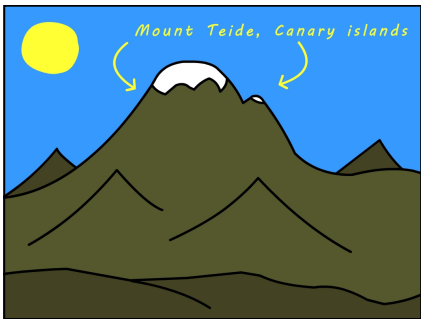

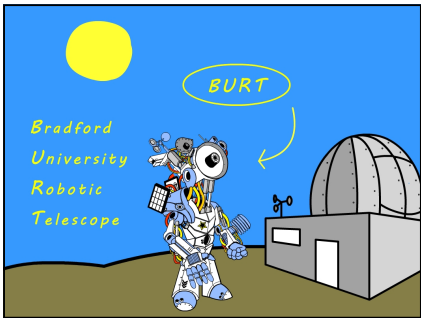

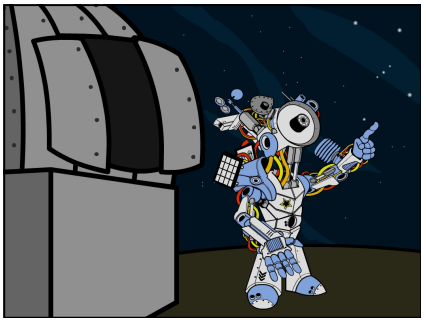

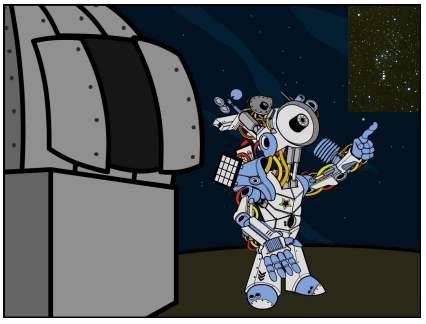

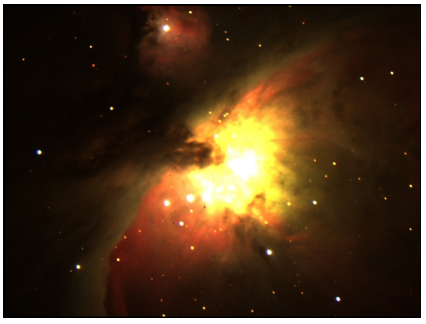

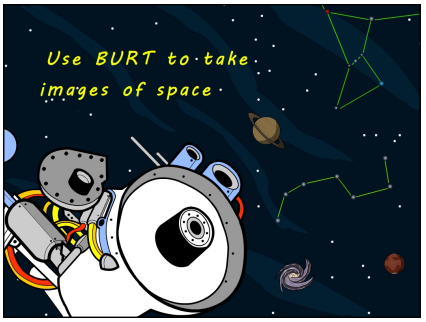
Use BURT to take images of space

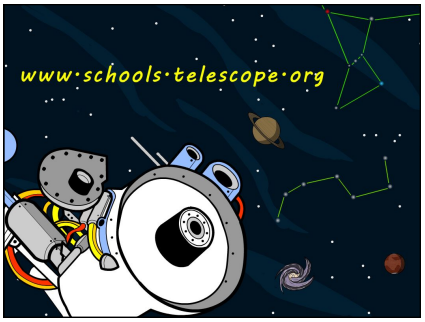
www.schools.telescope.org

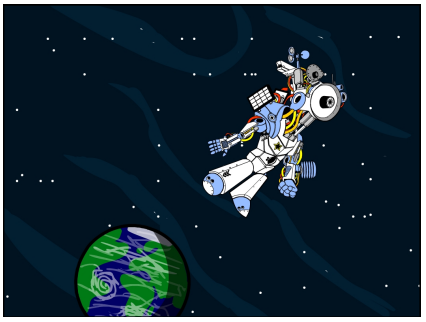

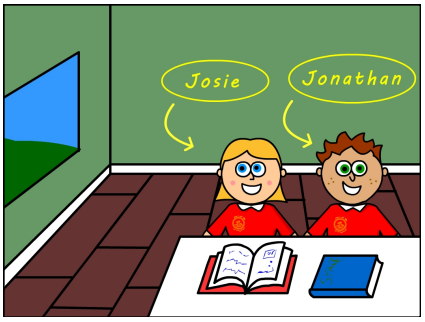
Josie
Jonathan

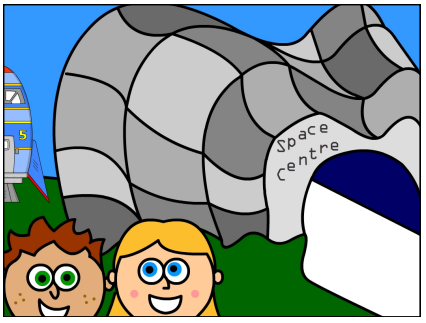
Space Centre


And the quest begins ...


MISSION TO
THE MOON
BRADFORD ROBOTIC TELESCOPE

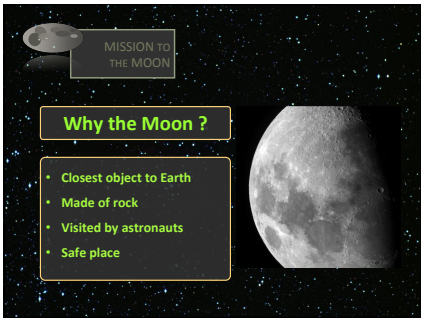
MISSION TO
THE MOON
Why the Moon ?
• Closest object to Earth
• Made of rock
• Visited by astronauts
• Safe place

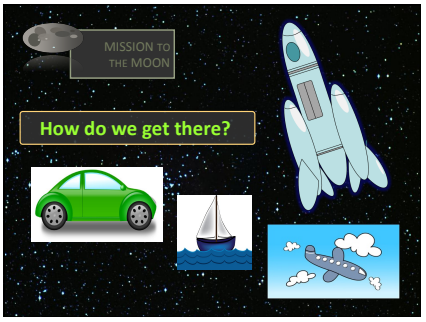
MISSION TO
THE MOON
How do we get there?

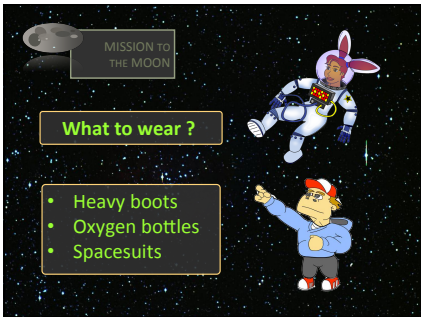
MISSION TO
THE MOON
What to wear ?
• Heavy boots
• Oxygen bottles
• Spacesuits

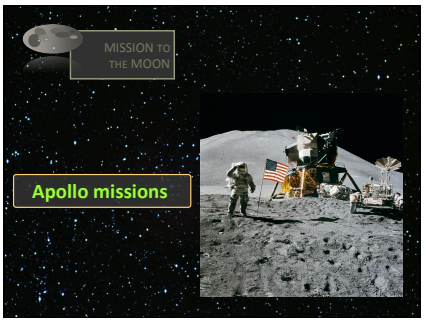
MISSION TO
THE MOON
Apollo missions

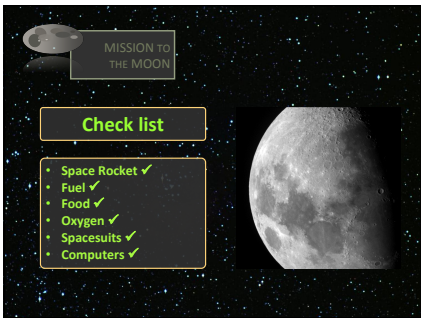
MISSION TO
THE MOON
Check list
• Space Rocket ✓
• Fuel ✓
• Food ✓
• Oxygen ✓
• Spacesuits ✓
• Computers ✓

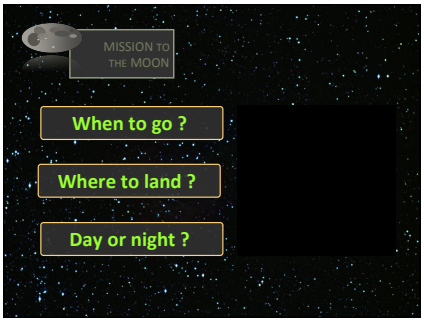
MISSION TO THE MOON
When to go ?
Where to land ?
Day or night ?


MISSION TO THE MOON
Schools.telescope.org
•Type in username and password
•Click link get started

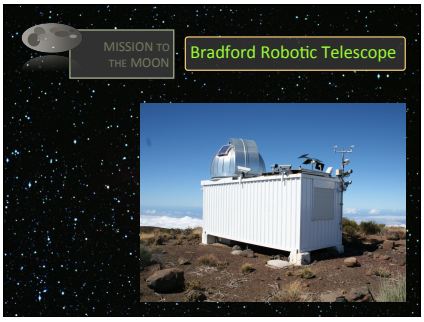
MISSION TO THE MOON
Bradford Robotic Telescope

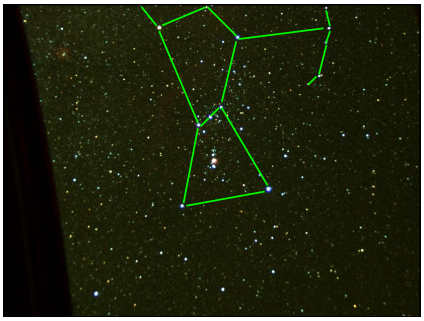

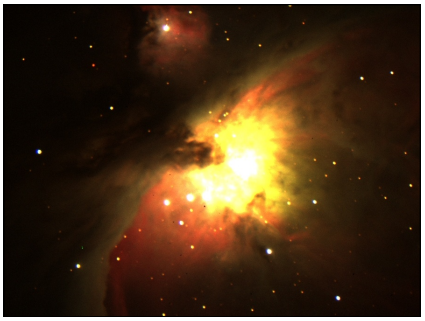

Secondary Schools

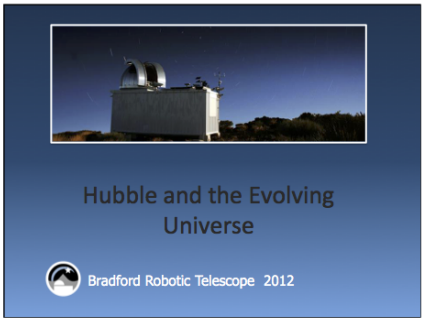

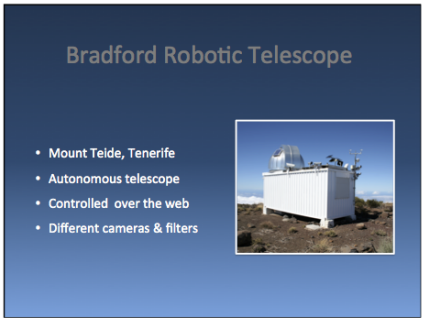

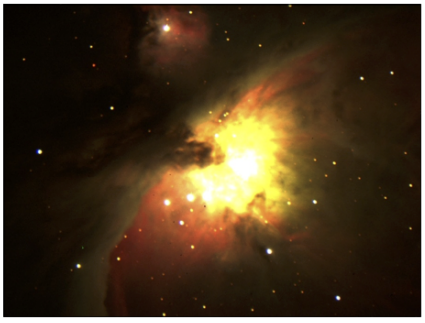

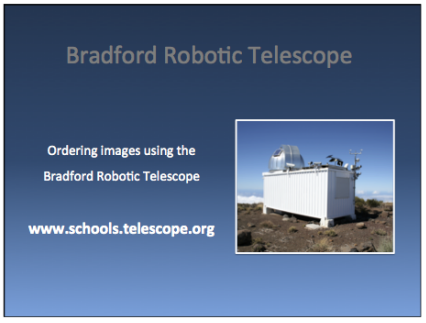

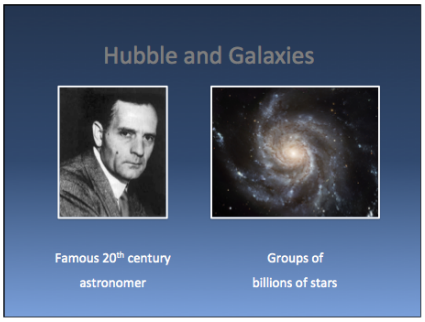

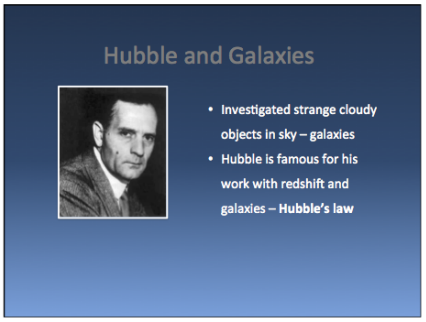

Galaxy or Nebula ?

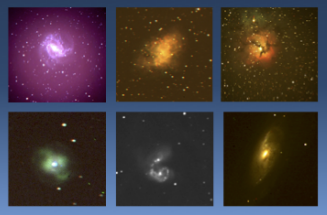

Galaxy or Nebula ?

Hubble's law

$$\text{velocity} = \frac{\text{distance}}{\text{time}}$$

The recessional velocity of galaxies is proportion to their distance from the observer

Hubble's law

How to measure galaxies velocities ?

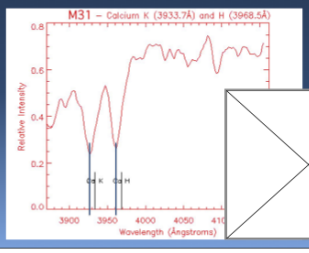

How to measure galaxies distances ?

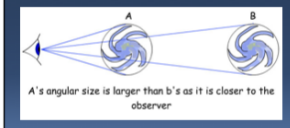

Angular sizes

Trigonometry or parallax

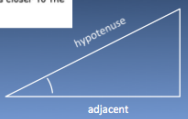

Hubble's law

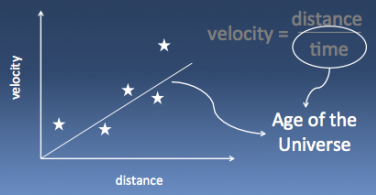

velocity = distance / time

Age of the Universe

Hubble Experiment

- You're going to measure the width of galaxies
- Each of the galaxies has a known speed
- Plot a graph of the galaxy's speed against its distance

Hubble and the Evolving Universe – part II

Bradford Robotic Telescope 2012

Speak about your method of measuring sizes

- Line of sight effects
- Galaxies are face on , edge on
- There is an inclination angle
- Brightness truncation
- Maybe we want to truncate all images to a certain brightness threshold an then measured the size

Edges of galaxies

Assessing where a galaxy "ends" is a complex topic of modern astrophysics

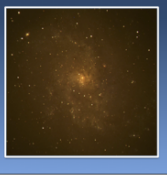

Edge on ? Face on ?

Galaxies (spirals) are thought to have circular shape but they are not often, face on